3

105500-57-F

Final Report

UTILIZATION OF SKYLAB (EREP) SYSTEM FOR APPRAISING CHANGES IN CONTINENTAL MIGRATORY BIRD HABITAT

by

Edgar A. Work, Jr.
Environmental Research Institute of Michigan
Ann Arbor, Michigan

and

David S. Gilmer
U.S. Fish and Wildlife Service
Northern Prairie Wildlife Research Center
Jamestown, North Dakota

Sponsored by
and
Prepared for

National Aeronautics and Space Administration
Lyndon B. Johnson Space Center
Houston, Texas
Contract No. T-4114B (EREP Investigation No. 486)

and

U.S. Department of the Interior
Fish and Wildlife Service
Washington, D.C.
Contract No. 14-16-0008-802

December 1975

ENVIRONMENTAL
RESEARCH INSTITUTE OF MICHIGAN

P.O. BOX 618 • ANN ARBOR • MICHIGAN • 48107

TECHNICAL REPORT STANDARD TITLE PAGE

1. Report No.	2. Government Accession No.	3. Recipient's Catalog No.
105500-57-F		

4. Title and Subtitle
Utilization of SKYLAB (EREP) System for Appraising Changes in Continental Migratory Bird Habitat

5. Report Date
December, 1975

6. Performing Organization Code

7. Author(s)
Edgar A. Work, Jr. and David S. Gilmer

8. Performing Organization Report No.

9. Performing Organization Name and Address
Environmental Research Institute of Michigan
P. O. Box 618, Ann Arbor, Michigan 48107

Northern Prairie Wildlife Research Center, U.S. Fish & Wildlife Service, Jamestown, North Dakota 58401

10. Work Unit No.

11. Contract or Grant No.
T-4114B

13. Type of Report and Period Covered
Final Report
May 1973 - Dec. 1975

12. Sponsoring Agency Name and Address
NASA Lyndon B. Johnson Space Center
Principal Investigator Management Office
Attn: Mr. Rigdon Joosten, Mail Code TF6
Houston, Texas 77058

14. Sponsoring Agency Code

15. Supplementary Notes

16. Abstract

A major effort pursued annually by the U.S. Fish and Wildlife Service is a survey of wetland conditions in the Dakotas, the southern portions of the prairie provinces, northwestern Canada and parts of Alaska. Data obtained from these surveys are utilized by biologists for establishing waterfowl hunting regulations and for satisfying certain research needs. Areas of particular importance are the glaciated prairies and adjoining prairie parklands of mid-continent because waterfowl production in these areas influences the entire continental population. This SKYLAB/EREP investigation has emphasized the monitoring of surface water, their numbers, frequency, size and the dynamics of seasonal change for a study site located in the glaciated prairies of eastern North Dakota. Data used were those collected by the SKYLAB multispectral scanner in the spring of 1973. As a primary task, thematic maps and statistics relating to open surface water were produced and analyzed. Discrimination of water was based upon water's low apparent radiance in a single, near-infrared waveband. An advanced technique using multispectral information for discerning water at a level of detail finer than the virtual resolution of the data was also successfully tested. The purpose of these efforts was to develop new remote sensing techniques which will enhance future waterfowl habitat production surveys.

17. Key Words	18. Distribution Statement
Wetlands Migratory Bird Habitat	

19. Security Classif. (of this report)	20. Security Classif. (of this page)	21. No. of Pages	22. Price
Unclassified	Not Applicable	111	

FORWARD

Satellites have provided man with a vantage point from which to peer deeper into space as well as to retrospectively and spynoptically view his home planet. The SKYLAB earth orbital satellite has been the first manned U.S. flight laboratory to be devoted principally to remote observations and experimentation in the unique environment of space. The project was conceived in the early 1960's as an extension of the Apollo program which during that decade emphasized space exploration. During the period of the 60's, application studies were consummated from which a proposed program for the conduct of solar observations and biomedical experiments evolved. In early 1970, the Apollo Applications Program was redesignated the SKYLAB Program and at about the same time the scope of the project was enlarged to include earth observation experiments. Earth observations were to be conducted with a variety of sensors including photographic cameras, an infrared spectrometer, a multispectral scanner (visible and infrared), and a microwave radiometer/ scatterometer and altimeter. These sensors together with onboard support equipment were designated the Earth Resources Experiment Package (EREP). A total of 146 proposed investigations were selected to comprise the EREP data-user program. This paper reports on the conduct and results of one of those investigations, specifically a study in the utilization of EREP data for monitoring changes in the breeding habitat of migratory waterfowl.

The authors wish to acknowledge Harvey K. Nelson who orginally conceived and developed the ideas behind this investigation. We are grateful too for the assistance of several individuals in the conduct of this work. In particular, we acknowledge the cooperation of our NASA technical monitor, Rigdon Joosten, the administrative guidance of W. Reid Goforth and the field assistance of A. T. Klett, the latter two individuals both of the Northern Prairie Wildlife Research Center. Finally, but far from last, we are indebted for the efforts of Diana Rebel of the Environmental Research Institute of Michigan for her labors with data processing and analysis.

TABLE OF CONTENTS

LIST OF FIGURES

LIST OF TABLES

CHAPTER 1

SUMMARY AND CONCLUSIONS

To explore procedures which could enhance the capabilities of the U.S. Fish and Wildlife Service for monitoring the breeding habitat of migratory waterfowl, an evaluation of the SKYLAB Earth Resources Experiment Package (EREP) has been conducted. A related study had previously been carried out utilizing data collected by the LANDSAT-1 satellite. The fact that the two studies have overlapped both chronologically and geographically has allowed the results of one to reinforce the other and has allowed for a comparison of the two sensor systems. In particular, we have emphasized the use of data collected by multispectral scanners and the processing of these data using general purpose and special purpose digital computers. The use of automatic data processing techniques is uniquely suited to this type of task because of the wide expanse of prime waterfowl breeding areas and because of the need to quickly assimulate and collate parametric information on habitat conditions.

The specific objectives of both the LANDSAT and this SKYLAB study were to map and tabulate statistics on surface water conditions and to determine changes in wetness between the spring breeding period and the fledging period of July or early August in a glaciated prairie region in east-central North Dakota. This study has principally considered habitat conditions related to open surface water (i.e., ponds and lakes). The study as originally planned envisioned the use of two sets of data collected by the SKYLAB multispectral scanner in May and again in July or early August. Because of operational constraints, the SKYLAB/EREP System was not able to achieve this repetitive coverage. Instead a single observation occurred on 12 June 1973. The timing of the observation has allowed us to supplement the single SKYLAB observation with bracketing LANDSAT observations which did occur on 14 May and 7 July of that year. This series of three sequential observations

provided an opportunity for tracking the dynamic water conditions over nearly a two month interval. Approximately the same areas were observed on the three different dates. The study area included portions of two different physiographic regions, a Coteau or moraine feature created by stagnation ice, and a drift plain or low relief feature of numerous ground moraines. Because of differences in wetland frequency between them, these physiographic features have served as a basis for stratifying the numerical results obtained in this study.

The mapping of open water has been carried out by two radically different techniques, a single-channel approach and a multiple-channel approach termed "proportion estimation". The single channel approach delineates water by thresholding or level slicing the scale of radiance values in a single near-infrared waveband. This approach is effective because the radiance of water relative to other terrain features was uniformly low. Proportion estimation processing involved the use of multiple data channels and a computational algorithm for estimating the fractions of pure materials present within the resolution cell of a multispectral scanner.

For the water delineation a single channel of near-infrared data was used to produce a computer generated thematic map and ralated statistics for an area encompassing 3833 km^2 (1480 square miles). This area included portions of both the Coteau and Drift Plain physiographic regions. The results were produced with a single near-infrared waveband of data gathered by the SKYLAB multispectral scanner (instrument experiment S-192). This multispectral scanner included a total of five near-infrared wavebands in the 0.78-to 1.75-μm range, all of which had good signal-to-noise characteristics. Our experience has indicated that any one of these bands would have been reasonably satisfactory for small scale water mapping by satellite. Given a choice, however, the 1.55- to 1.75-μm band was less ambiguous for water recognition and was easier to utilize in terms of training the computer. Use of the 1.55- to 1.73-μm band also held the promise that shallow water features when resolvable in the small scale satellite data were more likely to be recognized as open surface water.

Although the maps which were generated in this effort graphically portrayed water conditions, without further interpretation and quantification, such displays do not fully satisfy management and research needs. Quantification of the data was easily achieved when we used a digital computer to tabulate the size and location of each recognized water feature and thence to summarize the results. The summary indicated that the areal density of ponds in nearly all size classes considered (1 thru 50 acres) was generally an order of magnitude greater in the Coteau stratum than in the Drift Plain stratum. The data also indicated that the SKYLAB enumeration of ponds as a whole was consistent with enumerations made using LANDSAT data. This is to say, that a decline in pond numbers noted from May to July indicated by the LANDSAT observations was also reflected in the intermediate SKYLAB data. When individual ponds as represented in the SKYLAB data were studied, however, we saw that their areal display did not follow as consistent a pattern. Approximately 30 percent of the SKYLAB lakes examined were larger than expected while another 30 percent were smaller than expected. We have concluded that these deviations from the mean tended to balance each other and that the source of the problem was the conical scanning configuration of the sensor and the procedures used to subsequently convert the data into a rectangular grid of scene elements or pixels. Both the scanning format and the associated techniques for data conversion appear to have had the net effect of slightly but systematically altering areal measurements and the geometric fidelity of small scale scene features such as prairie ponds.

In another phase of the study, the limited testing of a unique technique for improving the apparent spatial resolution of multispectral data was undertaken. The technique, termed "proportion estimation," involved the use of a computational algorithm for estimating the fractions of pure materials present within the resolution cell of a multispectral scanner. To be effective, proportion estimation processing requires a high degree of spatial registration between spectral data channels. Our early work with SKYLAB multispectral scanner data in a line-straightened format (after conversion from a conical scan format) indicated the

occurrence of frequent but random channel to channel misregistration of as much as one or several pixels. The bulk of these registration errors were apparently introduced in the process of converting data from a conical-scan to a line-straightened format. Consequently all of our multispectral processing was accomplished with data in a conical-scan format although these data proved more difficult to handle and display.

Proportion estimation computations were applied to an area of 286 km^2 (110 square miles). The resultant computer output was a set of water proportions for each scene pixel. Results obtained from proportion estimation processing indicated that the minimum discernable pond size was four-tenths of the minimum size detected with the single-waveband thresholding algorithm. Ponds smaller than this could be detected, however, numerous errors of false recognition (commission errors) also occurred when the finer degree spatial resolution was attempted.

Proportion estimation processing of LANDSAT data had previously been applied to the same 286 km^2 site. It should be noted that nearly the same number of water features were identified in the LANDSAT data of 7 July 1973 as were observed with the SKYLAB observation data collected 25 days earlier on 12 June. If anything, this would indicate that the SKYLAB data did not yield as great a count of ponds as should be expected because some ponds should have diminished in size to the point of extinction over the interval. However, because of the deficiencies inherent in data which have undergone a format conversion, any inconsistencies of the small magnitude experienced could reasonably be attributed to the problems associated with data handling and conversion.

It is most significant to note that certain lakes, which had been only partially delimited in the LANDSAT proportion estimation processing, were in fact fully delimited with the SKYLAB data. The lakes in question were shallow alkaline lakes which were high in suspended solids and/or precipitated alkali bottom sediments and which had an anomalous appearance when compared to fresher lakes. We attributed

this improved recognition capability to the availability and utilization of several wavebands in the near-infrared spectral region. The SKYLAB scanner provided six wavebands of near infrared information to a maximum wavelength of 2.35 μm whereas only two near-infrared wavebands to a maximum wavelength of 1.1 μm were available from the LANDSAT system. In particular, we feel that a waveband in the 1.5-to 1.8-μm atmospheric window is important for the delineation of water and hygric scene features in general.

Finally, we should point out that it is difficult to state conclusively the results of this investigation because of numerous problems which became manifest during its course. Specifically, the two EREP observations upon which the measurement of habitat change was predicated were never realized. The single observation, which was obtained, did not occur during either the requested May or the requested July time periods. As a result the observation did not occur during an appropriate phenological period, and it did not coincide with supporting aircraft observations nor with the respective May and July breeding and production surveys routinely conducted by the U.S. Fish and Wildlife Service (FWS). These deviations from the originally planned experiment make it unrealistic and impractical for us to attempt at this time to assess the cost effectiveness of EREP data, as opposed to current techniques for predicting waterfowl populations.

The diurnal timing of the observation was less than optimal in that it took place at 06:19 local solar time, too early in the day for sufficient illumination. As a result, the poor signal-to-noise ratios in the visible and thermal infrared wavebands precluded the plenary use of those spectral channels. Furthermore, the multispectral scanner observation only marginally encompassed the study site and many areas of environmental interest were not surveyed nor did the SKYLAB observation spatially coincide with many of the supporting aircraft and ground survey transects. These were problems of an operational nature occasioned by satellite system complications which arose during and after launch and by the need to accommodate the requirements of both this and many other investigations in a relatively short time. One

source of difficulty which was inherent to the scanner system and which has already been referred to was associated with the conical scanning configuration and the subsequent data reformatting.

CONCLUSIONS

1. Satellite remote sensing techniques hold considerable promise for the rapid, synoptic assessment of waterfowl breeding habitat.
2. A simply implemented technique, requiring a single near-infrared waveband of data, exists for delimiting open surface water features. This capability with the use of automatic data processing techniques has the potential for being operationally incorporated into ongoing habitat assessment programs in the near future.
3. Trends noted in numbers and size distributions of water features were consistent between LANDSAT and SKYLAB data sets when considering a large observation scene as a whole.
4. The sizes of small individual water features were not, however, consistently determined. These areal inconsistencies of being rendered either too large or too small appeared to be due to the algorithm used to convert data from a curvilinear scan-line format to a straightened scan-line format and tended to average out when a large group of water features as a whole were considered.
5. The proportion estimation technique, utilizing the added information content of multiple spectral wavebands, has allowed for the recognition of a greater number of small ponds not previously identified and also greatly improved the area and peripheral shape definition of the larger ponds and lakes. The use of this technique has improved resolution capabilities for mapping open surface water by a factor of between two to three over the nominal resolution limit of the data. Further testing and refinement of the technique will be required.
6. Spectral information in the reflective infrared (0.7 to 3.0 μm) is often unique and useful for the thematic classification of terrain features. In particular, we feel that a waveband in the 1.5-to 1.8-μm atmospheric window is important for the delineation of water and hygric features in general.

7. The conical scanner while offering certain optical-mechanical advantages has in this program created problems of a data handling and display nature. It has been necessary to convert the data from a curvilinear scan format into a rectangular or straightened scan-line format. This procedure has diminished the spatial accuracy and geometric fidelity of the data.

2

INVESTIGATION BACKGROUND

The primary breeding areas of North American waterfowl (primarily ducks) are the Dakotas, the southern portions of the prairie provinces, northwestern Canada and parts of Alaska (Figure 1). These areas of the mid-continent are major contributors in sustaining the total continental duck population which amounts upwards to 120 million birds. Small ponds and lakes of the glaciated prairie region, commonly referred to as prairie potholes, are the backbone of duck production habitat in North America (Figure 2). The prairie pothole region, composed of the southern portions of Alberta, Saskatchewan, and Manitoba and parts of North and South Dakota, Minnesota, and Montana makes up only 10 percent of the total breeding area of North America yet produces 50 percent of the continental duck crop in an average year (Smith, et al., 1964). Because of the area's importance for waterfowl production the region is monitored annually by intensive systematic surveys conducted by the U.S. Fish and Wildlife Service in cooperation with the Canadian Wildlife Service and various states and provinces. Aerial surveys made in May and July are used with air-ground correction factors, to provide indices of breeding population size, habitat conditions, and waterfowl production. These indices serve to aid in making management decisions relating to annual hunting regulations and to answer certain research needs. Breeding ground survey data must be collected and summarized before early August when various national and regional waterfowl meetings convene to formulate annual hunting regulations. In some years breeding ground survey biologists are hard pressed to complete this task by early August. Descriptions of the operational aspects of the breeding ground surveys are given by Crissey (1957), Stewart, et al. (1958), and, more recently, Henny, et al. (1972). The use of survey statistics for modeling waterfowl production is discussed by Cooch (1969), Crissey (1969) and Geis, et al. (1969).

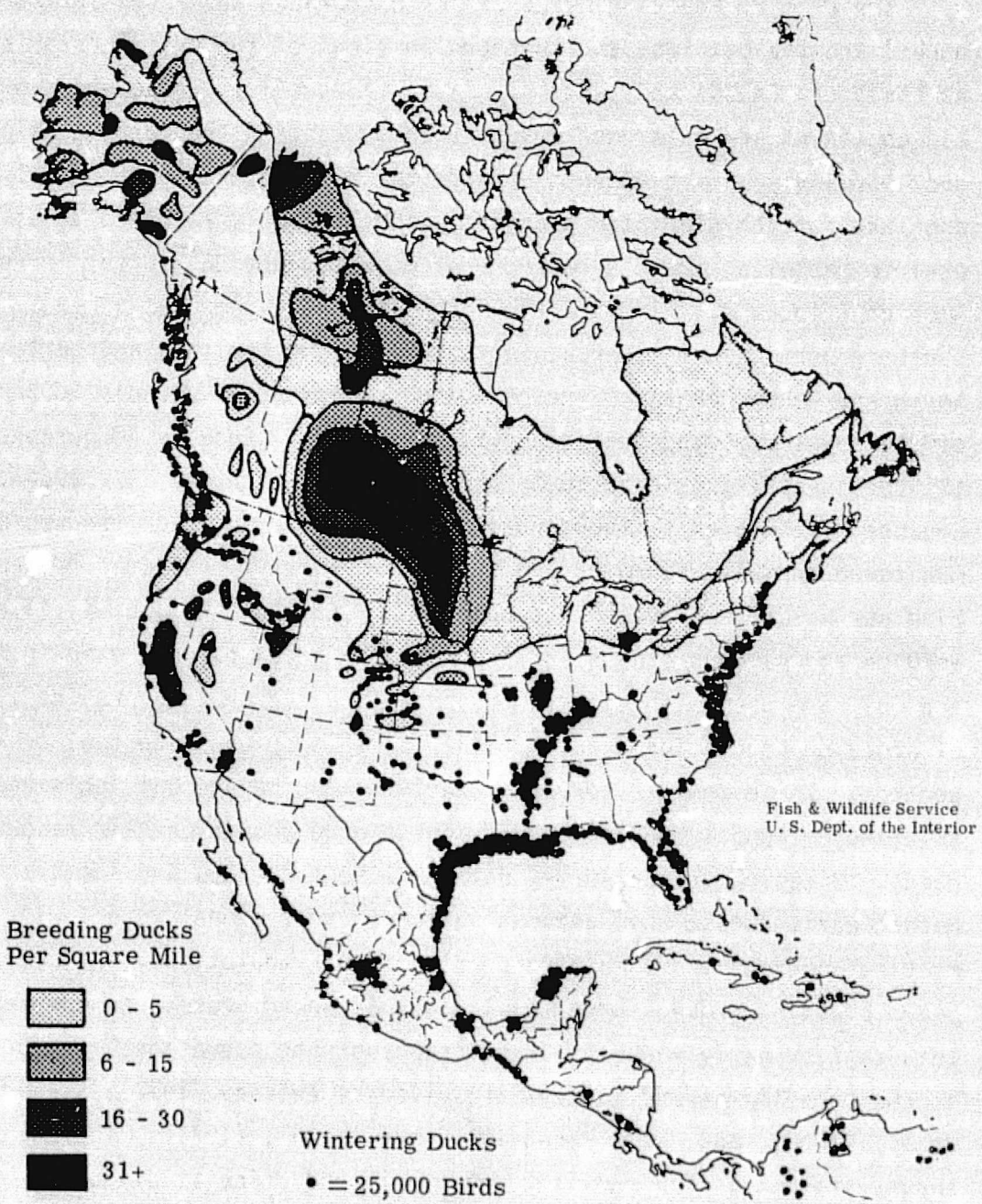

FIGURE 1. AVERAGE DISTRIBUTION OF NORTH AMERICAN BREEDING AND WINTERING WATERFOWL

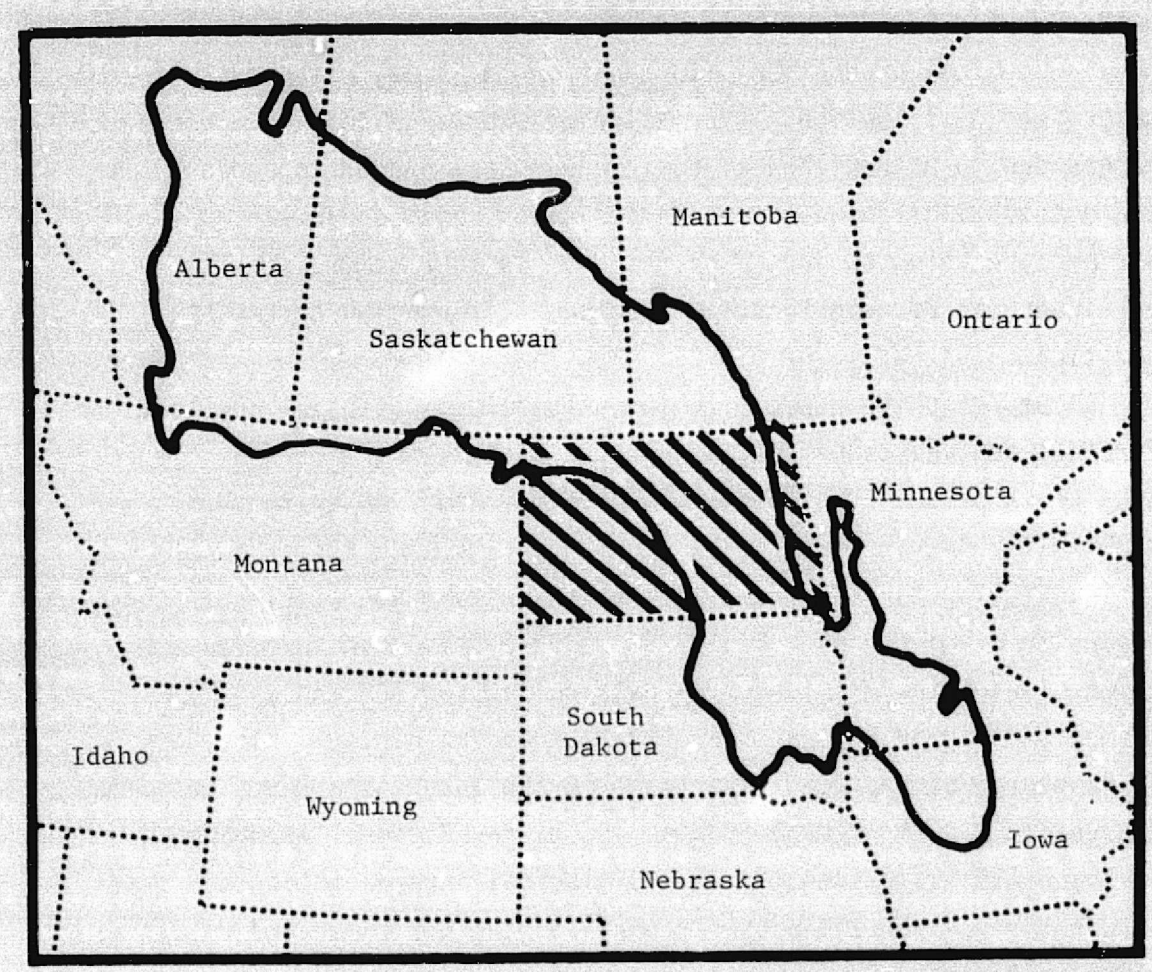

FIGURE 2. THE PRAIRIE POTHOLE REGION OF MID-CONTINENT NORTH AMERICA. (After Stewart and Kantrud, 1973.) The state of North Dakota is indicated by shading.

Canadian and U.S. investigators have suggested the importance of pond numbers in regulating annual waterfowl production (Cooch 1969, Crissey 1969). From the work of these and other researchers it has become evident that the degree of wetness, especially changes in pond numbers during May-July should provide a useful index for predicting annual waterfowl production. In addition to annual estimates of pond numbers and distribution, information on short and long term ecological changes due to natural and economic causes are needed to properly manage this wildlife resource. A series of research investigations have and are being conducted on the premise that remote sensing techniques can be used to assimilate such information on habitat conditions.

A comprehensive program to investigate the potential applications of remote sensing techniques as a tool in the management and scientific study of waterfowl populations was developed in 1968 by the U.S. Fish and Wildlife Service and the Environmental Research Institute of Michigan (prior to 1972 known as the Willow Run Laboratories of the University of Michigan). From 1968 to 1970 this work involved a series of airborne multispectral data collection and analysis experiments designed to assess waterfowl breeding habitat. The work was sponsored by the U.S. Department of the Interior's Earth Resources Observation Systems (EROS) Program and by the National Aeronautics and Space Administration (NASA). Biological interpretation and site coordination was provided by personnel of the U.S. Fish and Wildlife Service's Northern Prairie Wildlife Research Center at Jamestown, North Dakota.

These experiments emphasized data collection by airborne multispectral scanners and data reduction and analysis with computer aided techniques specifically developed for this task. This early work was reported by Burge and Brown (1970), Nelson, et al. (1970), and Work and Thomson (1974). A more recent program (Work 1974, and Work et al., in press) was conducted with LANDSAT-1 data.

The LANDSAT study was a natural extension of the earlier aircraft program. Its goals were to: 1) modify and utilize techniques which

evolved from the aircraft program, and 2) develop new techniques which would be suitable for high altitude, wide area (synoptic) surveys. Data were to be used principally to document the amount of surface water present during a May and a successive July observation. Data acquisition for the LANDSAT study was planned for the spring-summer of 1972. However, because of delays in the launch of the satellite, the bulk of that investigation was deferred until a May-July sequence of data was available from the 1973 season. As a result, the LANDSAT-1 program and the SKYLAB investigation with which this report is concerned have utilized data observations which have been nearly coincidential in a temporal and spatial sense. Because of this unique situation we have made occasional references and comparisons in this report of data from both sensor systems.

3

DESCRIPTION OF THE INVESTIGATION

Our overall goal for this investigation was to develop and test techniques for identifying and monitoring prairie waterfowl habitat using the EREP sensors. This and subsequent work is intended to bring us to our long term goal which is to define habitat quality indices which accurately relate to the dynamics of waterfowl production and which are discernable with remote sensing techniques. The application of high altitude (e.g., spacecraft) sensors and automated data handling is uniquely suited to monitoring waterfowl habitat because: (1) the survey is generally regional and international in scope, (2) the seasonal and annual changes in habitat conditions require repeated observations, and (3) the results are needed promptly for management decisions.

In undertaking this study our first objective was to monitor changes in the breeding habitat of migratory waterfowl between May, the peak nesting season for several species of ducks, and July or early August when most duckling broods have hatched. Proposed indicators of habitat quality were surface water, the general degree of terrain wetness, plant phenology, and land-use patterns. Primary emphasis, however, was placed upon the observations of ponds and lakes to include the assimilation of statistical data on their numbers, areal extent, frequency, distribution, and aggregation. Information on ponds and lakes is immediately important because it is currently used in models for predicting annual waterfowl production (Geis, et al. 1969).

Consistent with earlier work (Burge and Brown 1970, and Work and Thomson 1974), the use of data obtained by a multispectral scanner was stressed. Multispectral scanners offer the advantages of a multiplicity of spectral wavebands and quantified data values in the form of digital signals recorded on magnetic tape. The former advantage broadens the data's information content while the latter allows for

direct and rapid porcessing and analysis by digital computers. In addition to the primary role of scanner data in this investigation, photographic imagery was utilized in a secondary capacity for the selection of computer training data and for the verification of recognition maps resulting from automatic data processing.

The intended approach to carrying out this investigation was to use EREP multispectral scanner data collected over the same site in a sequence of May and July observations. The resultant data were to be processed for the recognition of surface water features and for a determination of habitat change as evidenced by changes in surface water conditions. Expected output of the automatic data processing was thematic maps of ponds and a tabulation of statistics on surface water conditions. From the onset of the program it was recognized that the EREP scanner would not be capable of consistently delineating ponds less than about two hectares (5.0 acres). Therefore, in addition to merely mapping resolvable surface water features, estimates of the presence of ponds smaller than the resolution limit were proposed by the use of a double sampling scheme in which low altitude aircraft data were to be collected at approximately the same time as each EREP data pass.

Because of operational delays in the launch and manning of the SKYLAB space station, data collection during the May 1973 breeding period did not occur. The subsequent compression of a large number of other planned earth observations into a foreshortened data acquisition period also precluded a second data observation as planned for July or early August of 1973. Instead a single data recording overflight occurred on 12 June 1973. Previously an overflight by supporting aircraft had occurred on 12 May 1973 and a subsequent aircraft overflight took place on 12 August 1973 on schedules which coincided with both the waterfowl nesting and brood rearing seasons. We had hoped for near simultaneous SKYLAB overflight and data observation. This failure to obtain a repetition of seasonal observations and the untimeliness of the single observation in terms of both season and coordination with supporting aircraft necessitated a modification of

project goals and emphasis. Originally the program had been intended as a stand alone investigation. Because of the circumstances, however, it seemed appropriate to integrate this investigation with another ongoing study which was utilizing LANDSAT-1 data. LANDSAT data collected on 14 May 1973 and 7 July 1973 had previously been obtained and analyzed. It therefore was advantageous to utilize EREP data as a third reference point in tracking the dynamic surface water conditions from May into July.

Our inability to obtain a temporally synchronized EREP and aircraft data set also precluded our conducting a double stage sampling experiment. In lieu of that experiment, we chose to utilize the manifold information of a multispectral data-set to systematically estimate percentage of surface water present in each of a scene's resolution elements (pixels). This approach potentially resulted in the detection and tabulation of surface water features smaller than the sensor's nominal optical resolution limits.

The text which follows includes a description of the EREP multispectral scanner and a description of the study area and site data coverage (Chapter 4), followed by the bulk of the technical report which discusses the methods and results of several analytic procedures used in this investigation. Chapter 5 is devoted to the mapping of surface water bodies with a single waveband of near-infrared data. This processing resulted in the generation of thematic water maps and statistics on water conditions and changes in these conditions. Chapter 6 is devoted to multispectral data analysis particularly the use of multiple wavebands of data for estimating within-pixel surface water content. Finally Chapter 7 contains a summary of investigation results and the conclusions derived from these results.

THE SKYLAB/EREP SURVEY OF WETLANDS IN EASTERN NORTH DAKOTA

This chapter provides additional background information regarding the principal EREP sensor system utilized for this investigation and characteristics of the study site.

SKYLAB/EREP Multispectral Scanner

The SKYLAB/EREP Multispectral Scanner (Instrument Experiment S-192) was an optical-mechanical scanner coupled with a spectral dispersing and detector system. The scanner assembly utilized a rotating mirror scanning in the image plane of the collector optics to perform a conical scan of the object plane (i.e., the earth's surface). The cone angle was 5°32' about the instrument axis (nominally spacecraft nadir). The spectrally dispersed electromagnetic energy received from the earth's surface simultaneously irradiated 13 detectors, each detector being responsive to a unique spectral region. The scan pattern consisting of the forward 116°15' of the 360° scanning cycle covered a curvilinear path on the earth's surface with a swath or chord length of approximately 72.4 km (39.1 nautical miles) and any desired length along the ground track of the satellite (Figure 3). Approximately 94.8 scans occurred each second resulting in a scan-line to scan-line forward displacement of approximately 72.4 m (238 ft). The sensor instantaneous-field-of-view was 79.3 m (260 ft) square. Thus the instrument had an overscan of about 10%. Each of the 13 detectors produced an electronic output signal corresponding to the average value of the radiance being received in its particular spectral band from a spot on the earth's surface contained in the instantaneous-field-of-view. The spectral range or waveband of each detector is given in Table 1. The analog video signals enamating from each of the 13 spectral detectors were sampled and digitized at either high or low rates with the exception of the thermal infrared band (13) which was sampled at both rates. The low sampling rate corresponded to an approximate 72.6 m (238 ft.)

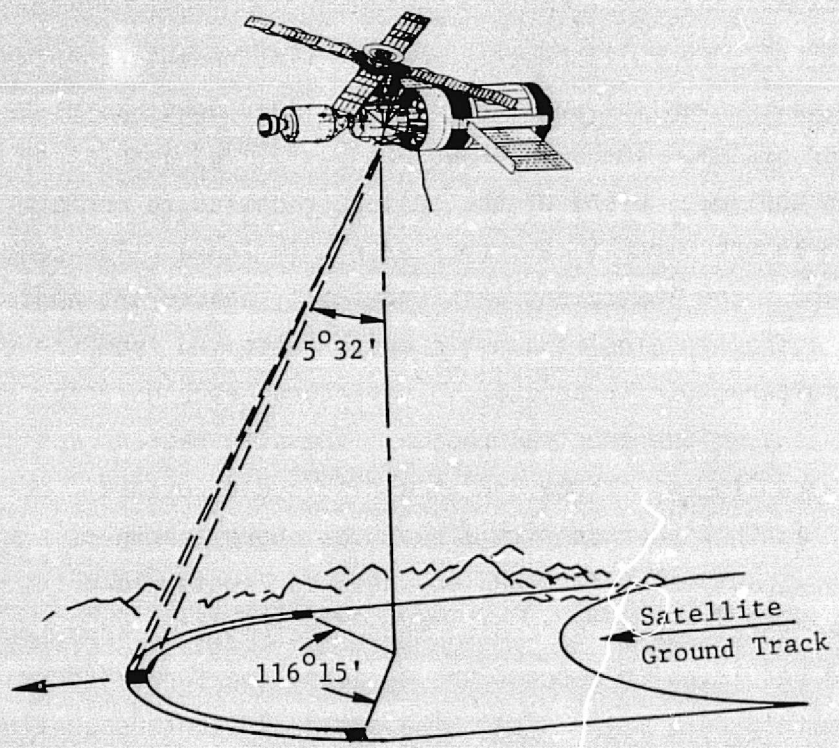

FIGURE 3. SKYLAB/EREP MULTISPECTRAL SCANNER CONICAL SCAN PATTERN

TABLE 1

SKYLAB/EREP MULTISPECTRAL SCANNER (S-192)
SPECTRAL RESPONSIVITY

Band No.	Description	Nominal Spectral Range (μm)*	Measured Spectral Range (μm)**	SDO Channel No.
1	Violet	0.41-0.46	0.420-0.447	22
2	Violet-Blue	0.46-0.51	0.451-0.503	18
3	Blue-Green	0.52-0.56	0.50-0.55	1 & 2
4	Green-Yellow	0.56-0.61	0.54-0.60	3 & 4
5	Orange-Red	0.62-0.67	0.599-0.654	5 & 6
6	Red	0.68-0.76	0.654-0.734	7 & 8
7	Infrared	0.78-0.88	0.770-0.890	9 & 10
8	Infrared	0.98-1.08	0.930-1.050	19
9	Infrared	1.09-1.19	1.030-1.190	20
10	Infrared	1.20-1.30	1.150-1.280	17
11	Infrared	1.55-1.75	1.550-1.730	11 & 12
12	Infrared	2.10-2.35	2.10-2.34	13 & 14
13	Thermal Infrared	10.2-12.5		15,16 & 21

* The nominal spectral range is referenced throughout this text.

** S-192 spectral response calibration per National Aeronautics and Space Administration (1974).

center-to-center spacing and was used for bands 1, 2, 8, 9, 10, and 13. The high sampling rate, equivalent to twice the low rate, approximated a 36.3 m (119 ft.) center-to-center sample spacing. Bands 3, 4, 5, 6, 7, 11, 12, and 13 were sampled at the high rate with even and odd numbered samples being handled as two low rate channels thereafter. The channels are referred to as SDO's (Scientific Data Output) in this report. In theory, all even numbered SDO's were in spatial registration with each other. Similarly all odd numbered SDO's were in spatial registration but one-half pixel out of registration with the even SDO's.

For the convenience of those investigators who utilized S-192 data and who desired data in a straight scan-line format, the conical data were available in a transformed line-straightened format. The algorithm used for this transformation was based on a nearest neighbor decision rule. After scan-line straightening, each high rate band was separated again into two low rate channels (SDO's) with the odd elements going into one SDO and the even elements going into another SDO as with the conical data described above. This investigation has utilized data in both a line-straightened format (Chapter 5) and a conical format (Chapter 6).

SKYLAB/EREP Mission Profile

The SKYLAB mission consisted of series of four launchings -- the first, to insert the large unmanned laboratory in earth orbit and thereafter three serial launches to carry crews to the orbiting laboratory. Each crew, consisting of three men transited from earth to the space laboratory, occupied the laboratory for an extended period, and subsequently returned to earth. The space laboratory was occupied for periods of 28, 60, and 85 days with intervals of 36 and 51 days respectively between the manned periods. This investigation utilized data collected during the first manned period which lasted from 25 May 1973 to 22 June 1973. During each occupation, the crews conducted a series of biomedical, astronomical, engineering, and earth survey experiments all of which had to be closely managed to fit within a tight mission schedule. In addition to the necessary imposition of a time budget,

other factors also posed restrictions to the earth resources survey program. They included spacecraft power limitations, the availability of consumables such as film and magnetic tape, spacecraft orbit location with respect to targets of interest, and the occurrence of suitable solar illumination and atmospheric viewing conditions.

Throughout its useful life the SKYLAB Orbital Workshop circumvented the earth in a circular orbit inclined at approximately 50° to the equator. The orbit was controlled to yield a five-day repeating ground track. However, it should be noted that the five-day orbital re-traces progressed through periods of darkness and daylight and that orbital drift, which at times became considerable, did occur.

Typical orbital paths projected onto the earth's surface are shown in Figure 4. The single earth observation made on behalf of this investigation occurred on 12 June 1973 on an ascending node of the orbital track crossing the state of North Dakota from the northwest corner thence east-south-east passing approximately over Fargo. Table 2 lists the parameters of this overpass.

The North Dakota Study Area

The study site chosen for this investigation, although small relative to the regional scope of the prairie pothole country was extensive enough to provide an adequate test of survey methods. The specified intensive study area was centered on Woodworth Station* and extended eastward to longitude 100°00'. The test site was situated completely within the North Dakota prairie pothole biotic area but did encompass two distinctly different groups of glacial landforms or physiographic divisions -- the Missouri Coteau and a Glacial Drift Plain. Figure 5 shows the biotic areas of North Dakota and the location of Woodworth Station. The Coteau overlying approximately two-thirds

*Woodworth Station is a field research site operated by the Northern Prairie Wildlife Research Center of the U.S. Fish and Wildlife Service. The Station, approximately 15.5 km^2 (6 mi^2) in size, lies 5 km (3 miles) east of the village of Woodworth, North Dakota or 48 km (30 miles) northwest of Jamestown. The station coordinates are 47°08'N and 99°14'W.

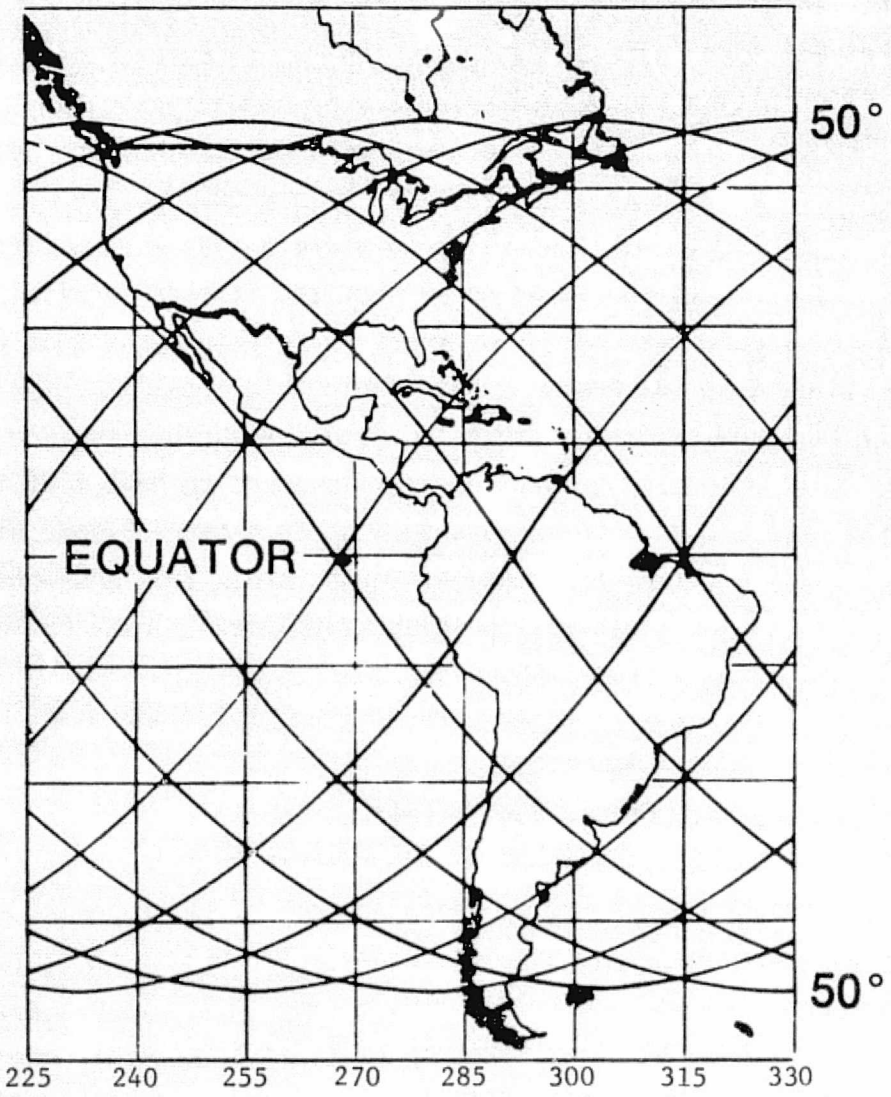

FIGURE 4. TYPICAL ORBIT PATHS OF THE SKYLAB ORBITAL WORKSHOP

TABLE 2

SKYLAB MULTISPECTRAL SCANNER (S-192) CHARACTERISTICS

Scan Format:	Conical
Scan Cone Angle:	$5^{o}32'$
Active Scan:	Forward $116^{o}15'$ of Scan
Scanner Optical Instantaneous-Field-of-View:	0.182 mrad (79.71 m @ Altitude Shown)
Scan Rate:	94.792 Scans/Second
Altitude:	437,957 m*
Ground Radius of Scan:	42427 m*
Sampling Rate (Along Scan):	Low Rate Channels -- 72.6 m Center to Center High Rate Channels -- 36.3 m Center to Center
Number of Samples per Scan:	Low Rate Channels - 1240 High Rate Channels - 2480
Ground Speed:	6866 m/sec*
Satellite Ground Distance Forward Per Scan:	72.43 m*
Analog to Digital Conversion:	8 Bit Words

* These parameters apply specifically to the North Dakota overpass of 12 June 1973.

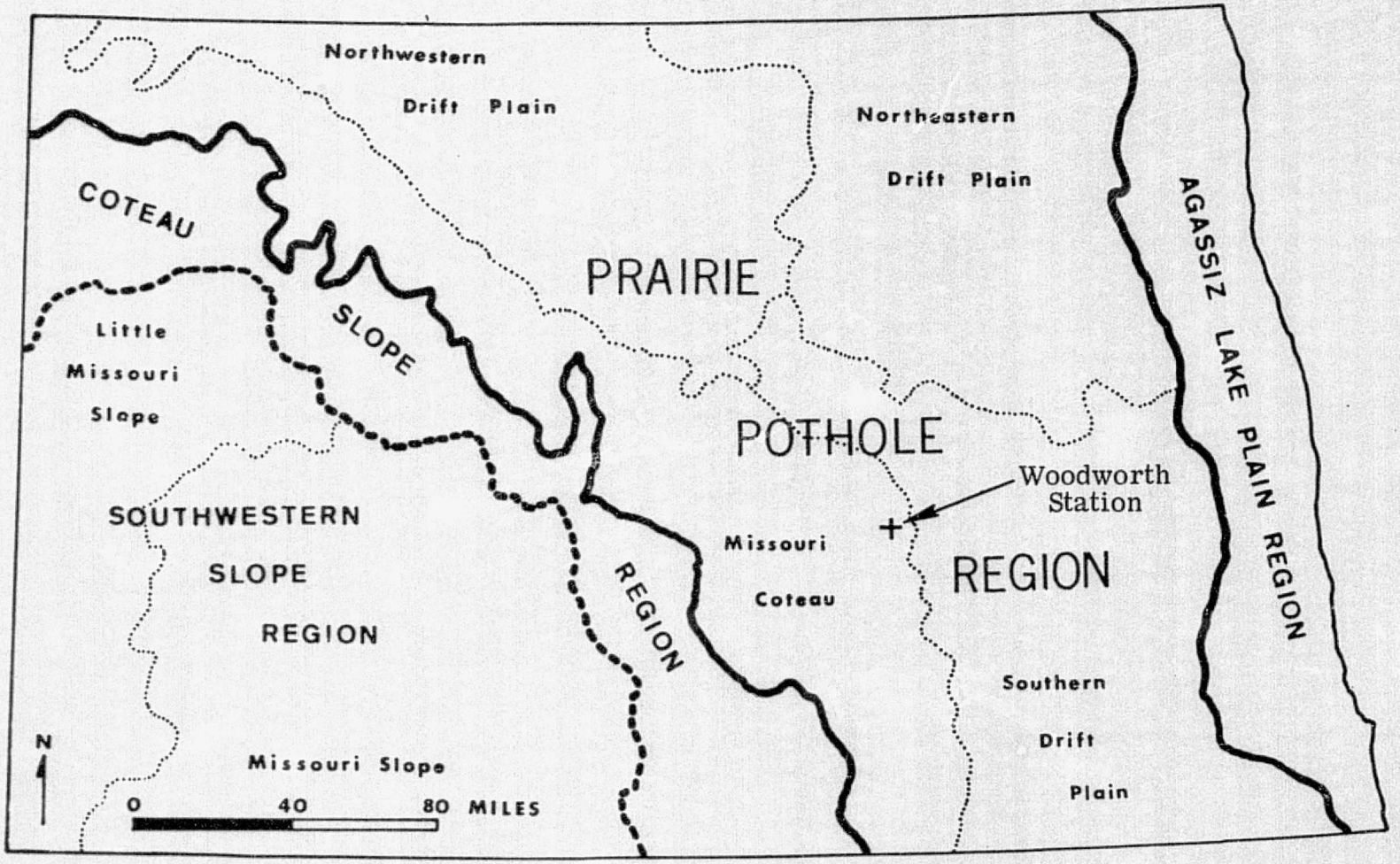

FIGURE 5. THE BIOTIC REGIONS OF NORTH DAKOTA. (After Stewart and Kantrud, 1973). The location of Woodworth Station with respect to the Missouri Coteau and a drift plain feature is indicated.

of the study area is characterized by the prominence of high underlying bedrock which acted to buttress the advance of Pleistocene ice sheets causing extensive glacial stagnation. In addition, the ice had become overlain with large quantities of superglacial till which caused protracted and irregular melting of the underlying ice. The resultant topography is hummocky, drainage is non-integrated, and lakes and sloughs are abundant as is characteristic of an area of collasped ice topography. The Coteau is said to contain some of the best waterfowl breeding areas in the 48 contiguous states (Clayton, 1967). The drift plain was formed by glaciation that possessed a margin which retreated in an orderly manner and which occasionally halted or readvanced. Drainage in the plain is integrated only along the edges of the large melt water channels. Numerous shallow, marshy depressions are present between these former channels. Relative to the Coteau, however, the Drift Plain has fewer potholes and because of its low relief has been subjected to numerous wetland drainage projects. This difference in wetland occurrence warranted a stratification of the statistical results in this investigation.

The areal extent of the multispectral scanner data utilized in this study is shown in Figure 6. Generally data which were common to three observations (two by LANDSAT and one by SKYLAB/EREP) are presented in this report. For the EREP S-192 observation, the spacecraft's ground track passed within 34 km (21 statute miles) of Woodworth Station on a heading approximately 109°. Because of the relatively narrow lateral field-of-view of the EREP multispectral scanner and the short data-take period, Woodworth Station was on the extreme margin of the scanner's coverage and scanner coverage only minimally included areas lying within the Coteau physiographic division which lay generally to the west and southwest of Woodworth Station. It is unfortunate that many of the sampling transects flown by the supporting aircraft were also outside the area actually observed by the EREP S-192 scanner. The short along-track duration of the S-192 observation, however, was necessitated by the limited supply of magnetic recording tape carried aboard the spacecraft.

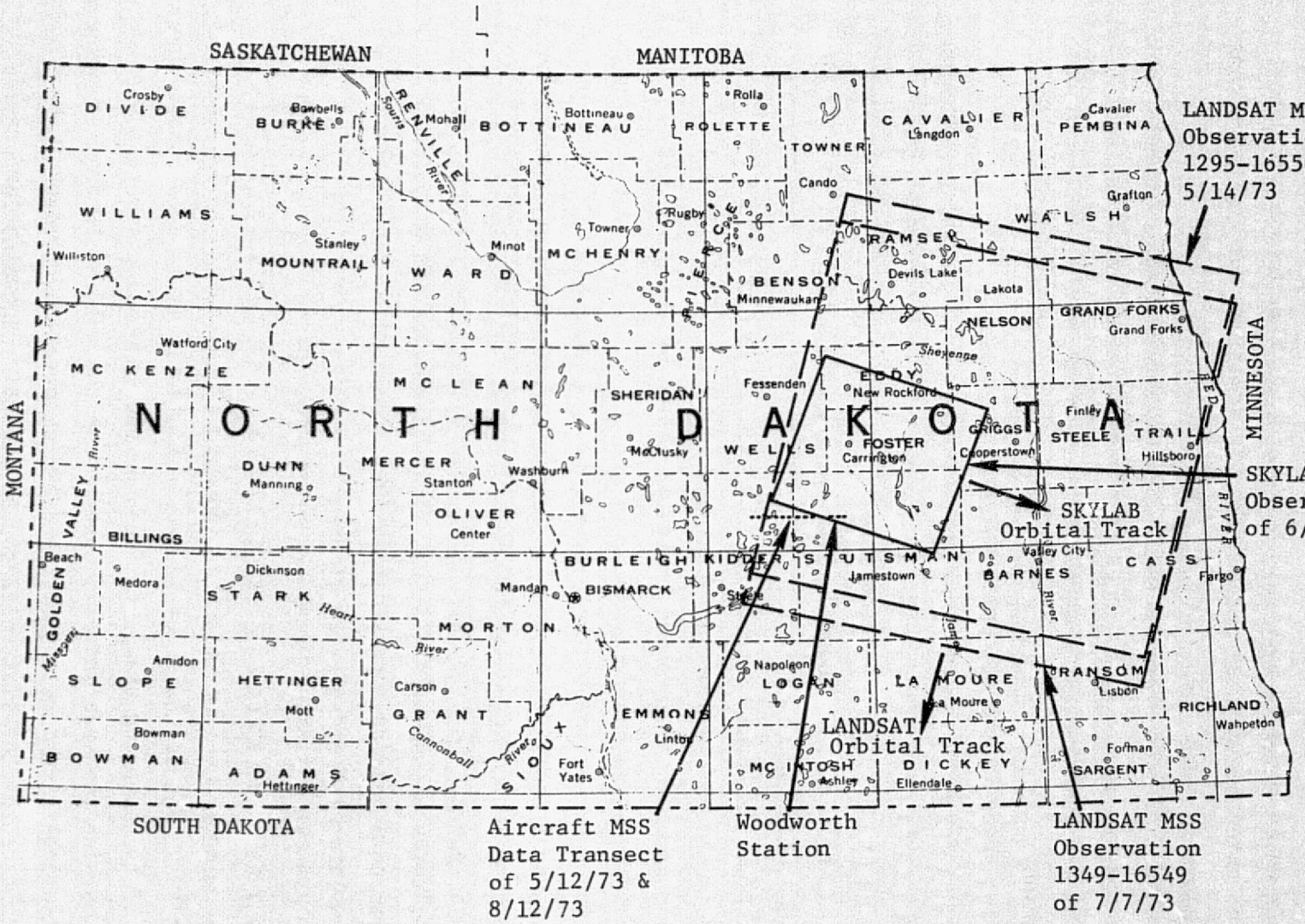

FIGURE 6. GEOGRAPHIC LOCATION OF SATELLITE AND AIRCRAFT OBSERVATIONS. The larger lakes and major streamcourses within the state of North Dakota are indicated.

5

DETECTION OF SURFACE WATER FEATURES USING A SINGLE WAVEBAND OF NEAR-INFRARED DATA

Level thresholding of a radiation signal in a single near-infrared waveband is a reliable and simple technique for delineating surface water. This technique is effective because at near-infrared wavelengths the apparent radiation of water is usually uniform and lower than for other terrain objects. Thus using an appropriate near-infrared waveband, water may be delineated by accepting scene points with low radiance values (classified as water) while rejecting all values above a certain threshold (non-water).

In this text, we have termed this form of surface water detection "thresholding". To appreciate the effectiveness of thresholding, it is helpful to have an understanding of the interaction of incident radiation* with water.

Spectral Radiance of Water

The apparent radiance of a body of water is the result of: (1) reflections at the air-water interface, (2) reflections from particulate matter suspended in the water, and (3) reflections from the bottom. Because the fields-of-view of the LANDSAT and SKYLAB multispectral scanners have been limited to near vertical observations and because water surfaces reflect specularly, radiation reflected by water to the scanners must have emanated from a sky position near the zenith. Given the northerly latitudes which characterize the glaciated prairies, satellite scanners viewing only near nadir generally do not view water-reflected direct solar radiation (i.e. the ground specular point is a considerable distance outside the field-of-view of the scanner). This leaves only that fraction of diffuse skylight which emanates from a near-zenith sky location to impinge upon the water surface and thence

*This discussion excludes consideration of thermal or self-emitted infrared radiation and is therefore limited to radiation in the visible and near-infrared at wavelengths somewhat less than 4 μm.

to be reflected to the scanner. In relative magnitude; however, diffuse skylight is much weaker than direct solar radiation, especially in the near-infrared and under clear sky conditions when optimal satellite observations are possible. McDowell (1974) illustrated the magnitude and spectral differences between diffuse skylight and direct solar radiation (Figure 7). In addition, the reflected skylight component is further diminished because water surfaces are a uniformly weak reflector of radiation which impinges at any but very oblique angles (Figure 8).

In considering reflections emanating from particulates within the water volume and from the bottom surface, water's absorptivity must be considered. In the near-infrared, that fraction of radiation which penetrates the air-water interface is largely absorbed, the extent of absorption being dependent upon the wavelength and the length of the water path. This situation is shown quantitatively in Figure 9 which illustrates the spectral transmission of pure water for a variety of path lengths. Consequently, a sensor viewing a water body in a near-infrared band receives little or no radiation that may have been reflected by the bottom or volume suspended particulates.

In an earlier study utlilzing aircraft data, Work and Thomson (1974) evaluated the relative merits of various near infrared bands for mapping surface water. They compared bands in the 0.73- to 0.92-μm, 1.0- to 1.4-μm, and 1.5- to 1.8-μm ranges and concluded that all produced reasonably good results. Given a choice, however, the longer wavelength bands did provide some marginal improvement. Longer wavelength alone should not predicate the choice of a water mapping waveband however. For example, the use of a waveband in the 2.0- to 2.6-μm atmospheric window is not optimal because of the decreasing amount of solar radiation at these wavelengths. It must be remembered that most terrestrial objects are relatively strong diffuse reflectors and that with adequate solar illumination such targets will contrast sharply with surface water features which consistently are darker. Work and Thomson (1974) concluded that an ideal waveband for delineating surface water lay within the 1.5- to 1.8-μm atmospheric window.

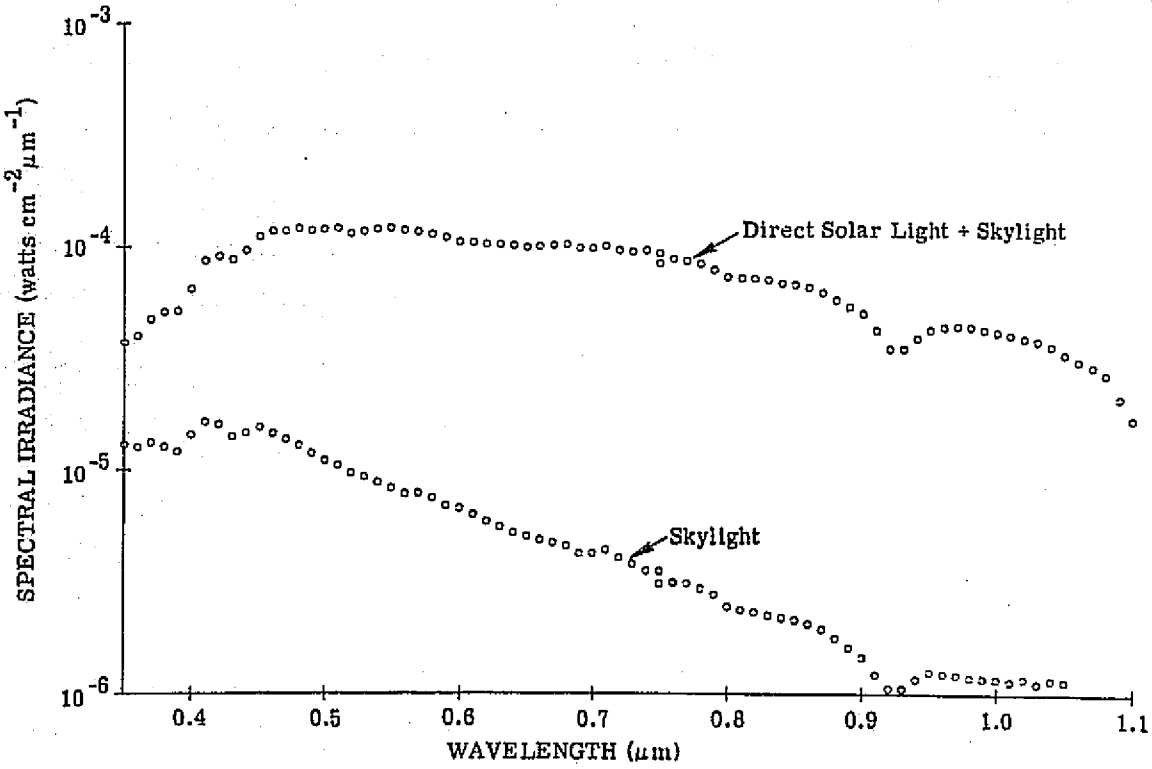

FIGURE 7. SCENE IRRADIANCE COMPONENTS FOR A CLEAR DAY. (After McDowell, 1974.) Spectral irradiance levels attributable to skylight alone may be significantly different and variable with wavelength due to variations in atmospheric haze. The conditions shown were recorded on an exceptionally clear day in New Mexico on 30 October 1970 at a sun elevation angle of 43°.

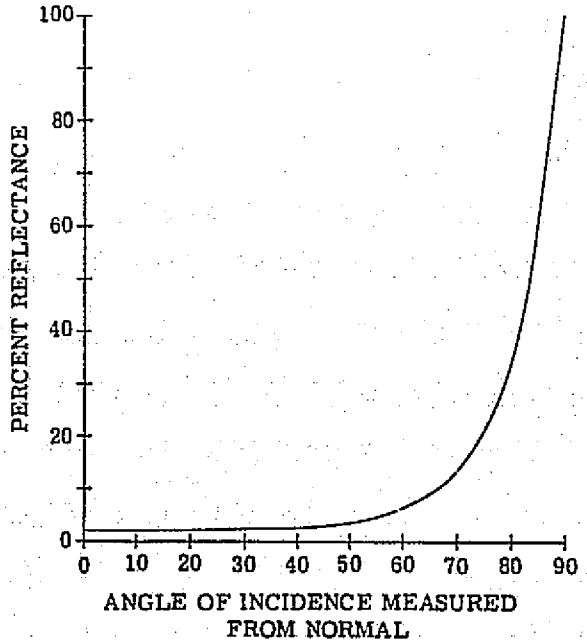

FIGURE 8. VARIATION OF REFLECTING POWER OF THE AIR-WATER INTERFACE AS A FUNCTION OF THE ANGLE OF INCIDENCE (Natural or unpolarized light of wavelength 0.589 μm).

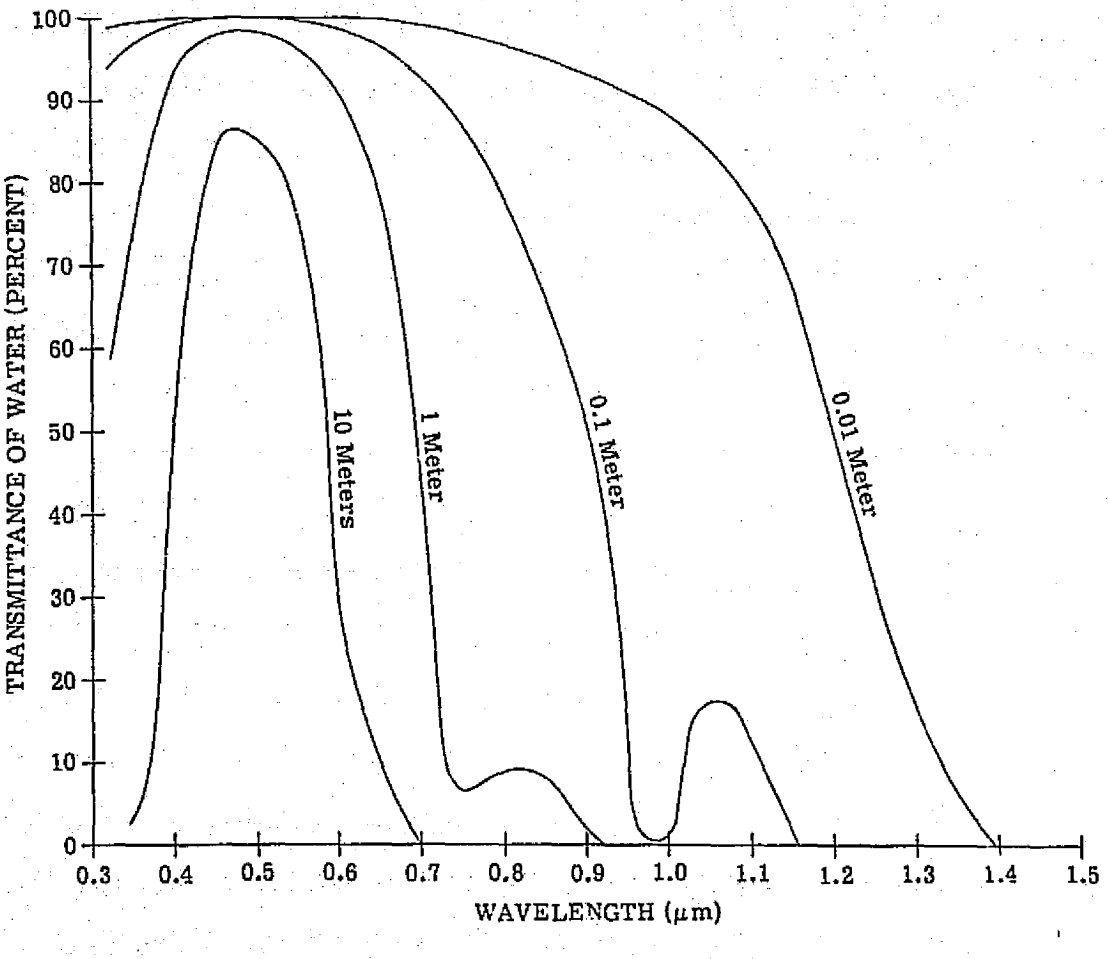

FIGURE 9. SPECTRAL TRANSMITTANCE OF PURE WATER FOR DIFFERENT PATH LENGTHS. (Plotted after data from Sverdrup et al., 1942.)

A graphic illustration of the relative utility of different near-infrared bands for detecting water may be seen in Figure 10. Illustrated is imagery acquired by an airborne multispectral scanner flown in support of this study. For the three infrared bands illustrated (0.67- to 0.94-μm, and 1.0- to 1.4-μm), standing water is rendered as a dark feature in the imagery due to the low level of radiant energy emanating therefrom. These wavebands are generally comparable to the SKYLAB multispectral scanner bands 7, 10, and 11 respectively (0.78- to 0.89-μm, 1.20- to 1.30-μm, and 1.55 to 1.75-μm).

The 0.67- to 0.94-μm imagery of Figure 10 illustrates an anomalous condition for at least one pond. The pond labeled "a" contained several light-toned, pincer-shaped features which occurred within the pond perimeter but which did not appear in the imagery at wavelengths greater than 1.0 mm. These features were due to a floating algal mat and possibly to plant submergents (water-milfoil, Myriophyllum exalbescens, and bladderwort, Utricularia vulgaris) which may have been exposed by low water levels. In the 0.67- to 0.94-μm band, this vegetation was a moderately strong reflector of incident radiation, and consequently a light-toned rendition occurred in the imagery thus masking the underlying water.

In general, the radiance of vegetation is largely affected by the critical reflection of incident light from cell walls within a leaf (Gates, et al., 1965, Gausman, 1974). Although radiation may be reflected several times before leaving the leaf, most of the radiation will be returned if there is little absorption by leaf tissues. This would seem to be true for the floating vegetation in the 0.67- to 0.96-μm waveband of Figure 10. However, beyond 1.0 μm, water's increasing near infrared absorptance (per Figure 9) appears to influence the radiance of plant materials. In the 1.0- to 1.4-μm imagery of Figure 10, the floating vegetation was no longer discernable from its water background due, possibly, to the high moisture content of aquatic plant tissues. In addition, the fact that the algal mat may have been floating several millimeters below the pond surface would also have precluded a strong return of radiation.

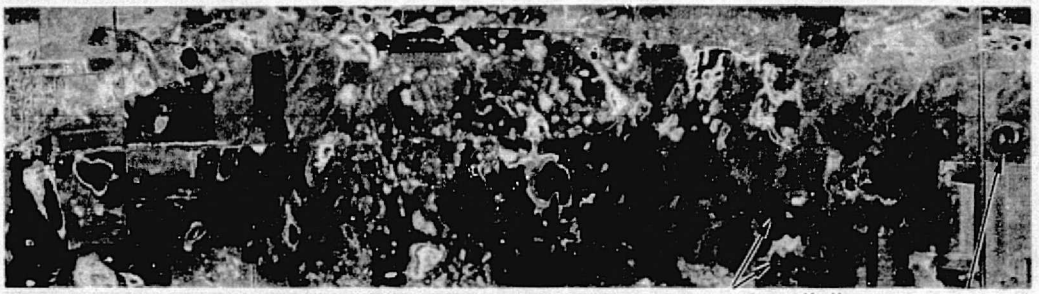

Bare Soil "a"-Floating Vegetation

Video Reproduction of 0.67-0.94μm Scanner Data

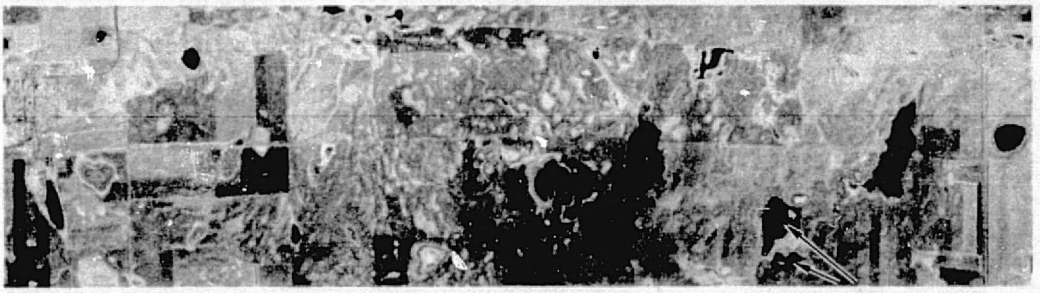

Bare Soil

Video Reproduction of 1.0-1.4μm Scanner Data

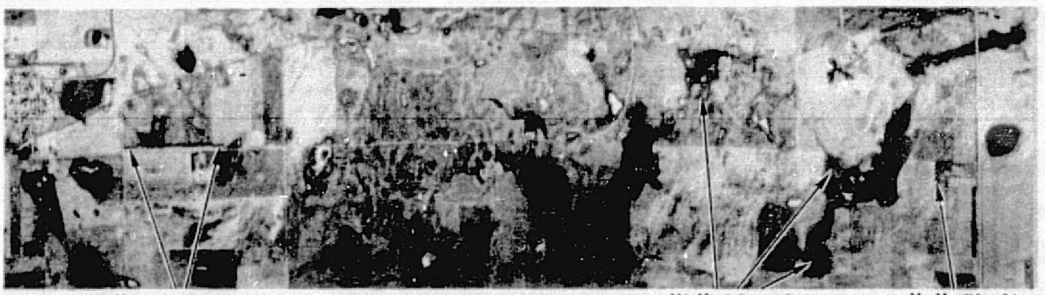

"c"-Shelterbelt "b"-Marsh "c"-Shelterbelt

Video Reproduction of 1.5-1.8μm Scanner Data

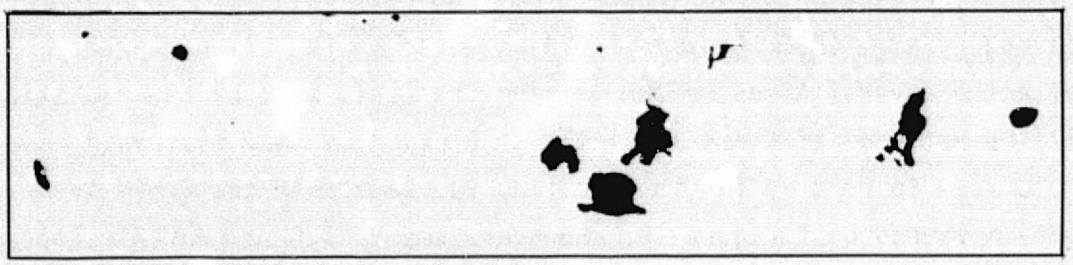

Water Recognition Map Produced By Thresholding 1.5-1.8μm Data

FIGURE 10. COMPARISON OF SEVERAL NEAR-INFRARED WAVEBANDS FOR RENDERING STANDING WATER AND OTHER MOISTURE RELATED CONDITIONS. The floating vegetation at location "a" partly obscured the standing water in the 0.67-0.94μm data only. The marshes at locations "b" and the shelterbelt trees at locations "c" had foliar vegetation containing liquid water. Many of the upland herbaceous plants were highly desiccated. These hygric to xeric conditions are discernible by tonal differences in the 1.5-1.8μm data. The above data were collected by an airborne multispectral scanner operated at an altitude of 4500ft. above the Woodworth Station on 12 August 1973, 1633 GMT.

Liquid water within a leaf is largely the cause of moderate absorption beyond 1.4 μm and according to Gates, et al. (1965) very strong absorption beyond 2.0 μm. Other investigators including Olson (1969), Rohde and Olson (1970), Myers, et al. (1970), and Gausman (1974) have demonstrated the influence of leaf water in suppressing reflectivity beyond 1.5 μm. This situation is illustrated at locations "b" and "c" in the 1.5- to 1.8-μm imagery of Figure 10. At locations labeled "b", marsh vegetation consisting predominantly of bulrushes (Scirpus spp.) and cattails (Typha spp.) was present. Deciduous trees comprised the shelterbelts at locations labeled "c". Both of these communities had received some moisture during the usually dry summer, either because they were deep rooted (i.e., the trees) or because they were rooted in standing water (i.e., the marsh vegetation). Gross differences in moisture conditions did exist in the scene. Specifically, an extremely desiccated condition is exhibited by much of the dry herbaceous upland vegetation, most of which was dead. Reflections from these materials were high, and they contrast sharply with the marsh and shelterbelt communities in the 1.5- to 1.8-μm imagery.

The water recognition map included in Figure 10 was generated by thresholding 1.5- to 1.8-μm data. The recognition map illustrates that in spite of the apparent low radiance of water, marsh, and shelterbelt features, standing water was unique for its low radiometric signature. Had water been mapped by thresholding the 0.67- to 0.94-μm band or any of the SKYLAB multispectral scanner bands between 0.7 and 1.0μm, the pond at "a" and other similarly occluded or shallow water features would at best have been only partially recognized.

Methods

Implementation of the thresholding technique was accomplished by observing radiance values for known water features within a scene and comparing these values with those of other terrain features also known to exhibit relatively low radiance characteristics. A decision boundary or threshold was then selected which effectively separated surface water from all other scene objects on the basis of their relative brightnesses

(i.e., differences in apparent radiance). Experience has shown that various scene objects exhibit radiances that may or may not be close to the low radiance of water depending on (1) the specific near-infrared band under consideration, (2) the geographic locale, and (3) the phenologic state of some scene objects.

In eastern North Dakota, dark prairie soils, Mollisols (formerly referred to as Chernozems), have consistently approached the low radiance values of water in near-infrared wavebands of less than 1.4 μm. In the 1.5- to 1.8-μm atmospheric window, vigorous green vegetation most nearly approach water's low apparent radiance (these water, soil, and green vegetation radiance characteristics were previously illustrated in Figure 10). For our North Dakota study site, the practice was to threshold or differentiate between water and either bare soil or vigorous green vegetation depending upon the particular near-infrared waveband utilized.

The SKYLAB multispectral scanner had five wavebands in the wavelength range 0.78 to 1.75 μm, any of which were potentially useful for discriminating open surface water using the thresholding technique. Thus the SKYLAB data offered a further opportunity to appraise the relative usefulness of several near-infrared wavebands. Such an evaluation was conducted, the results of which are presented in Figures 11 through 14. In the waveband considered in Figures 11 through 13 (0.78- to 0.88-μm, 0.98- to 1.08-μm, and 1.20- to 1.30-μm respectively), bare soil was the terrain feature most likely to be mistaken for open surface water. Each histogram represents a sample size of about 350 pixels drawn from throughout the observation scene. The overlap of water and bare soil histogram tails generally decreases with increasing wavelength. In the 1.55- to 1.75-μm waveband (Figure 14), the terrain material most likely to be mistaken for open water was vigorous green vegetation; but there was no overlap of histograms in this waveband. Our conclusion, reaffirmed by these data, was that the 1.55- to 1.75-μm channel was the least ambiguous for water discrimination. For this waveband a threshold boundary of 10 volts and less was selected for the delineation of open surface water. In affixing units to this threshold value, no inference

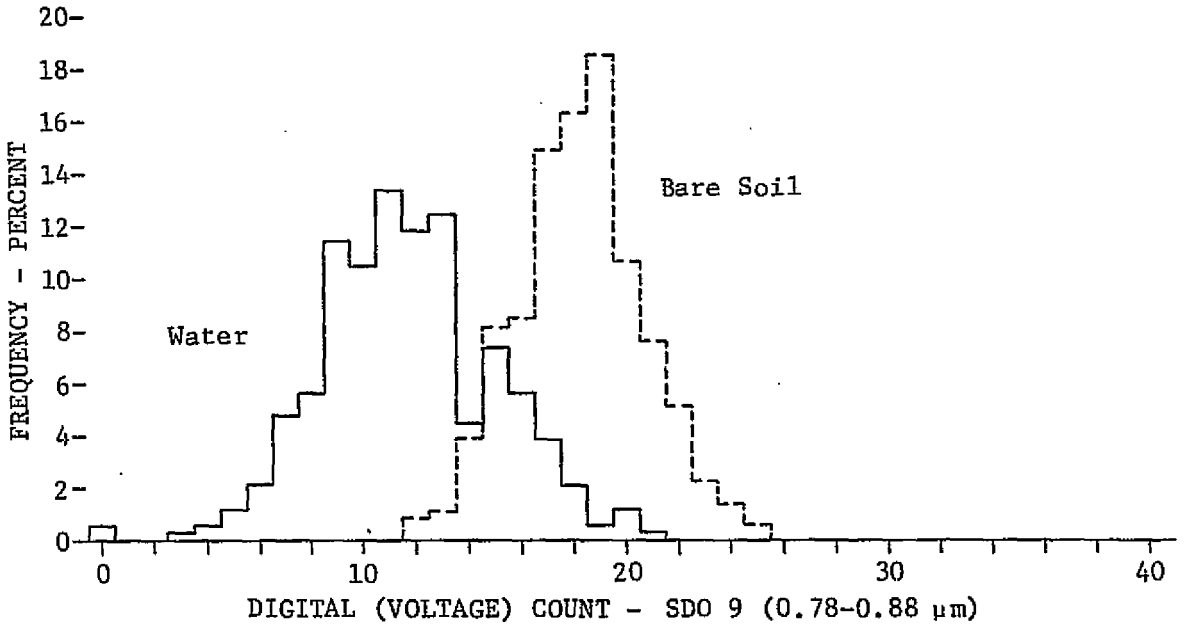

FIGURE 11. HISTOGRAMS OF REFLECTANCE VALUES IN THE 0.78- to 0.88-μm WAVEBAND. The distributions each represent approximately 350 pixels sampled from throughout a SKYLAB multispectral scanner observation made 12 June 1973 over eastern North Dakota.

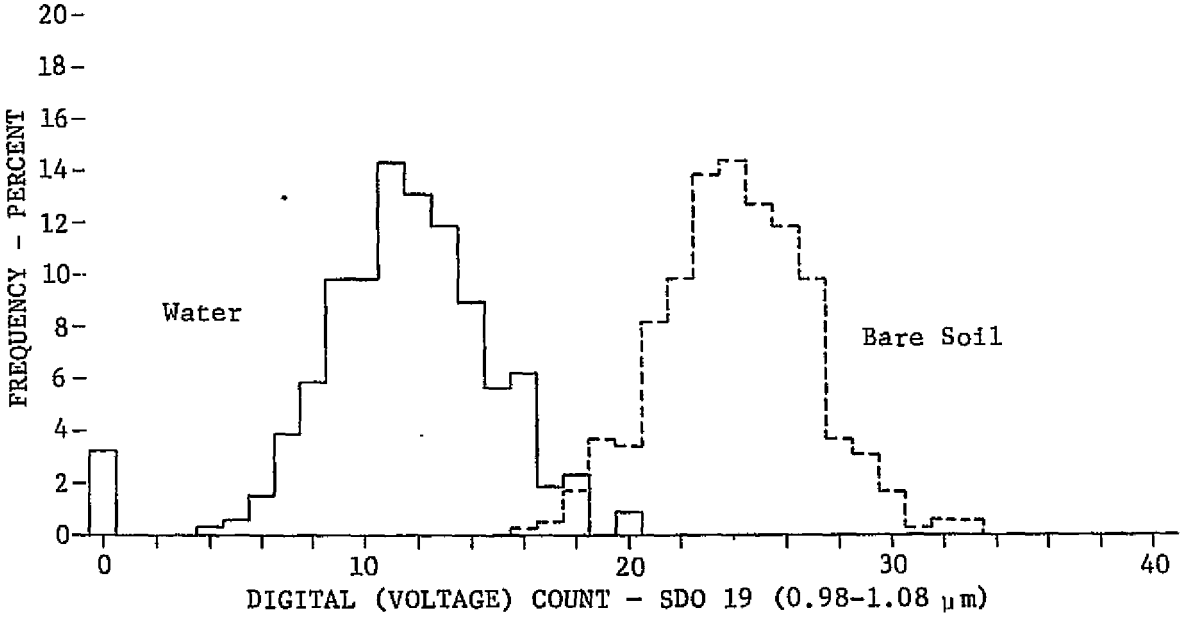

FIGURE 12. HISTOGRAMS OF REFLECTANCE VALUES IN THE 0.98- to 1.08-μm WAVEBAND. The distributions each represent approximately 350 pixels sampled from throughout a SKYLAB multispectral scanner observation made 12 June 1973 over eastern North Dakota.

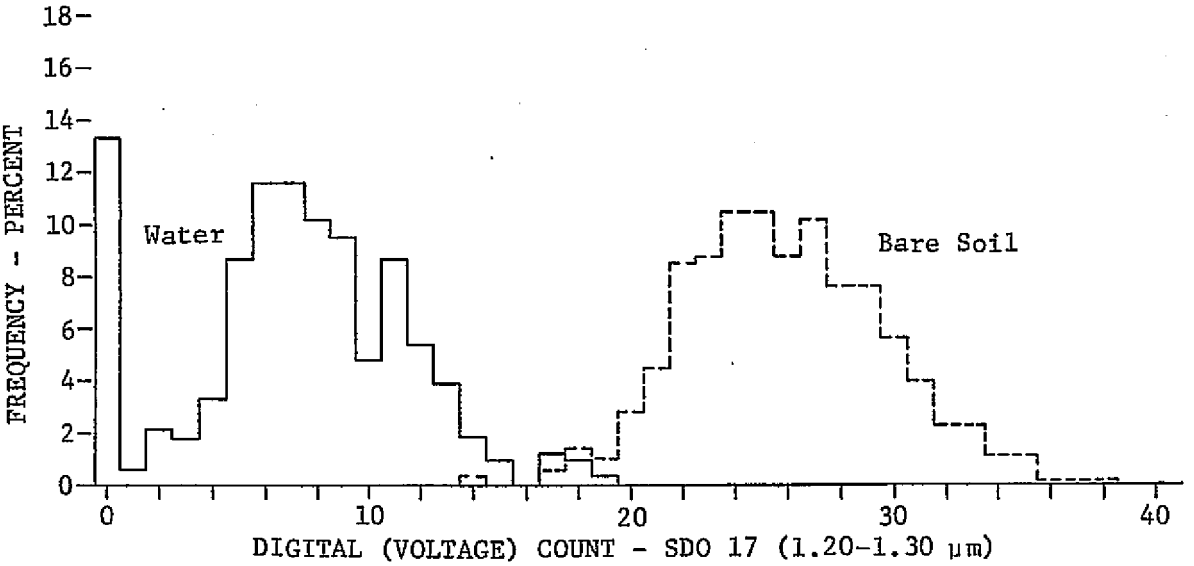

FIGURE 13. HISTOGRAMS OF REFLECTANCE VALUES IN THE 1.20- to 1.30-µm WAVEBAND. The distributions each represent approximately 350 pixels sampled from throughout a Skylab multispectral scanner observation made 12 June 1973 over eastern North Dakota.

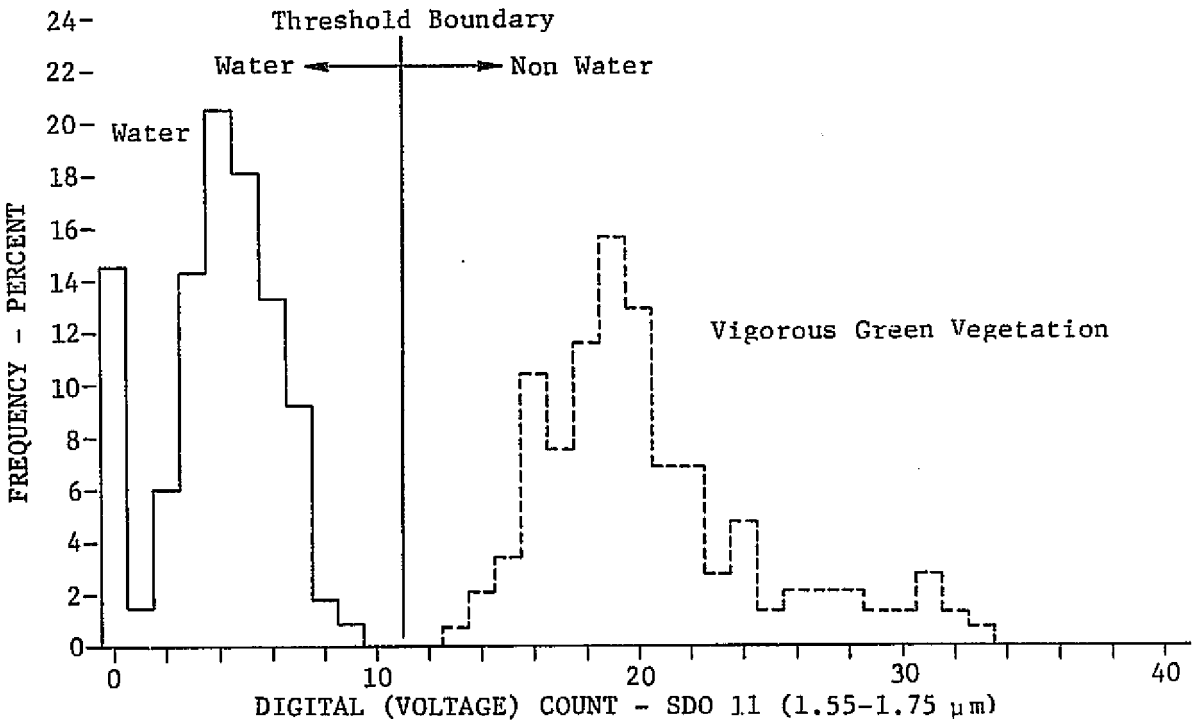

FIGURE 14. HISTOGRAMS OF REFLECTANCE VALUES IN THE 1.55- to 1.75-µm WAVEBAND. The distributions each represent approximately 350 pixels sampled from throughout a Skylab multispectral scanner observation made 12 June 1973 over eastern North Dakota.

of radiance values was intended. Indeed, we have only been concerned with relative differences of radiance between target types and consequently have made no attempt, using available calibration data, to relate the digital (voltage) count recorded on the data tapes to absolute radiance levels.

In this investigation, the selection of an appropriate threshold boundary was manually accomplished, based upon a visual examination of a computer generated statistical analysis (i.e., histograms or frequency distributions). Given the limited amount of data to be analyzed and the clear separability between terrain classes (i.e., open surface water versus vigorous green vegetation), this manual interaction in the recognition process has been satifactory. The procedure could have been automated, however, and the computer could have been used to perform a one channel linear recognition between two object classes in a manner similar to maximum likelihood classification recognition (or pattern recognition). Such an approach should be appropriate when it is necessary to handle large amounts of data which represent a variety of scene and illumination conditions.

Results of Single Channel Water Recognition

A computer-generated thematic map identifying open surface water over a 3621 km^2 (1397 mi^2) area as observed by the SKYLAB/EREP scanner was produced by thresholding a 1.55- to 1.75-μm waveband (Figure 15). The tract shown partially overlapped both the Missouri Coteau (25%) and the Drift Plain (75%) strata. It is evident from this map that the Coteau (lower left) had a considerably higher density of ponds and lakes. The larger lakes in the Drift Plain were frequently the result of major impoundments on the James River watercourse (Jamestown Reservoir, Jim Lake, Mud Lake, Arrowwood Lake, and Juanita Lake).

The SKYLAB/EREP observation of 12 June 1973 was interleaved between two LANDSAT observations which occurred on 14 May 1973 and 7 July 1973. Thematic water maps resulting from those LANDSAT observations are shown in Figures 16 and 17 respectively. Only the upper 40 percent of each of the LANDSAT maps is common to the area mapped by SKYLAB. Note, too,

FIGURE 15.
COMPUTER GENERATED
SURFACE WATER MAP FROM
A SKYLAB MULTISPECTRAL
SCANNER OBSERVATION OF
12 JUNE 1973

Jamestown, North Dakota lies immediately south of the reservoir shown in the lower right corner.

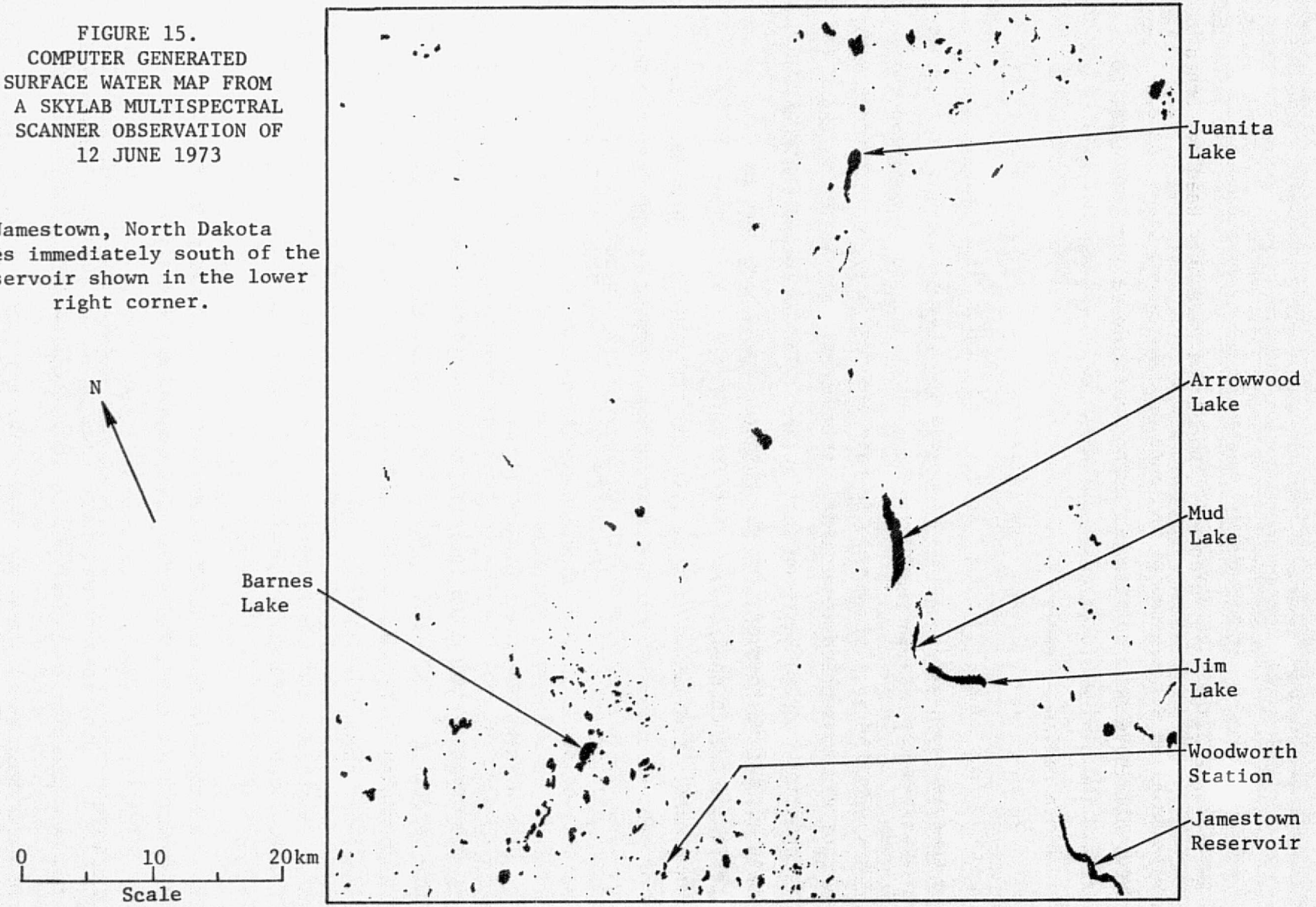

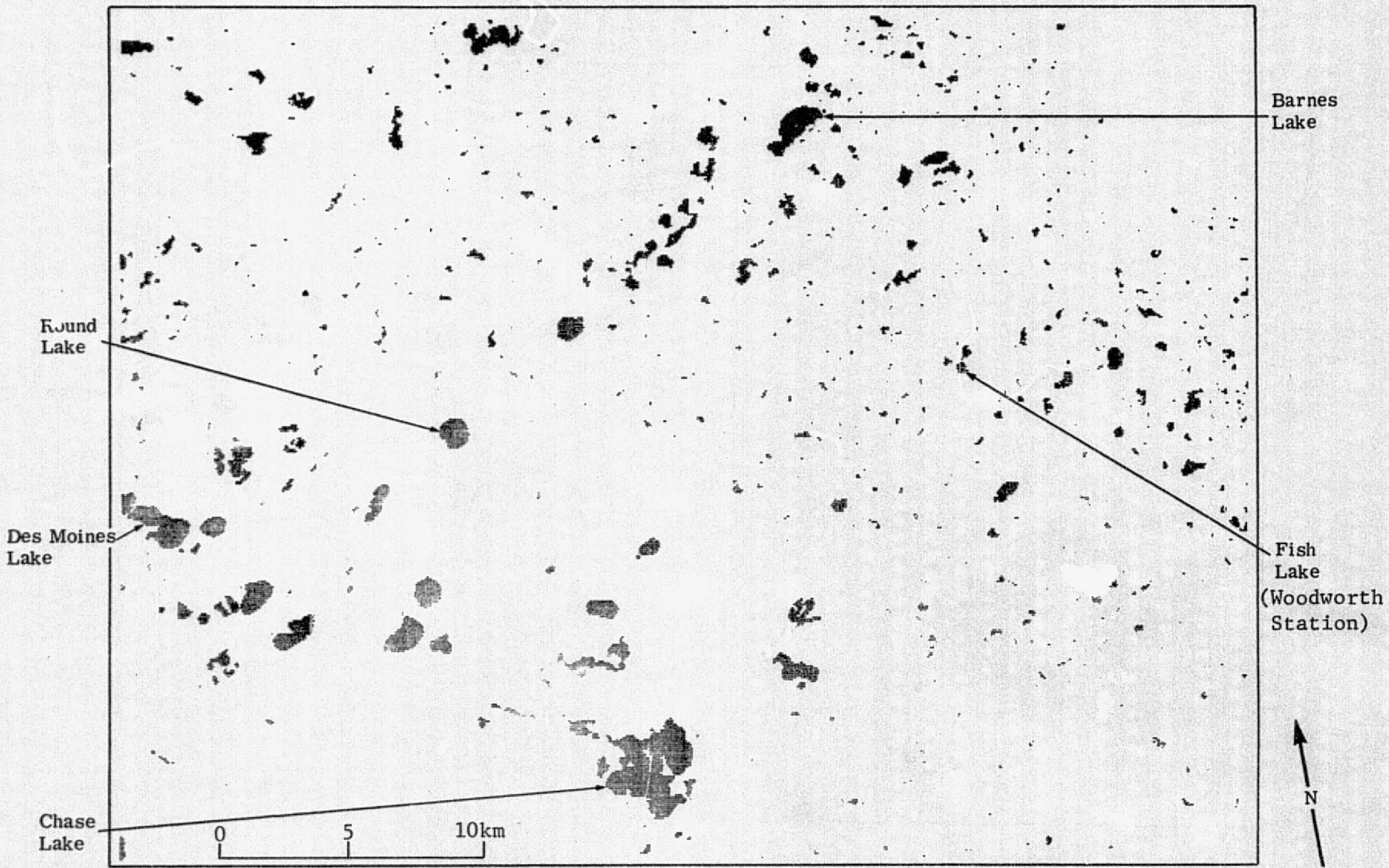

FIGURE 16. DIGITAL WATER RECOGNITION MAP FROM ERTS OBSERVATION 1295-16550 OF 14 MAY 1973. The map, obtained by thresholding channel MSS-7, encompasses approximately 1520 sq. km.

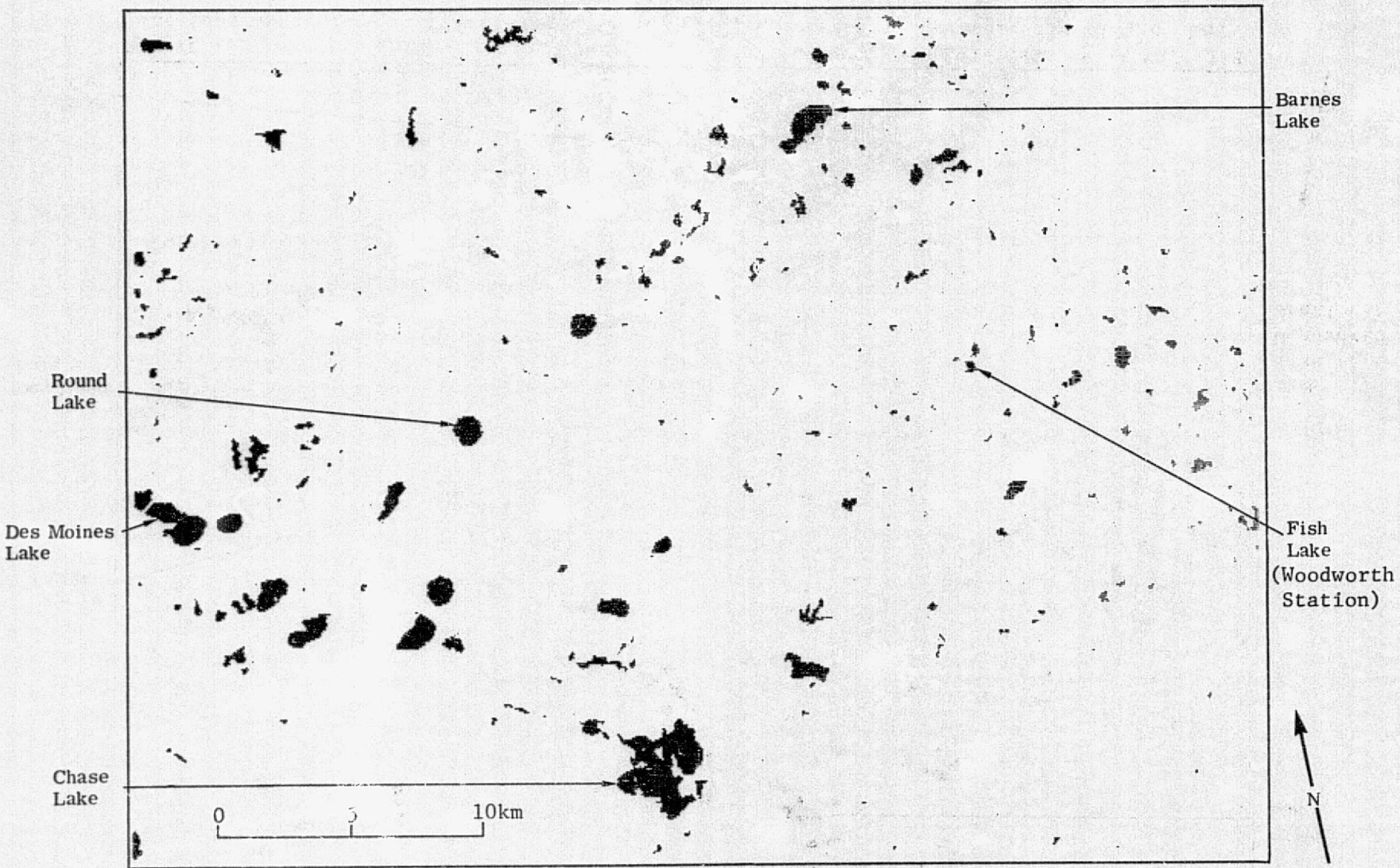

FIGURE 17. DIGITAL WATER RECOGNITION MAP FROM ERTS OBSERVATION 1349-16543 OF 7 JULY 1973. The map, obtained by thresholding channel MSS-7, encompasses approximately 1520 sq. km.

that the maps scales differ. The LANDSAT maps were initally generated at a scale of 1/24,000 using a general purpose, digital printer writing 132 pixel columns per each 15-inch wide paper strip. The LANDSAT maps illustrated each consisted of six printed strips which were manually abutted and subsequently photo-reduced to a convenient size. The SKYLAB map was initally generated at a scale of 1/155,000 using a computer controlled, ink-jet printer. This format was of a more convenient size and was considerably easier to reproduce. Thus the ink-jet map represented a significant reduction in production time and labor.

The three sequential observations represented by Figures 15, 16, and 17 spanned a time period of low precipitation and progressive desiccation. The diminishing of prairie ponds and lakes is normally to be expected during a May to July period. Visually, however, it is difficult to discern from the maps what the changes in surface water conditions were, and without extensive manual interpretation it is impossible to quantify these changes. For purposes of analysis, therefore, the data are more conveniently assessed if they are assembled in statistical form by automatic data processing techniques. Figure 18 illustrates such a statistical tabulation as generated from tape recorded data gathered by the SKYLAB scanner over the Coteau physiographic stratum. The upper tabulation (only partially illustrated) is an enumeration of all recognized surface water features while the lower tabulation summarizes the frequency of pond occurrence by size. For the biologist concerned with the management of waterfowl populations this summary provides a ready assessment of habitat conditions over wide (synoptic) areas. The SKYLAB map and the related statistics have been generated from tape recorded data which was made available to us in a scan-line straightened format. Existing software and printers were capable of handling data in only this format.

The statistical tabulations were produced by a software program designed specifically for use with satellite data. The program was adapted from a pre-existing program which was used with wide field-of-view, low altitude (aircraft) scanner data. These programs function by the use of a threshold decision criterion for classifying a grouping

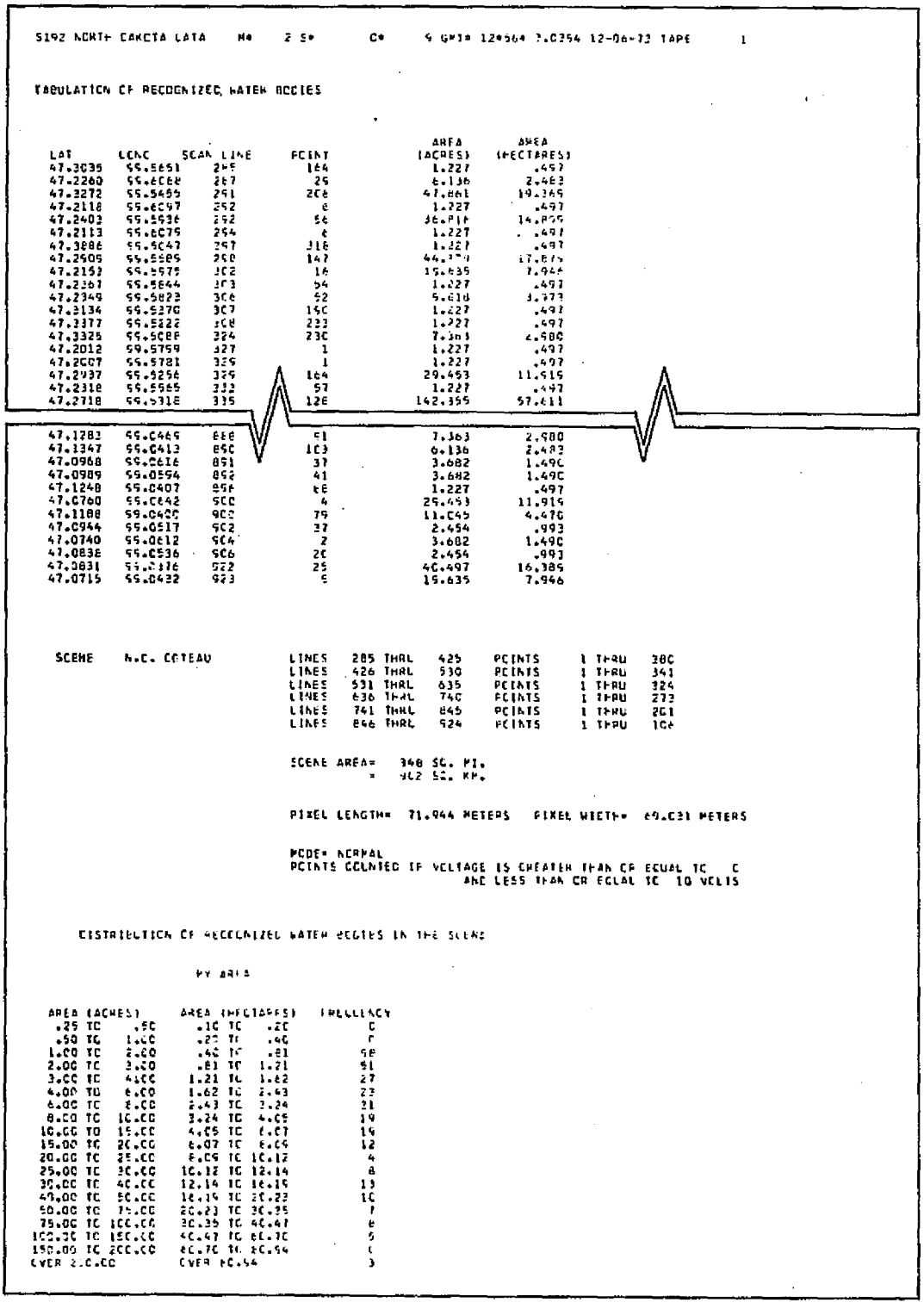

```
S192 NORTH DAKOTA DATA    M0    2 S0       C0     9 GM1# 12#564 2.0254 12-06-72 TAPE      1

TABULATION OF RECOGNIZED WATER BODIES

                                                          AREA        AREA
  LAT       LONG     SCAN LINE      POINT                (ACRES)   (HECTARES)
 47.3035   99.5851      285          164                   1.227        .497
 47.2260   99.6088      287           25                   6.136       2.483
 47.3272   99.5459      291          268                  47.886      19.379
 47.2118   99.6097      292            8                   1.227        .497
 47.2403   99.5936      292           56                  36.818      14.899
 47.2113   99.6079      294            6                   1.227        .497
 47.3886   99.5047      297          316                   1.227        .497
 47.2505   99.5885      298          147                  44.1[illegible]  17.875
 47.2152   99.5975      302           16                  19.635       7.946
 47.2367   99.5844      303           94                   1.227        .497
 47.2349   99.5823      306           42                   9.818       3.973
 47.3134   99.5370      307          150                   1.227        .497
 47.3377   99.5222      308          223                   1.227        .497
 47.3325   99.5088      324          230                   7.363       2.980
 47.2012   99.5759      327            1                   1.227        .497
 47.2007   99.5781      329            1                   1.227        .497
 47.2937   99.5256      329          164                  29.453      11.919
 47.2318   99.5565      332           57                   1.227        .497
 47.2718   99.5318      335          128                 142.355      57.611

 47.1283   99.0469      888           91                   7.363       2.980
 47.1347   99.0413      890          103                   6.136       2.483
 47.0968   99.0616      891           37                   3.682       1.490
 47.0989   99.0594      892           41                   3.682       1.490
 47.1248   99.0407      896           66                   1.227        .497
 47.0760   99.0642      900            4                  25.453      11.919
 47.1108   99.0409      902           79                  11.045       4.470
 47.0944   99.0517      902           37                   2.454        .993
 47.0740   99.0612      904            2                   3.682       1.490
 47.0838   99.0536      906           20                   2.454        .993
 47.0831   99.0336      922           25                  40.497      16.389
 47.0715   99.0432      923            9                  19.635       7.946


 SCENE    N.D. COTEAU          LINES   285 THRU   425    POINTS     1 THRU   380
                               LINES   426 THRU   530    POINTS     1 THRU   341
                               LINES   531 THRU   635    POINTS     1 THRU   324
                               LINES   636 THRU   740    POINTS     1 THRU   273
                               LINES   741 THRU   845    POINTS     1 THRU   261
                               LINES   846 THRU   924    POINTS     1 THRU   164

                               SCENE AREA=   348 SQ. MI.
                                         =   902 SQ. KM.

                               PIXEL LENGTH=  71.944 METERS   PIXEL WIDTH=  69.031 METERS

                               MODE= NORMAL
                               POINTS COUNTED IF VOLTAGE IS GREATER THAN OR EQUAL TO   0
                                                  AND LESS THAN OR EQUAL TO  10 VOLTS


    DISTRIBUTION OF RECOGNIZED WATER BODIES IN THE SCENE

                        BY AREA

  AREA (ACRES)        AREA (HECTARES)    FREQUENCY
   .25 TO    .50      .10 TO   .20          0
   .50 TO   1.00      .20 TO   .40          6
  1.00 TO   2.00      .40 TO   .81         98
  2.00 TO   3.00      .81 TO  1.21         91
  3.00 TO   4.00     1.21 TO  1.62         27
  4.00 TO   6.00     1.62 TO  2.43         23
  6.00 TO   8.00     2.43 TO  3.24         31
  8.00 TO  10.00     3.24 TO  4.05         19
 10.00 TO  15.00     4.05 TO  6.07         14
 15.00 TO  20.00     6.07 TO  8.09         12
 20.00 TO  25.00     8.09 TO 10.12          4
 25.00 TO  30.00    10.12 TO 12.14          8
 30.00 TO  40.00    12.14 TO 16.19         13
 40.00 TO  50.00    16.19 TO 20.23         10
 50.00 TO  75.00    20.23 TO 30.35          7
 75.00 TO 100.00    30.35 TO 40.47          6
100.00 TO 150.00    40.47 TO 60.70          5
150.00 TO 200.00    60.70 TO 80.94          0
OVER 200.00         OVER  80.94             3
```

FIGURE 18. EXAMPLE OF COMPUTER PRINTOUT OF POND AND LAKE STATISTICS FOR AN AREA WITHIN THE MISSOURI COTEAU PHYSIOGRAPHIC PROVINCE OF NORTH DAKOTA. The above statistics resulted from a SKYLAB multispectral scanner (S-192) observation of 12 June 1973.

of pixels as a water body and thereafter computing the area of each specific water feature. Perimeter and shape factor (a measure of shape complexity) calculations were also possible. Because of the small size of many of the ponds and the potential that the shorelines of larger ponds and lakes could vary widely in length at scales finer than the resolution limit of the data, perimeter and shape factor calculations were not performed. Appendix A of this report describes in detail the computer program used to generate these statictical data while Appendix B includes a complete tabulation of surface water statistics derived from the SKYLAB scanner observation of 12 June 1973.

In the statistical tabulations, we identified each pond and lake and defined its position with each of two coordinate systems based on a scan-line and point number scheme and a more conventional latitude and longitude system. The scan-line and point number information was inherently available from the digital tapes. Conversion to latitude and longitude coordinates was accomplished by a regression analysis which used several control points located within the scene. The convention used to reference each water body was to identify the body by the number of the last scan-line with at least one pixel in the water body and the point number of the greatest numbered water pixel of that scan-line.

Graphical summaries of pond frequency for the two observed strata are shown in Figure 19. These data were normalized so that comparisons between the different sized strata are possible. Note that the ordinate or density scales for the two strata are logarithmic and that the two density distributions differ between strata by approximately an order of magnitude in all size classes. A summary of seasonal change in pond numbers over several consecutive time intervals is illustrated in Figures 20 and 21. These changes were observed in the Coteau stratum by the use of a combination of LANDSAT and SKYLAB observations*. The

*A similar measure of surface water change for the Drift Plain is not available because the processed LANDSAT data did not represent a large enough sample in this stratum.

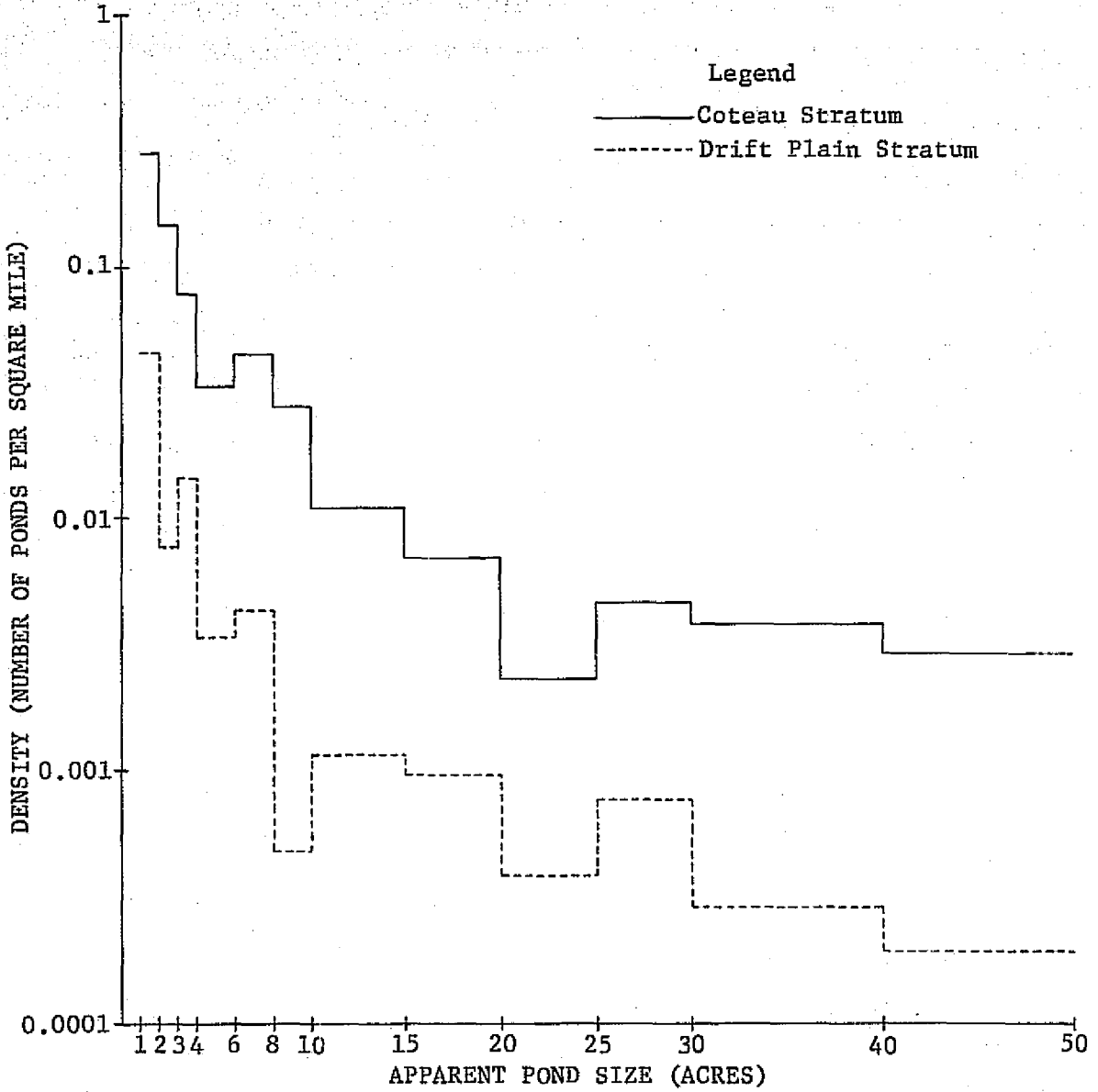

FIGURE 19. SUMMARY OF SIZE DISTRIBUTION OF PONDS IN THE COTEAU AND DRIFT PLAIN STRATA AS DETERMINED USING SKYLAB MULTISPECTRAL SCANNER DATA COLLECTED 12 JUNE 1973. Where the pond size increments are greater than one acre, the data have been averaged over the increment.

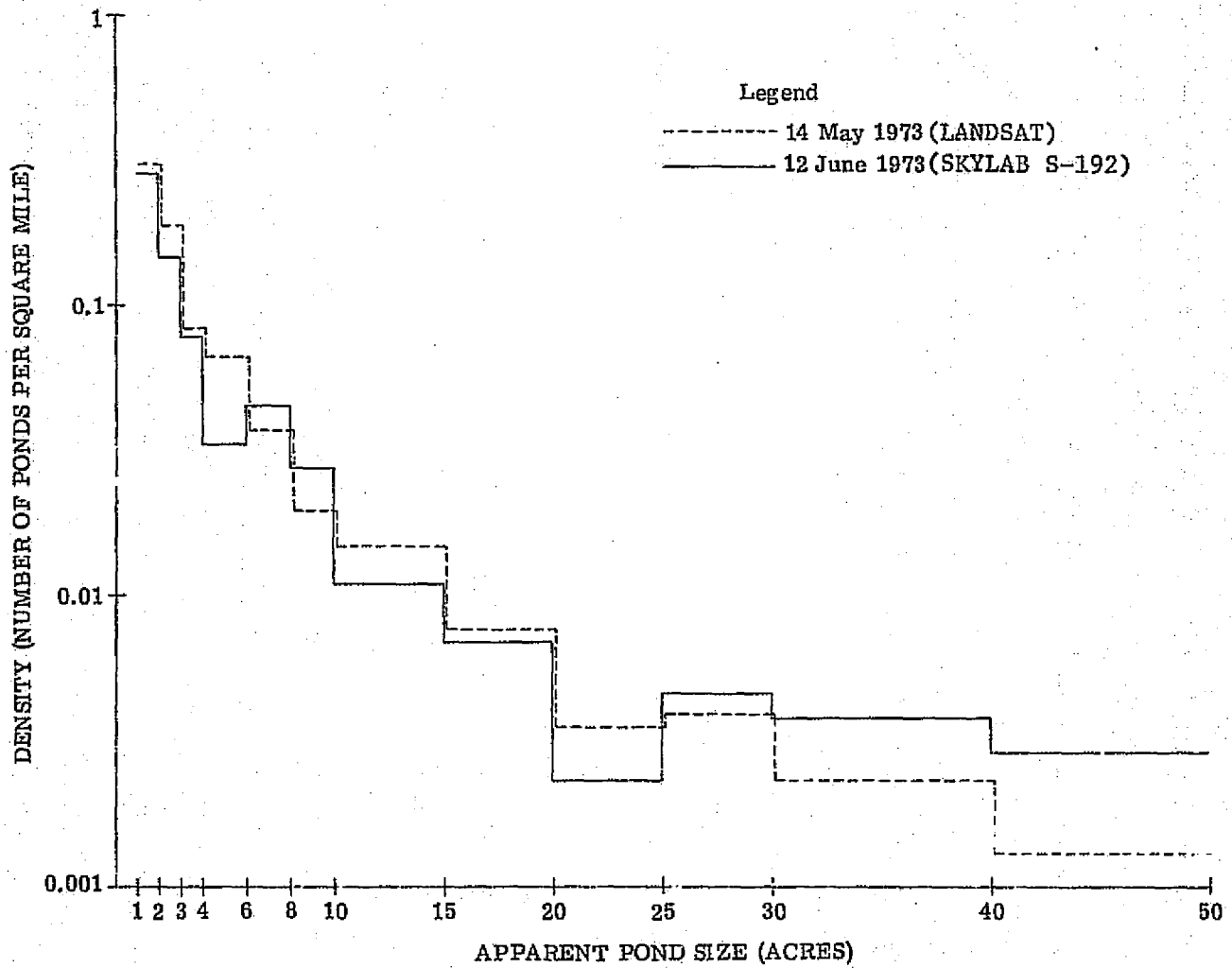

FIGURE 20. SUMMARY OF SIZE DISTRIBUTION OF PONDS IN THE COTEAU STRATUM FOR A 29-DAY MID SPRING INTERVAL. Where the pond size increments are greater than one-acre, the data have been averaged over the increment.

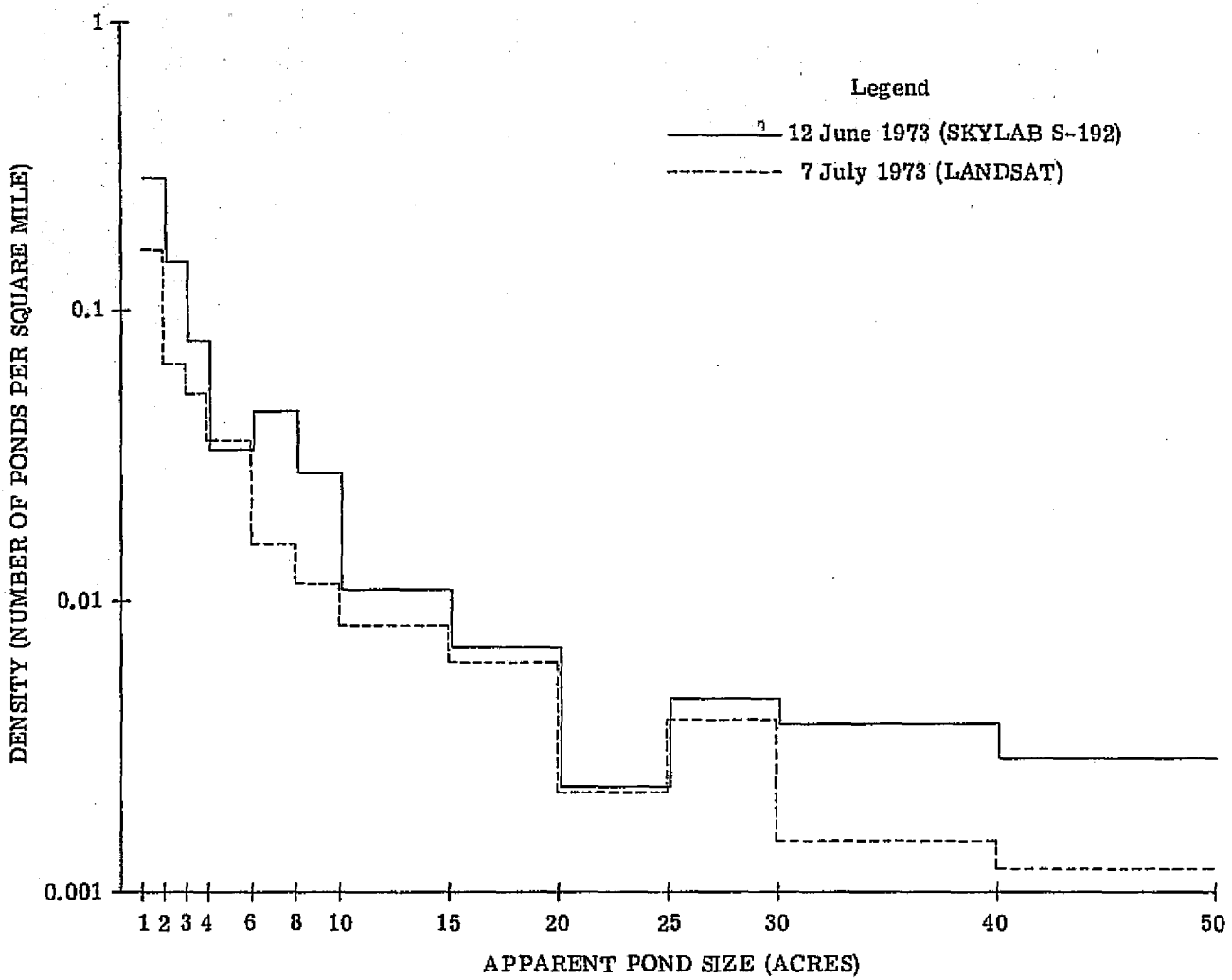

FIGURE 21. SUMMARY OF SIZE DISTRIBUTION OF PONDS IN THE COTEAU STRATUM FOR A 25-DAY LATE SPRING/SUMMER INTERVAL. Where the pond size increments are greater than one acre, the data have been averaged over the increment.

graphical data indicate a progressive drying trend for May thru June to July. However, the trend appeared to be protracted during the 14 May to 12 June interval after which ponds diminished in size and numbers at a more rapid rate. On a synoptic basis, at least, it appears that the two sensor systems (i.e., SKYLAB and LANDSAT) were consistent in that both data sets indicated a decline in both area and numbers of surface water features. It should be noted, however, that the data are for sampled areas which were not specifically the same for each of the three observations. As a result, the observed trends for the larger ponds and lakes were not always consistent because of the low sampling frequency.

The trends, as noted above, appeared to be manifested in both the SKYLAB and LANDSAT observations when each of the data sets was considered as a whole. One may then ask whether individual ponds and lakes as observed by both the SKYLAB and LANDSAT scanner systems also adhered to the group trend. To answer this question, 21 ponds and lakes ranging in size from 2 to over 190 hectares were randomly selected for comparison. Figure 22 is an enlargement of a section of the thematic water map shown previously in Figure 15. Indicated in Figure 22 are the names and locations of the 21 ponds and lakes studied. Table 3 is a listing of these water bodies along with their geographic coordinates as listed in the computer output stream. Note that the coordinates are consistent between data sets but that slight differences exist between the SKYLAB and LANDSAT observations. These discrepancies can be attributed to the fact that the computed coordinates from the SKYLAB data were for the northeastern corner of each water body while the LANDSAT data were for the southeastern corner. This difference is particularly apparent for the larger water bodies, for example, Barnes Lake.

Table 4 is a listing of water body size for the same 21 ponds and lakes. The LANDSAT data indicated a decline in pond size from May to July in all but two instances, Lawrence Lake and Fish Lake, which virtually remained constant. On the other hand, the SKYLAB pond and lake data which were collected intermediate between the LANDSAT

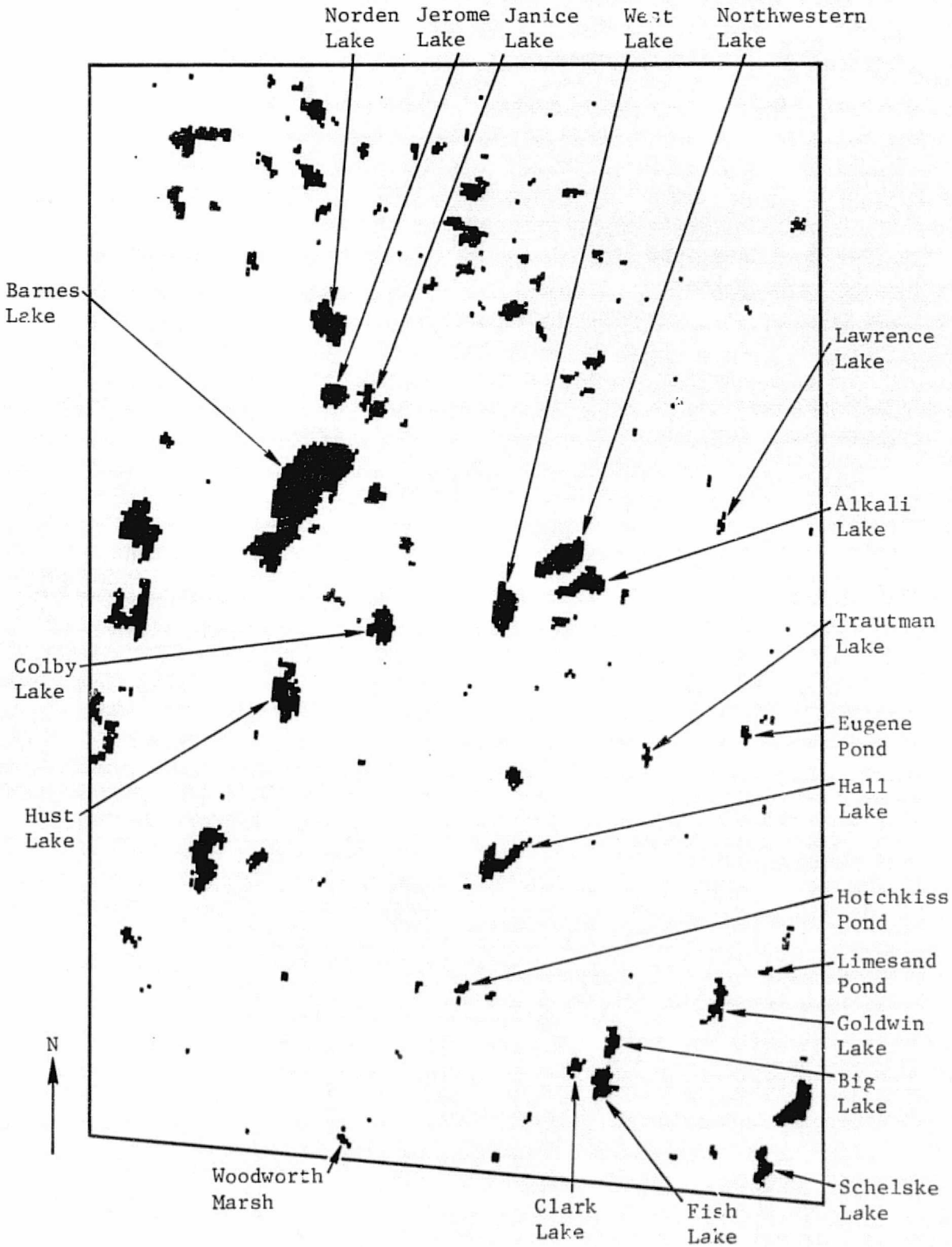

FIGURE 22. THEMATIC WATER MAP OF A TRACT LYING IN THE COTEAU PHYSIOGRAPHIC PROVINCE AND OBSERVED BY THE SKYLAB MULTISPECTRAL SCANNER ON 12 JUNE 1973. Approximate Scale: 1/62,500.

TABLE 3.
COMPARISON OF COMPUTED LATITUDE & LONGITUDE COORDINATES
PER LANDSAT & SKYLAB OBSERVATIONS

	Computed Latitude (Deg. N) Per Observation of:			Computed Longitude (Deg. W) Per Observation of:		
	LANDSAT 5/14/73	LANDSAT 7/7/73	SKYLAB 6/12/73	LANDSAT 5/14/73	LANDSAT 7/7/73	SKYLAB 6/12/7:
Barnes Lake	47.224	47.225	47.239	99.286	99.286	99.260
Norden Lake	47.255	47.255	47.260	99.258	99.258	99.255
Jerome Lake	47.246	47.246	47.248	99.261	99.261	99.259
Janice Lake	47.242	47.242	47.246	99.250	99.250	99.249
Colby Lake	47.208	47.208	47.211	99.262	99.263	99.260
Northwestern Lake	47.210	47.210	47.214	99.217	99.215	99.206
Alkali Lake	47.204	47.205	47.208	99.205	99.205	99.203
Trautman Lk.	47.177	47.178	47.179	99.200	99.200	99.201
Hall Lake	47.167	47.168	47.172	99.250	99.250	99.237
Hotchkiss Pond	47.151	47.151	47.153	99.263	99.264	99.262
Clark Lake	47.134	47.135	47.136	99.238	99.236	99.236
Fish Lake	47.130	47.130	47.130	99.234	99.231	99.229
Big Lake	47.135	47.136	47.138	99.229	99.227	99.226
Goldwin Lake	47.136	47.137	47.140	99.196	99.196	99.195
Limesand Pond	47.139	47.140	47.140	99.182	99.182	99.182
Schelske Lk.	47.108	47.111	47.111	99.196	99.195	99.194
Hust Lake	47.200	47.201	47.206	99.293	99.294	99.289
West Lake	47.203	47.204	47.209	99.232	99.231	99.297
Lawrence Lk.	47.208	47.208	47.212	99.168	99.169	99.168
Eugene Pond	47.175	47.176	47.177	99.174	99.174	99.174
Woodworth Marsh	47.134	47.135	47.135	99.300	99.300	99.302

TABLE 4.
COMPARISON OF COMPUTED WATER AREAS PER
LANDSAT & SKYLAB OBSERVATIONS

	(a)	(b)	(c)	(d)		(e)
	Computed Surface Water Areas (Hectares) Per Observation of:			LANDSAT Observed Mean Area		SKYLAB Departure from LANDSAT Mean
	LANDSAT 5/14/73	SKYLAB 6/12/73	LANDSAT 7/7/73	(Hectares)	(No. of Pixels)	(No. of Pixels)
Barnes Lake	191.15	197.17	180.01	185.58	368	+18.24
Norden Lake	33.11	35.76	30.67	31.89	63	+6.09
Jerome Lake	16.78	17.38	13.78	15.28	30	+3.02
Janice Lake	17.66	17.38	16.45	17.06	34	+0.52
Colby Lake	22.07	23.84	20.45	21.26	42	+4.06
Northwestern Lk.	42.38	38.74	37.34	39.86	79	-1.76
Alkali Lake	29.14	26.32	24.45	26.80	53	-0.74
Trautman Lake	8.83	3.97	6.22	7.53	15	-5.59
Hall Lake	32.67	27.32	23.11	27.89	55	-0.76
Hotchkiss Pond	7.06	3.48	4.00	5.53	11	-3.23
Clark Lake	7.06	5.96	3.56	5.31	11	+0.99
Fish Lake	16.33	17.88	16.45	16.39	33	+2.34
Big Lake	13.24	11.42	12.00	12.62	25	-1.89
Goldwin Lake	13.24	13.91	8.89	11.07	22	+4.47
Limesand Pond	5.30	2.48	1.78	7.08	7	-1.66
Schelske Lake	14.57	12.91	8.00	11.29	22	+2.56
Hust Lake	38.85	37.75	31.11	34.98	69	+4.35
West Lake	32.67	30.79	31.56	32.12	64	-2.08
Lawrence Lake	5.74	3.48	5.78	5.76	11	+3.59
Eugene Pond	7.06	4.47	4.89	5.98	12	-2.37
Woodworth Marsh	4.86	2.48	1.78	3.32	7	-1.31
				Totals	1034	+21.66

observations do not consistently follow this trend. Six of the water features observed by the SKYLAB scanner had computed areas greater than, six less than, and the remaining nine within the range of the respective LANDSAT observations. Since the SKYLAB observations occurred midway between the two LANDSAT observations we have, for the sake of comparison, assumed that the SKYLAB observed ponds should have had areas equal to the mean of the two LANDSAT observations (column d of Table 4). We then tabulated the departure of the actual SKYLAB observations from this mean and expressed the departure in terms of equivalent pixels (column e). An algebric summation indicated a cumulative deviation of only 21.7 pixels for the 21 ponds whose summed area was equivalent to a count of 1034 pixels. Thus it appeared that the SKYLAB observed individual pond areas varied randomly and that those ponds which were larger than expected tended to be balanced by those which were smaller than expected. We have examined the data including aerial photography and ground-truth photography in an attempt to explain these individual variations in the SKYLAB observations. We have not been able to relate these variations to differences in water quality, to the presence or absence of aquatic plants, to phenological circumstances, or to differences in the near-infrared wavebands which were used to delineate surface water features*. We must conclude, therefore, that such factors were not contributory. Furthermore, it appears that for relatively small targets such as prairie ponds and lakes, the SKYLAB multispectral scanner was not able to achieve as consistent a measure of area as was obtained with LANDSAT. We attribute this to the fact that the SKYLAB multispectral scanner utilized a conical scan. With such a system, problems of varying pixel overlap and data redundancy were inherent (Figure 23). The problems were further compounded when the data were converted into a straight line format using a nearest neighbor decision rule. The mapping of picture elements (pixels) of a conical scan-line into a

*Water was delineated in the case of LANDSAT data with a 0.8 to 1.1 μm waveband and, in the case of SKYLAB S-192 data, a 1.55 to 1.75 μm waveband was used.

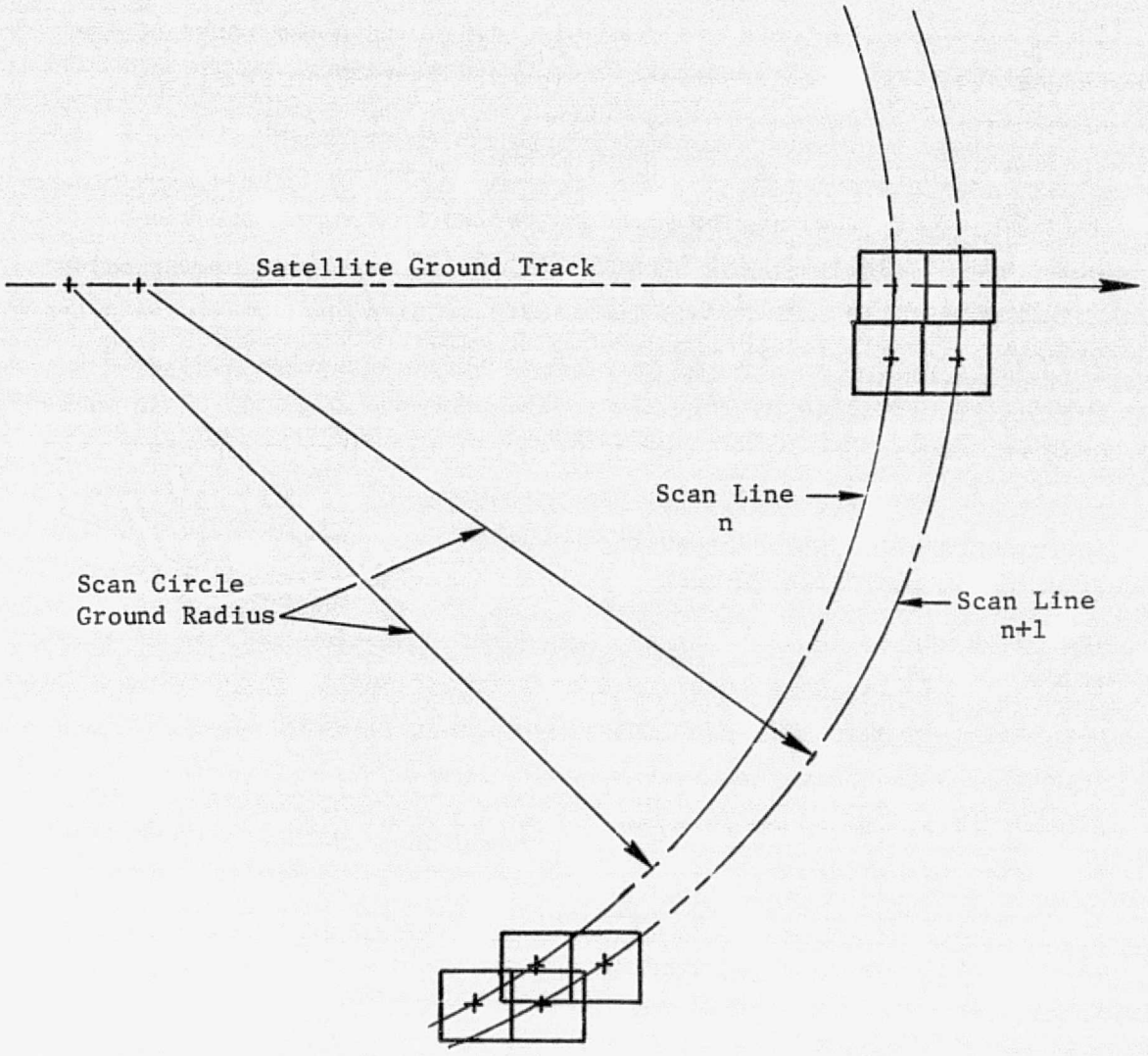

FIGURE 23. RELATIONSHIP OF ADJACENT PIXELS IN THE GEOMETRY OF A CONICAL SCANNER. The figure depicts increasing pixel overlap with displacement away from the ground track.

straightened scan-line must of necessity result in the discarding of a certain number of data pixels and slight dislocation of nearly all pixels from their true geographical position so that they can be fitted into a rectangular pixel grid. These actions have the net affect of slightly and systematically affecting areal representations and geometric fidelity.

With regard to surface water area measurements, it is important to stress one other point. The pond sizes listed by the computer must in practice be termed "apparent size", because each pixel of data was examined and determined to be either totally water or not water. Many pixels lying on the perimeters of ponds and lakes undoubtedly contained some unrecognized and untabulated water. This caused the surface areas of virtually all water features to be underestimated. Percentage-wise, the errors were greater for the smaller ponds and for those of irregular shape (i.e., those having a high ratio of perimeter length to area). The very small ponds, of course, would not be recognized at all. In theory a pond must have filled or nearly filled the scanner's instantaneous-field-of-view (IFOV) to be recognized*. The IFOV of the SKYLAB multispectral scanner was 0.635 hectares in size. Recognition of a pond of this size would have been dependent upon whether the pond was wholly included in one digital sample or fractionally distributed over several samples. This would be governed by both the size and shape of the pond, by the frequency response of the scanner's electronics, and by the random occurrence of the pond with respect to the scanner's sampling grid (i.e. the occurrence of the pond with respect to a scan-line and the digital samples along that scan-line). In general, we feel that it is problematic whether ponds in the 0.6 to 2.5 hectare size class were recognized whereas

*Since there was some variability in the radiance signals received from water targets (per the histograms of Figures 11 through 14), it is possible that a water target did not completely fill the scanner's instantaneous-field-of-view but was nevertheless dark enough to be classified as water.

above 2.5 hectares it is most probable that they were recognized but not necessarily recognized at their full areal extent. The next chapter is devoted to the processing of multispectral data and particularly to the use of such data for detecting water elements smaller than the nominal resolution limits of the scanner.

CHAPTER 6

PROCESSING OF MULTISPECTRAL DATA FOR THE IMPROVED SPATIAL RESOLUTION OF WATER FEATURES

As discussed in the previous chapter, signal level thresholding of a single near-infrared waveband of data is a simple and effective method for delineating surface water. With the advent of satellite programs, however, many workers in the field of remote sensing have been uncomfortable with the diminished resolving capabilities inherent in the operation of high altitude sensors, particularly scanners. Because prairie ponds are frequently smaller than one-half hectare (1.2 acre), it was apparent in both our LANDSAT and SKYLAB studies that many water features were not delineated by single channel thresholding. As part of these studies we have attempted to test a technique which takes advantage of the added information content of multiple spectral channels to estimate the proportion of materials present within a scanner's instantaneous-field-of-view (IFOV)*. The technique termed "proportion estimation" or "mixtures estimation" was first outlined by Horwitz et al. (1971) and further described by Nalepka et al. (1972). Before the LANDSAT and SKYLAB studies, the application of this technique was largely developmental in nature. Its use in these studies must be considered to be among the first attempts to test its applicability in a limited operational context.

General Theory

When the IFOV of a multispectral scanner is large with respect to the scene objects being scanned, a single resolution cell may contain

*The terms "IFOV" and "pixel" are often used interchangeably. However, the terms are not synonymous for LANDSAT and SKYLAB data. The SKYLAB multispectral scanner optics provide an IFOV of approximately 79 x 79 meters while the data are sampled and digitized at a rate which equates a pixel to an area of approximately 72 x 72 meters. In the strictest sense, a description of the proportion estimation approach must make reference to the sensor's optical IFOV. In the actual processing and display of output data, however, reference will be made to the pixel or digitized sample.

a number of different material classes (i.e., the IFOV may be composed of a mixture of materials). The proportion estimation algorithm when applied to such data provides an estimate of the proportion of objects present within each of the scanner's IFOV's.

A discussion of proportion estimation theory is beyond the scope of this paper, however, the essence of the technique can be described in geometric terms. Assume that a data set made up of two spectral channels, λ_1 and λ_2, contains three pure and unique materials -- A, B, and C. This situation can be depicted as in Figure 24 where the signature means for the three materials are shown in two-dimensional signal space. The signature simplex is the geometric figure formed by the lines connecting each pair of signature means. In the non-degenerate case, each pure signature is a distinct vertex of this simplex. If an unknown scene element (IFOV) consists of a mixture of all three materials, the signature of this material, X, lies within the simplex. An estimate of the pairwise proportion of pure materials constituting the unknown element is obtained by drawing a line from a vertex through the unknown signature to the opposite leg of the simplex. The inverse ratio into which each leg is divided defines the pairwise proportional composition of the unknown. In Figure 24, the unknown happens to lie at the centroid of the triangle, and its composition would be in the ratio of 1/3, 1/3, and 1/3 of materials A, B, and C, respectively. A case requiring special geometric interpretation is shown in Figure 25. In this instance the unknown, Z, lies outside or on the edge of the signature simplex. The unkown is determined to be made up of only materials A and C in the inverse ratio by which the simplex triangle's leg A-C is divided by a line drawn from Z orthogonally to that leg. If the unknown is quite distant from the signature simplex (described in terms of a χ^2 distance) the algorithm is capable of designating the unknown as an alien object or an object composed of none of the simplex materials.

Although the above description has been limited to three pure and unique materials in two-dimensional signal space, the concept is easily expanded to situations where many object materials exist in spectral

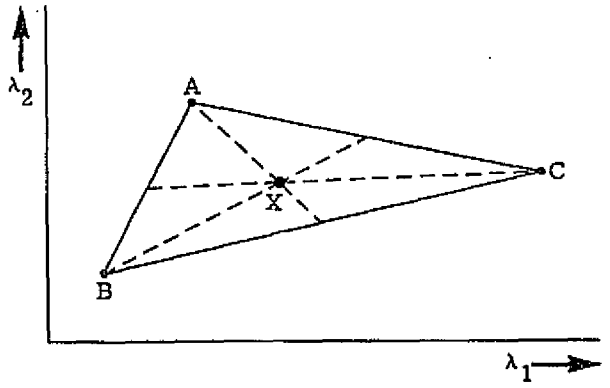

FIGURE 24. GEOMETRIC INTERPRETATION OF MEANS OF SIGNATURE MIXTURES. In the case illustrated, the unknown, X, is a mixture of three pure materials -- A, B, and C -- which form the vertices of the signature simplex.

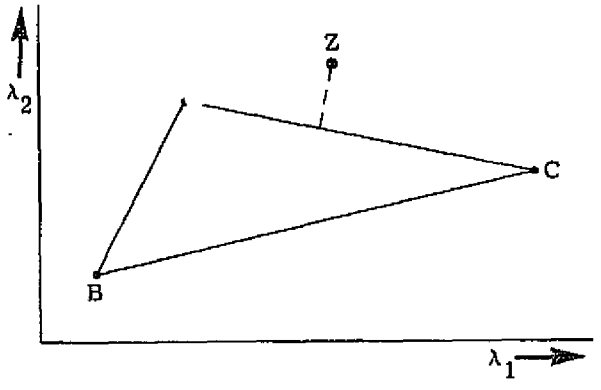

FIGURE 25. GEOMETRIC INTERPRETATION OF ESTIMATE FOR A SPECIAL CASE. The unknown, Z, lying outside the signature simplex is a mixture of materials A and C.

hyperspace. In applying the algorithm, however, it is necessary to observe two operational constraints. Firstly, at least n-1 spectral channels of information are required to satisfactorily estimate mixtures of n-object materials. Secondly, if the signatures for the materials in a mixture are similar or if one of them comes too close to a weighted average of the others, the estimates of the proportions may be poor. The latter condition is illustrated by Figure 26. Figure 26a shows a valid signal simplex for three signatures and two channels of data. Here covariance matrices interpretable in terms of loci of constant probability are shown. Figure 26b is a nearly degenerate signature simplex in which the vertex of one signature has come close to the weighted average of the other two signatures. A measure of what is "too close" is dependent upon the size and shape of the unit contour ellipsoid about the vertex or more specifically upon the covariance matrix.

A Note About the Data Utilized For Multispectral Processing

In multispectral data processing, a necessary condition is that all channels of information utilized must be spatially registered. In accordance with the SKYLAB scanner design, all the even numbered SDO's as a group and all the odd numbered SDO's as another group should have been in registration within a group but one-half pixel out of register between groups. In evaluating several near-infrared wavebands as part of the single channel water mapping task (Chapter 5), it became apparent that misregistration existed not only between even and odd SDO groups but also within groups. This condition was discovered during an examination of several maps of two large lakes, each map generated by thresholding a different near-infrared waveband. If any two wavebands had been spatially registered, all land/water interface pixels should have occupied the same geographic position in each of the respective threshold maps. The examination indicated, however, that for any two SDO's within either the even or odd numbered SDO groups, between 30 and 50 percent of a lake's peripheral pixels were randomly out of register by one or several pixels.

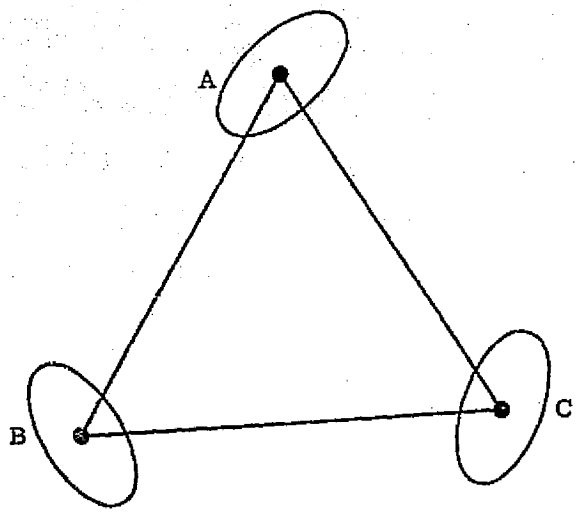

(a) Signature Simplex with Unit Contour Ellipsoids

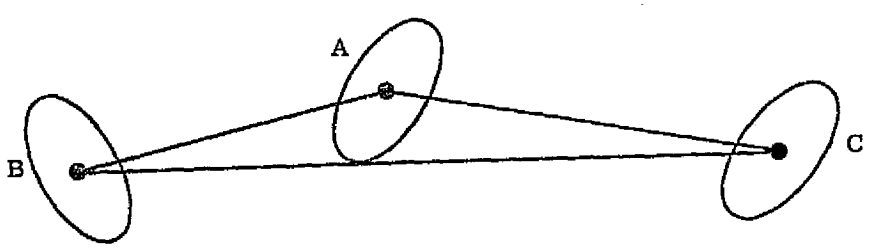

(b) Nearly Degenerate Signature Configuration

FIGURE 26. GEOMETRIC CONFIGURATIONS FOR THREE SIGNATURES AND TWO CHANNELS

A similar lack of registration was independently discovered and more rigorously documented by Morgenstern et al., (1975) who used SKYLAB data collected over a Michigan test site. Band to band misregistration could have occurred due to lags in the analog electronics or due to data displacements in the digital electronics either onboard the spacecraft or during ground processing. Braithwaite and Lambeck (1975) have shown that this source of misregistration was minor in most SDO's. Morgenstern et al. (1975), after examining data in both a conic scan format and a line straightened format, concluded that serious misregistration was created in the data by the scan-line-straightening algorithm.

The above stated registration errors posed potential problems to any multispectral processing and especially for proportion estimation processing. Consequently, we felt it inappropriate to use the scan-line straightened data which was currently on hand and which had been utilized for the single-channel water mapping task (Chapter 5). We, therefore, requested data for the same observation only in a conic scan-line format. These data were subsequently supplied to us by the Data Distribution Center of NASA/Johnson Space Flight Center. The remainder of this discussion will be devoted to the processing and analysis of this conic scan-line data.

Proportion Estimation Processing

In this phase of the study, the primary objective was to delineate open surface water in a mixutre of several scene materials. This should have made it possible to both improve the size estimates of larger ponds and to detect small ponds which would have been undetected. Since models currently used for estimating waterfowl production utilize pond numbers, we have emphasized the detection and enumeration of ponds rather than their areal measurement. Secondarily, we were interested in detecting wetland components which were characterized by marsh vegetation, the canopies of which largely occlude standing surface water. Such marsh conditions are usually peripheral to open water and are often too small to be delineated in whole pixel recognition.

Before processing began, the multispectral data (in a conic scan format) was evaluated by visually assessing electronic screening imagery produced from the data tape. Table 5 presents a summary of that assessment while Figure 27 presents examples of both good and poor quality imagery. Note that in terms of target contrast, only those bands in the near or reflective infrared were of good quality. All visible and thermal-infrared bands were of lesser quality in terms of contrast and other forms of electronic noise. This condition can perhaps be explained by the time of day during which the observation occurred -- 12:56 GMT or 06:19 local solar time. This places the observation at about two hours after sunrise, at a time when the solar altitude was less than 20°. It is conjectured that the near-infrared detectors produced a cleaner output signal under these conditions than did the visible detectors because; (1) with the longer atmospheric path occasioned by the low sun angle, infrared radiation was scattered considerably less than was visible radiation, (2) the bandwidths of the infrared detectors were broader than were the bandwidths of the visible detectors, and (3) a vegetation dominated terrain has generally a higher reflectance in the infrared than in the visible. Furthermore, the SKYLAB multispectral scanner was designed for optimal performance at solar altitude angles in excess of 30° (National Aeronautics and Space Administration 1973). The poor contrast in the thermal infrared is again attributed at least in part to the time of the observation. Generally, during a brief period shortly after dawn and again after sunset, temperature differences between most terrain objects will be muted. This is due to the warming effect of the sun and the differing heat capacities of terrain features.

Figure 28 further illustrates characteristics of the data utilized. In this case, a one-percent systematic sample was extracted from the data set. The figure indicates the data value range of 95 percent of the sampled pixels. Generally the samples had an approximate Gaussian (normal) distribution between the extremes shown. For the observation of 12 June 1973, the data values were generally depressed and lacked dynamic range. These depressed data values can largely be attributed

TABLE 5. EVALUATION OF SKYLAB MULTISPECTRAL SCANNER ELECTRONIC SCREENING IMAGERY FOR DATA OF 12 JUNE 1973 COLLECTED OVER EASTERN NORTH DAKOTA

BAND	λ RANGE (μm)	SDO	IMAGERY CONTRAST	LOW FREQ. NOISE	NOISE BANDING*	1/f NOISE	COMMENTS
1	0.41-0.46	22	very poor	yes	yes	no	
2	0.46-0.51	18	poor	yes	yes	no	
3	0.52-0.56	1	poor to fair	yes	yes	no	some sync. dropout
	0.52-0.56	2	poor to fair	yes	yes	no	some sync. dropout
4	0.56-0.61	3	poor	yes	yes	no	some sync. dropout
	0.56-0.61	4	poor	yes	yes	no	some sync. dropout
5	0.62-0.67	5	very poor	yes	yes	no	
	0.62-0.67	6	very poor	yes	yes	no	
6	0.68-0.76	7	good	yes	no	yes	
	0.68-0.76	8	good	yes	no	yes	
7	0.78-0.88	9	good	no	no	no	
	0.78-0.88	10	good	no	no	no	
8	0.98-1.08	19	good	no	no	no	
9	1.09-1.19	20	good	no	no	no	
10	1.20-1.30	17	good	no	no	no	
11	1.55-1.75	11	good	no	no	no	
	1.55-1.75	12	good	no	no	no	
12	2.10-2.35	13	good	yes	no	no	some sync. dropout
	2.10-2.35	14	good	yes	no	no	some sync. dropout
13-2	10.20-12.50	15	very poor	yes	no	no	some sync. dropout
	10.20-12.50	16	very poor	yes	no	no	some sync. dropout
13-1	10.20-12.50	21	very poor	yes	yes	no	

*Noise banding is noise occurring in phase with the scan frequency. In these particular cases it was evidenced by two cycles of alternate dark and light bands which occurred throughout the imagery parallel to the ground track.

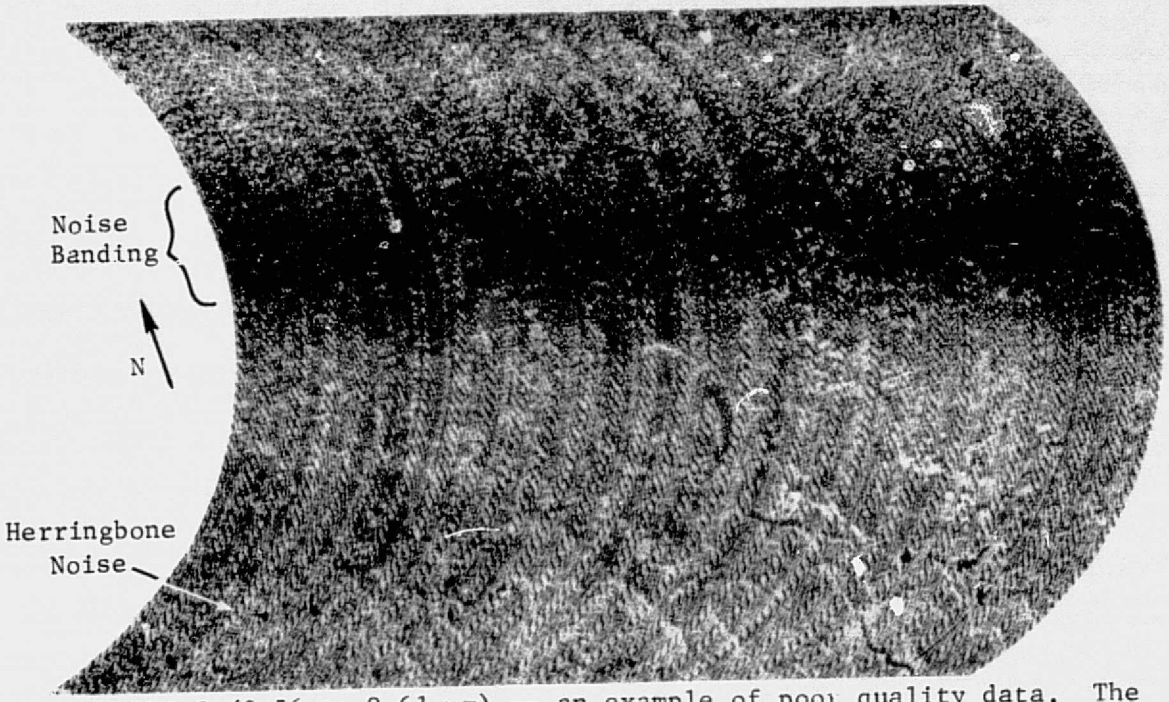

(a) SDO 3 (0.56 to 0.61 μm) -- an example of poor quality data. The alternate light and dark scan line striping is low frequency noise.

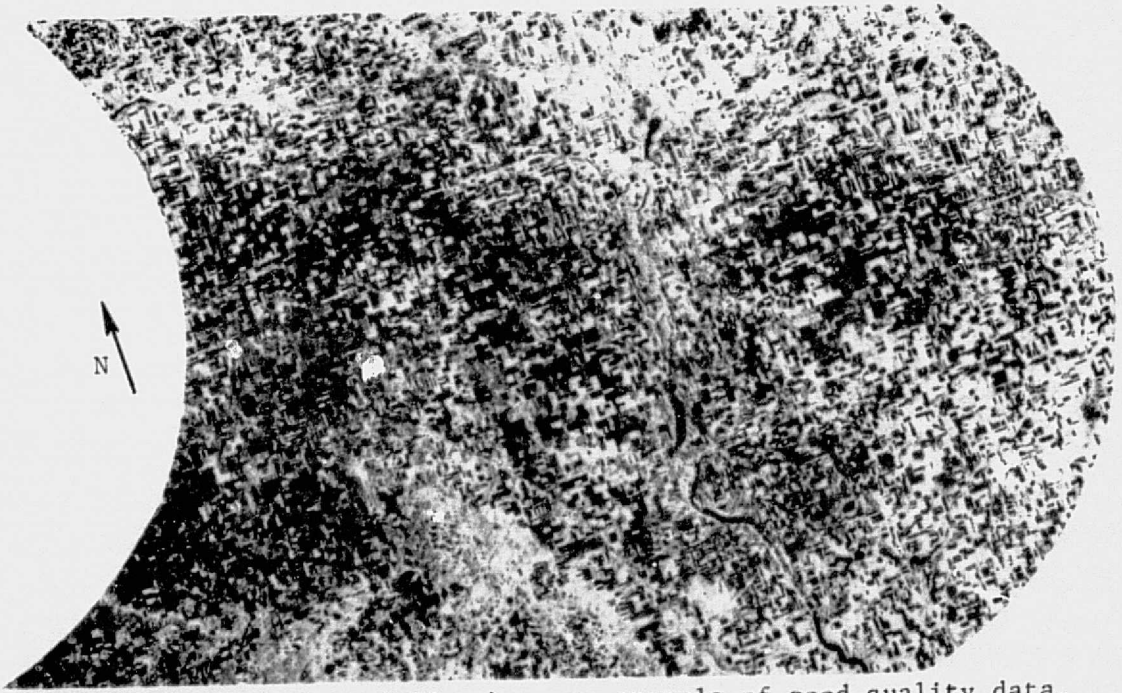

(b) SDO 9 (0.78 to 0.88 μm) -- an example of good quality data.

FIGURE 27. EXAMPLES OF ELECTRONIC SCREENING IMAGERY USED TO EVALUATE DATA QUALITY AND TO DETERMINE SITE COVERAGE. This SKYLAB multispectral scanner observation was made over eastern North Dakota on 12 June 1973 at approximately 12:56 GMT (06:19 local solar time).

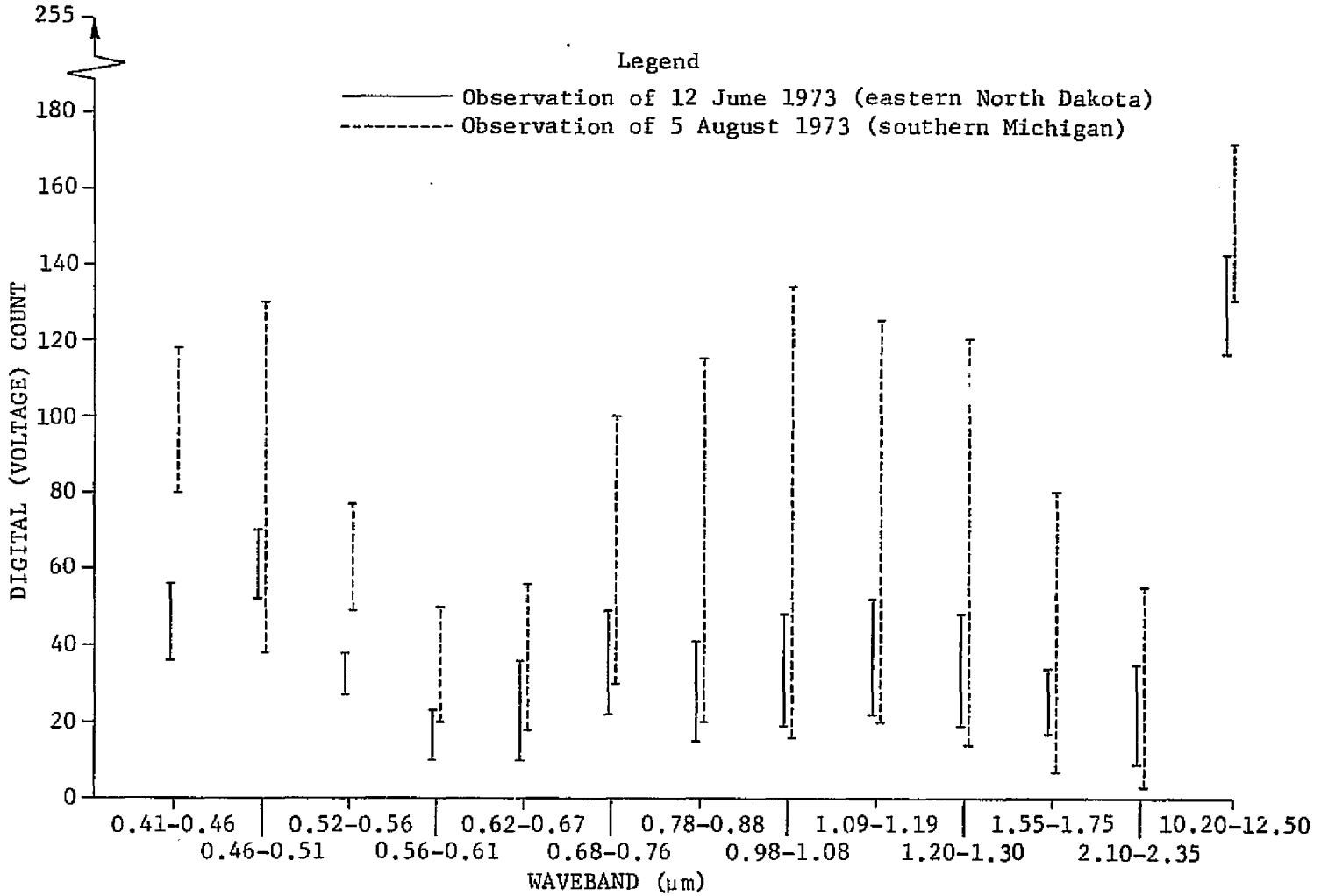

FIGURE 28. DYNAMIC RANGES OF SKYLAB MULTISPECTRAL SCANNER DATA COLLECTED OVER EASTERN NORTH DAKOTA ON 12 JUNE 1973 AND, FOR COMPARISON, OVER SOUTHERN MICHIGAN ON 5 AUG. 1973. The ranges are based on a 1% systematic sample taken throughout the data.

to the low sun angle and the generally poor illumination conditions which existed. For comparison, the figure also includes similar data samples obtained from a SKYLAB scanner observation made over southern Michigan on 5 August 1973 at 15:00 GMT or about 09:30 local solar time. Note that these latter samples have much broader dynamic ranges in nearly all spectral bands and that the ranges are not depressed.

The actual implementation of proportion estimation processing involved as a first step the securing of spectral signatures for object materials occurring in the observation scene. Multispectral signatures extracted from actual scene elements (training sets) for the SKYLAB observation of 12 June 1973 are shown in Figure 29. Only even numbered SDO's were utilized and, in addition, data in the 0.41- to 0.46-μm and 10.20- to 12.50-μm wavebands were discarded because of poor quality. In selecting the training sets, care was taken to pick resolution elements that were pure in their constituency. In order to obtain representative samples, however, the signatures were obtained by combining several training sets which consisted of like materials. For example, the water signature represents a combination of several ponds and lakes which ranged in water quality from the relatively clear to the moderately turbid. As a result, the signature for water in this instance has a larger standard deviation than would normally be expected. Similarly, other signatures represent a variety of field and marsh situations. Note from the figure that the signatures are not well differentiated in the visible wavebands -- a further manifestation of poor contrast as observed for these bands in the electronic screening imagery.

The deep marsh signature was obtained from several communities of bulrushes (Scripus spp.) and cattails (Typha spp.). Bulrushes commonly occur in solid stands and frequently in association with cattails. Cattails occur less frequently in solid stands and consequently were not as dominant in the deep-marsh composite signature as were the bulrushes. Signatures for the shallow marsh class were obtained from plant associations of whitetop (Scolochloa festucacea) and sedges (Carex, spp.). Whitetop is a tall, lush marsh grass that

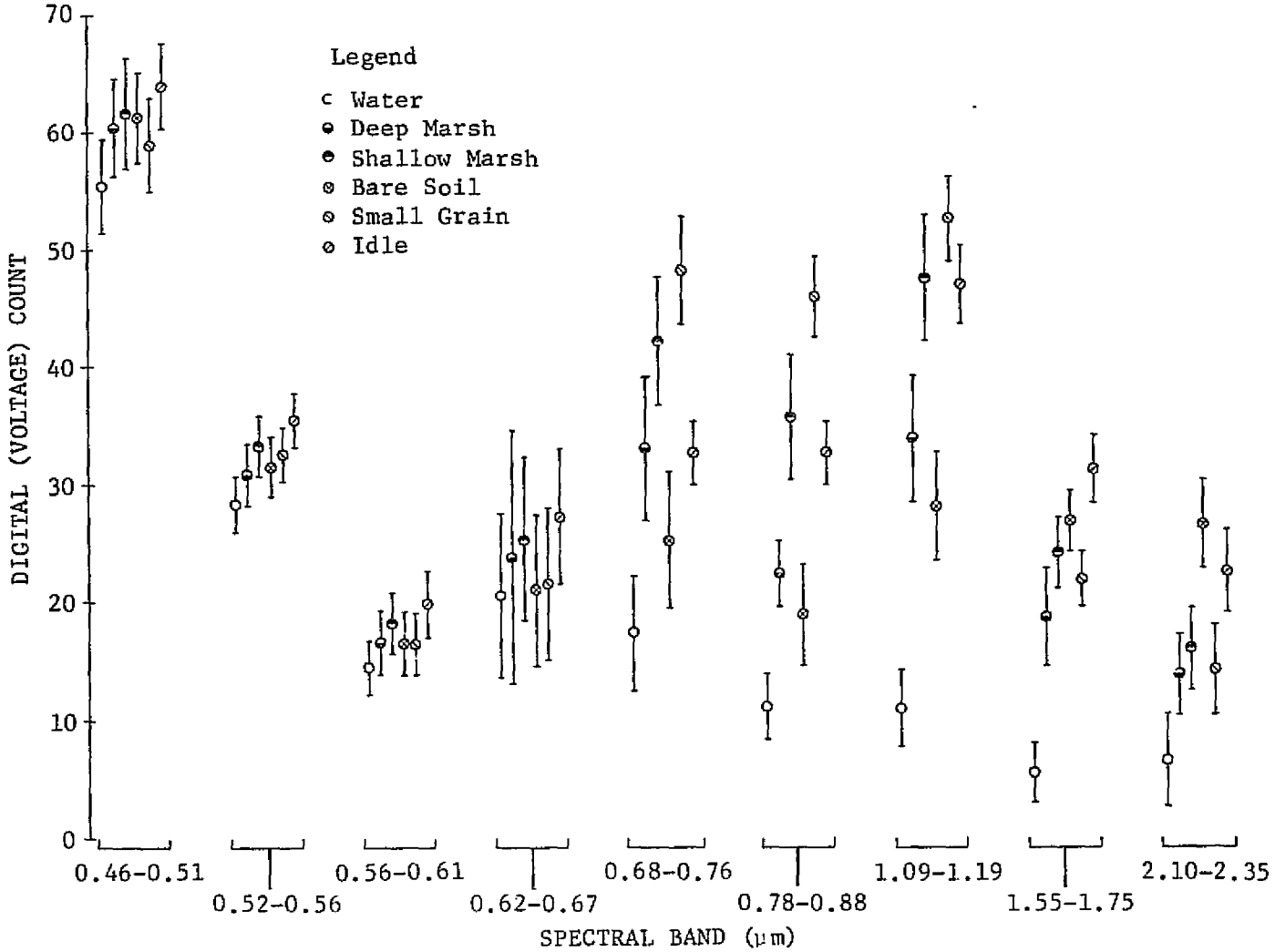

FIGURE 29. SPECTRAL SIGNATURES USED IN THE PROCESSING OF SKYLAB MULTISPECTRAL SCANNER DATA COLLECTED 12 JUNE 1973 OVER EASTERN NORTH DAKOTA. The signature mean and plus and minus one standard deviation are shown.

often grows in solid stands and, in drier years, is cut for hay. Haying stimulates the growth of whitetop allowing the species, in the long term, to become dominant over the sedges. On the other hand, pasturing tends to suppress the whitetop and allows sedges to become dominant. Both of these marsh classes frequently occur in narrow concentric rings surrounding central areas of open water. Continuous, large expanses of these communities are less common. It is this latter situation which must be selected as a training set and, as a result, the selection was often limited.

The small grain signature represented those grains typically grown in this area of North Dakota -- hard red wheat, durum wheat, barley, and oats. These grains, all springplanted, were in an early growth stage during the observation on 12 June. Grain fields throughout the region were represented by a wide range of phenological stages because of variations in planting dates. Some fields had only recently been planted, thus bare soil was predominant. Other fields had been planted for up to one month and had reached a stage where a nearly closed, homogeneous canopy existed. It is this latter condition that is represented in the small grain signature. The "idle" signature represents primarily grasslands (i.e., pasture, open range, and/or native prairie situations). In general, grasslands in early June were represented by a predominance of above ground, dead, herbaceous standing or matted biomass remaining from the previous year's growth of grasses and forbs. Few green plants had as yet emerged from this standing or matted dead biomass.

The signatures selected were evaluated with an automated statistical analysis program. The purpose of the analysis was to determine whether the position of the signatures in multispectral hyperspace permitted a meaningful mixture estimation. If, for example, three signature means, A, B, and C, were in a line, then one would have no way of knowing whether a data point between B and C was a mixture of B and C, a mixture of A and C, or a mixture of all three (an approximation of this situation was illustrated previously in Figure 26b). The results of our analysis of a set of six, five, and four

signatures respectively are presented in Table 6. In the first case, where the full complement of six signatures was tested, the separability of four of the six signatures was poor and for water and bare soil was only moderate. In the second iteration the shallow marsh signature was eliminated, but water's separability did not improve. Finally the set was pared to four signatures, at which time the separability of all signatures, but particularly of water, improved drastically. Our rationale in discarding the deep marsh signature was that this signature probably contained some water along with vegetation particularly due to the timing of the observation when water levels were high and the new year's vegetative growth had not fully developed. In eliminating the shallow marsh signature we felt that its characteristics were duplicated by either the small grain signature (if a flush of new growth had occurred) or by the "idle" signature (if the present year's growth was still masked by the previous year's dead biomass).

As a result of the analysis described above, we chose to perform proportion estimation processing using four signatures - water, bare soil, small grain, and idle. For this set of signatures the small grain signature had in essence become a surrogate for all green herbaceous vegetation. (Woody plants at any significant scale were not present.) The fact that the estimation was to be done without the deep marsh signature also meant that some of these marsh components would be recognized and tabulated as open water. We felt it better to bias the error in this direction as compared to drastically underestimating water, particularly pond numbers. In fact, the transition between open water and closed stands of emergent plants is often a continuum which can vary both with the season and with position within a wetland. As a result, the delineation between open water and an emergent marsh community is often a judgment decision.

The proportion estimation algorithm was applied to multispectral information in a conical scan-line format. The output of this processing, for purposes of display and statistical analysis, was then scaled and converted into a scan-line straightened format. The line straightening

TABLE 6. ANALYSIS OF SIGNATURE SEPARABILITY - A Test for the Uniqueness of a Signature for Use in Proportion Estimation Processing

Number of Signatures Used for Processing	Distance*					
	Water	Deep Marsh	Shallow Marsh	Bare Soil	Small Grain	Idle
6 Signature Set	2.2788	0.7810	0.4534	2.4743	1.2150	0.9668
5 Signature Set	2.3477	1.6264		2.8670	4.6227	1.4359
4 Signature Set	7.3618			3.2506	4.8842	2.7381

* The distance in standard deviation units of the signature mean from the weighted average of the remaining signatures.

algorithm was similar to that which had been used by the Earth Resources Production Processing System of NASA/Johnson Space Center except that compensation for the earth's rotation was not performed.

Results

For the proportion estimation computation, the output was a set of proportions for each pixel. A water recognition map generated from this output is shown in Figure 30. For comparison a map generated with the single-waveband thresholding algorithm is shown in Figure 31. The data in both figures have been scaled (so that the digital pixels have a height/width ratio compatible to a line printer) and converted to a line straightened format. Both maps represent the identical 286 km^2 (110 square mile) area. In the proportion estimation map, the symbol density is related to the proportion of water estimated for that pixel. In order for the map to accurately portray the scene, certain percentage or acceptance limits were determined for the output of the algorithm. For example, it seemed appropriate to count pixel values of 0.81 and above as totally water. This procedure tended to account for the likelihood that a value close to a signature mean (i.e., close in terms of the probability contours) may in fact have been a pure sample related to that mean. Similarly, pixels showing less than 0.40 water were assumed to be false alarms (i.e., nonwater pixels classified as water), and they were excluded from any consideration as surface water. These limits were established after an examination of a small portion of the processed data and a comparison with multispectral scanner data and photography collected by supporting aircraft.

In general, a detailed comparison of the classification maps and related imagery indicated that proportion estimation significantly improved both pond shape definition and the recognition of smaller water features which otherwise would not have been detected.

In the proportion estimation processing of LANDSAT data, a difficulty encountered was the inablilty to adequately delineate alkaline lakes. Such lakes are scattered throughout prairie areas of non or poorly integrated drainage but particularly in glacial

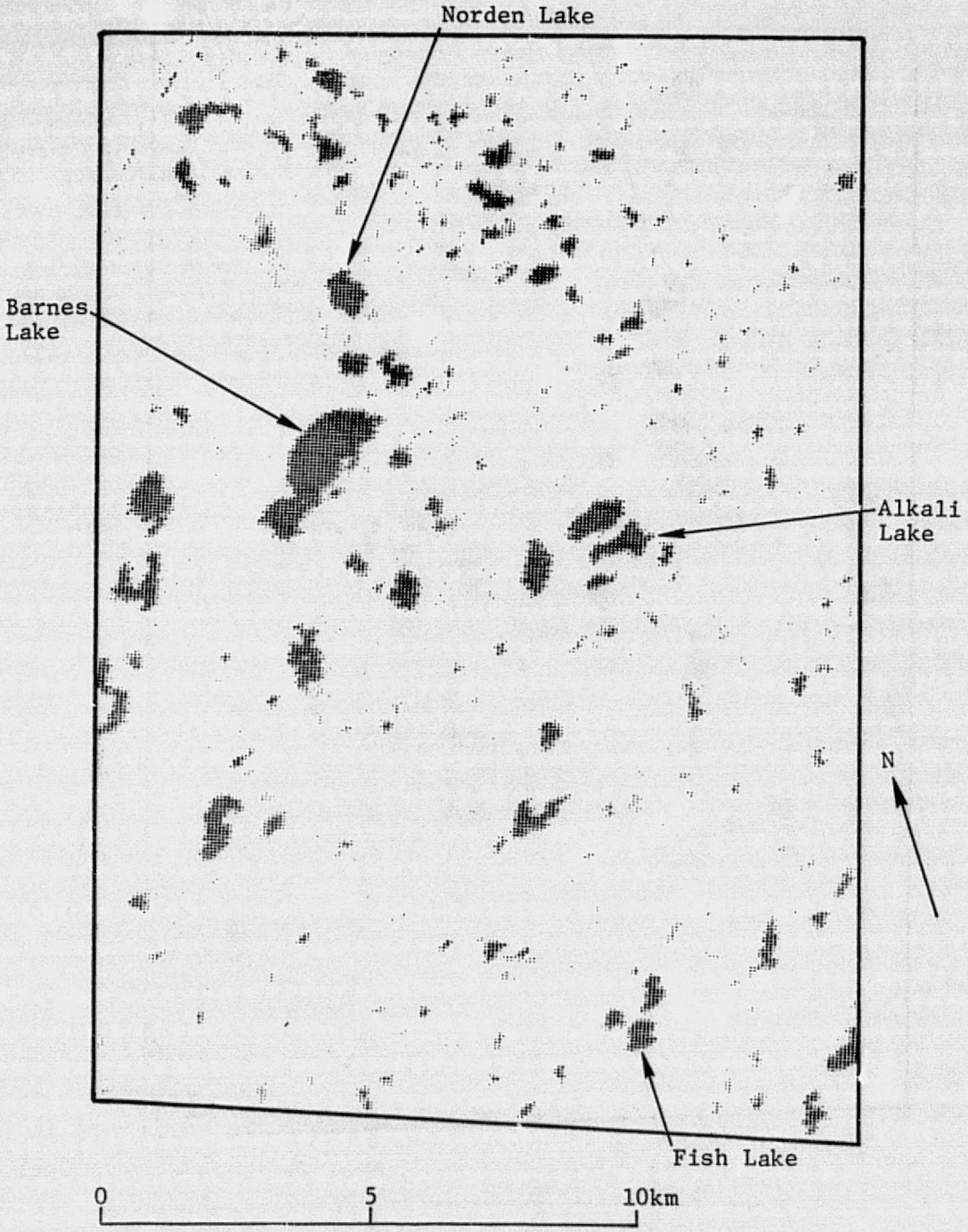

FIGURE 30. WATER RECOGNITION OBTAINED BY THE USE OF THE PROPORTION ESTIMATION ALGORITHM APPLIED TO SKYLAB SCANNER DATA COLLECTED 12 JUNE 1973. The symbol density is related to the proportion of water estimated for that pixel.

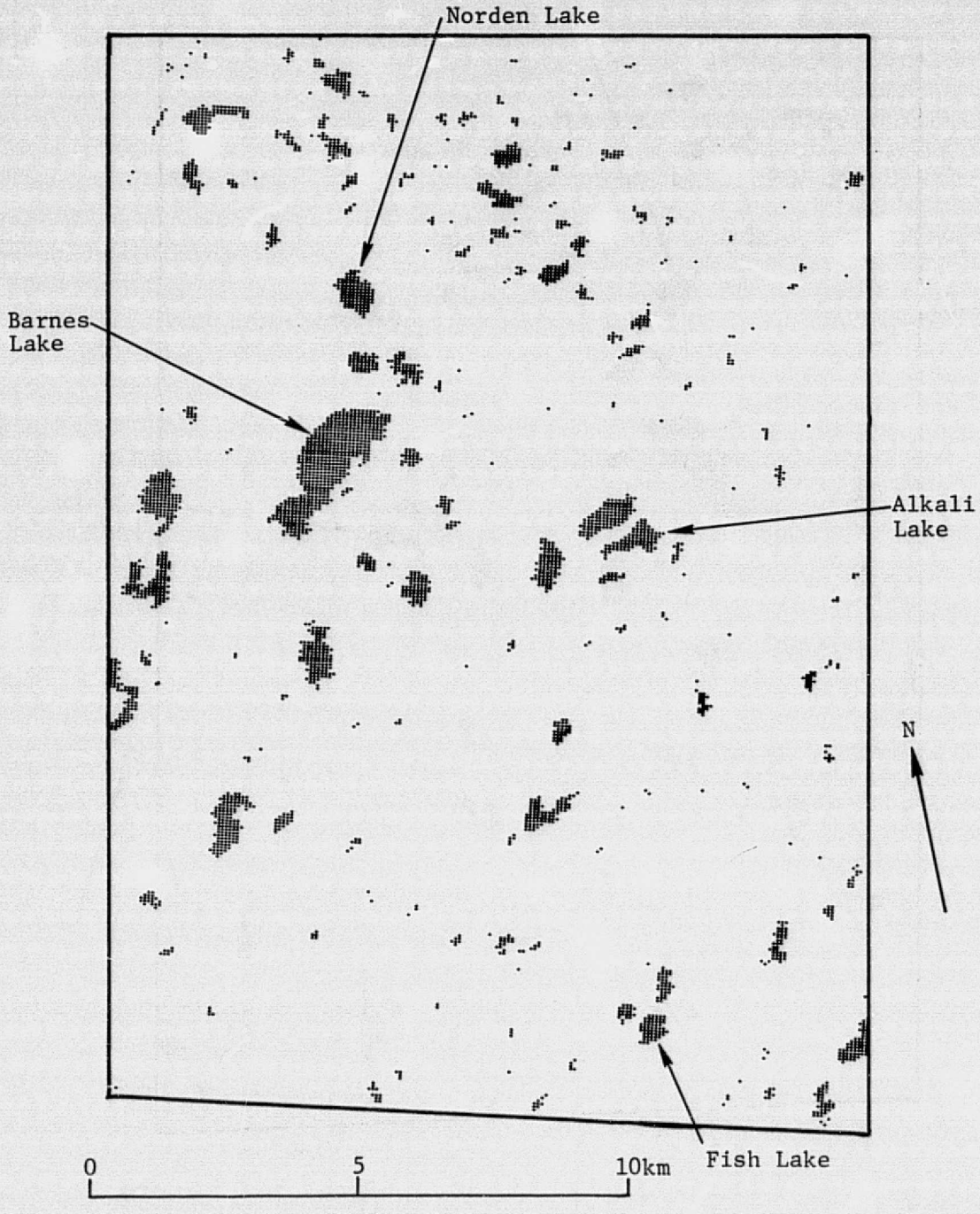

FIGURE 31. WATER RECOGNITION OBTAINED BY THE USE OF THE SINGLE CHANNEL THRESHOLDING ALGORITHM APPLIED TO SKYLAB SCANNER DATA COLLECTED 12 JUNE 1973. The decision criteria is such that each pixel has been classified as either totally water or not water.

outwash areas of the Missouri Coteau. A proportion estimation water map which closely matches the areal coverage of our SKYLAB map (Figure 30) and which was produced from LANDSAT data collected 25 days after the SKYLAB observation is included here as Figure 32. Both Alkali Lake and Norden Lake in the LANDSAT map were only partially recognized. Both lakes at the time contained large amounts of suspended solids and possibly precipitated alkali bottom sediments. These conditions are especially prevalent during periods of low water as was the situation during the summer of 1973. The anomalous detection of these lakes, we had felt, could have been improved had there been additional spectral information available beyond what was available with the LANDSAT multispectral scanner. In particular, we had thought that the additional near-infrared wavebands and especially the 1.55- to 1.75-μm waveband available on SKYLAB would provide improvements in the recognition of these anomalous lake features. A comparison of Figure 30 and 32 indicates that a dramatic improvement was, in fact, realized. We are unable, however, to determine in a quantitative sense how accurately the areas of the two lakes were estimated since no current low altitude planimetric data for the lakes were available.

Quantitative comparisons were made of certain other surface water features which coincided with an aircraft data transect located in the vicinity of the Woodworth Station. The strip maps of Figure 33 were plotted from processed SKYLAB scanner data while still in a conic scan-line format. The data were quantitatively analyzed in this format in order to avoid errors which would be introduced by the scan-line straightening algorithm. The map symbols used are plotted at the areal centroid of the respective pixel, the symbol size being equivalent to the proportion of water found in that pixel. Note that the symbols are not equally spaced. This is due to the overlapping of adjacent pixels in a direction orthogonal to the ground track of the satellite and in direct proportion to the distance of the pixel from the ground track (see Figure 23).

Figure 33a resulted from the thresholding of a single waveband of data (1.55 to 1.75 μm). Figure 33b is a proportion estimation map

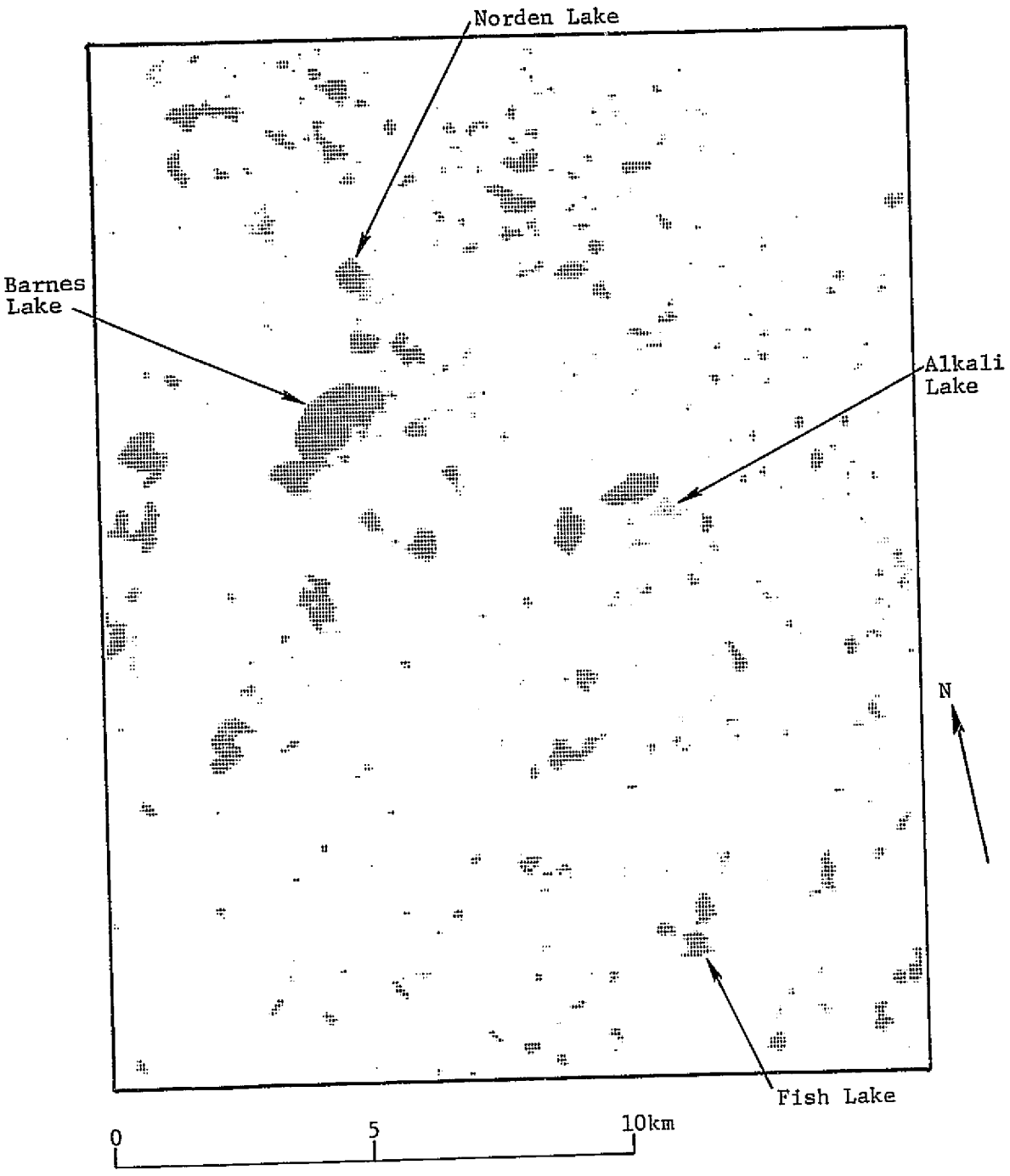

FIGURE 32. WATER RECOGNITION OBTAINED BY USE OF THE PROPORTION ESTIMATION ALGORITHM APPLIED TO LANDSAT DATA COLLECTED 7 JULY 1973. The symbol density is related to the proportion of water estimated for that pixel.

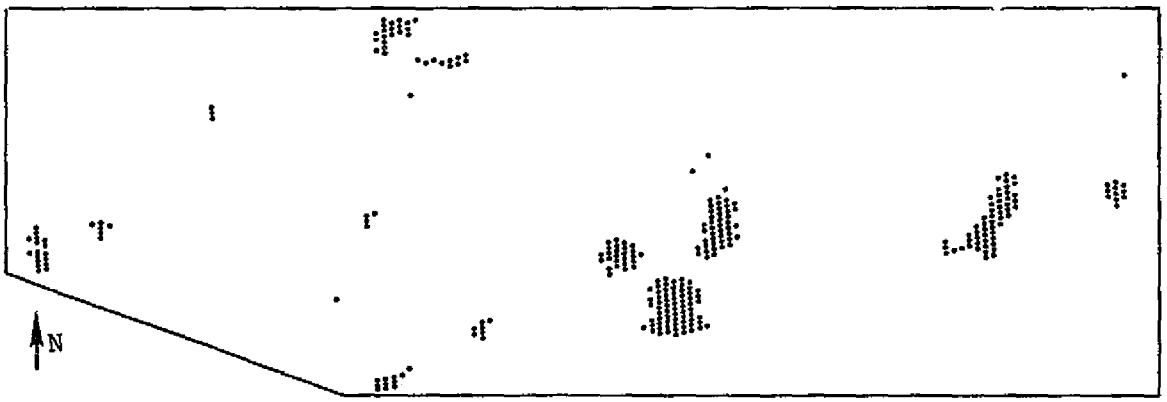

(a) Water Recognition by Thresholding 1.55- to 1.73-μm SKYLAB Scanner Data Collected 12 June 1973.

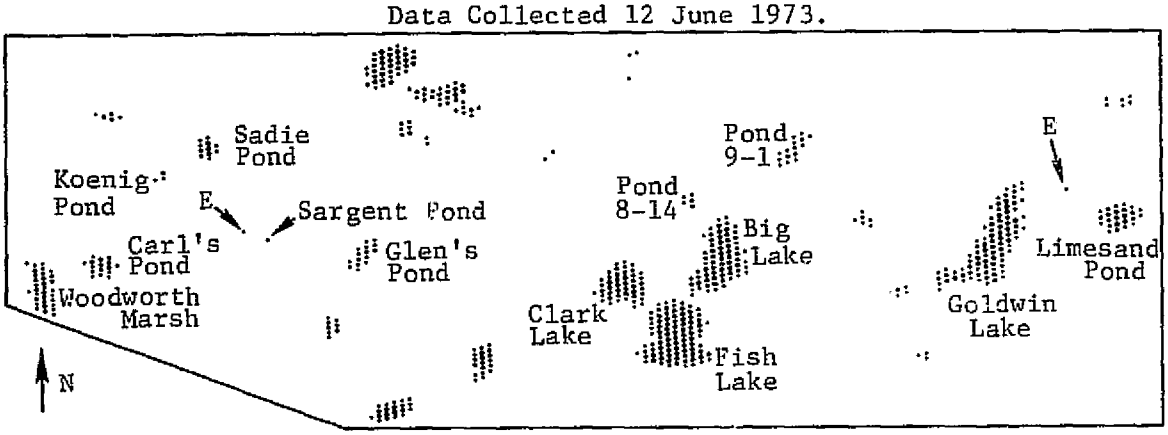

(b) Water Recognition by Proportion Estimation Processing of SKYLAB Multispectral Scanner Data Collected 12 June 1973. The minimum fractional acceptance limit for water was 40% per pixel.

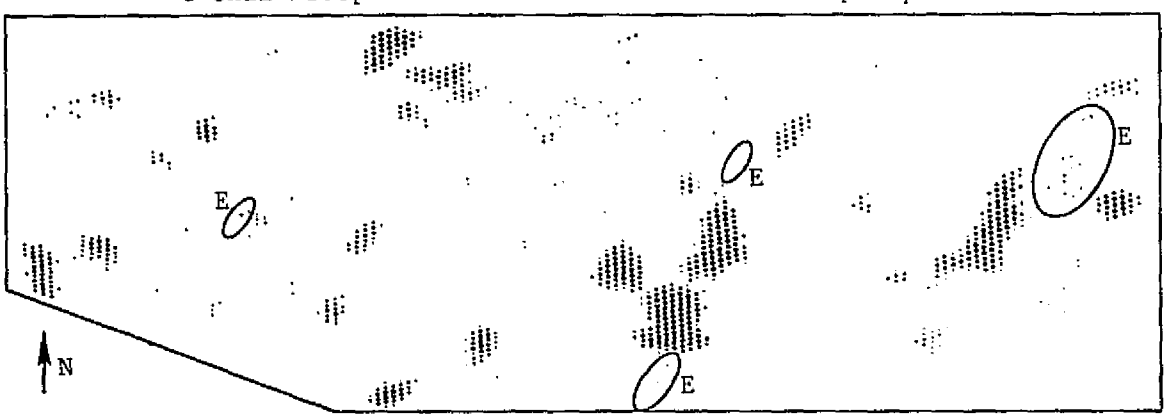

(c) Water Recognition by Proportion Estimation Processing of SKYLAB Multispectral Scanner Data Collected 12 June 1973. The minimum fractional acceptance limit for water was 31% per pixel. Pixel water fractions in the range 31 thru 39% are indicated by small open symbols.

FIGURE 33. WATER RECOGNITION IN THE VICINITY OF WOODWORTH STATION, NORTH DAKOTA. The proportion estimation recognition maps (b and c) differ only in the minimum fractional acceptance limit used in plotting the map. In both of the proportion estimation maps, symbol size is related to the percent of water detected in that pixel. The symbols labelled "E" are confirmed commission errors. Scale: 1/62,500.

which uses a minimum acceptance level of 40 percent (i.e., pixels tabulated as containing less than 40 percent water were assumed to contain no water at all). In this map, it is apparent that a major improvement in both the detection of small ponds and the detection of peripheral pond features was realized. The map contains two confirmed commission errors at locations "E". Many other smaller ponds were not identified as may be attested by a comparison with the electronic aircraft imagery of Figure 34.

Referring again to Figure 33b, the smallest confirmed recognized water feature was Sargent Pond. Figure 33c is also a proportion map similar to the previous map except that an acceptance level of 31 percent was utilized. (Pixels in the 31- to 39-percent range are indicated by small open symbols. The map differs only from the previous map with the inclusion of these symbols.) Clearly many of these added symbols do represent water, but it is equally evident that many also were commission errors as at locations labelled "E". It was because of the proliferation of these errors that the minimum acceptance level was set at 40 percent. In addition to these maps which can only qualitatively illustrate a range of proportions, the areal extent of each of the several ponds and lakes named in Figure 32b, was calculated based upon the exact proportion of water listed in the algorithm output stream (and excluding pixels containing less than an estimated 40 percent water).

Before describing the results, however, we present here a brief discussion of the areas which were assigned to each pixel. The IFOV of the SKYLAB multispectral scanner was 80 x 80 m but, since the scene was overscanned in the direction of the satellite's velocity vector and since the data were oversampled in a direction orthogonal to this vector, there was overlap in the ground patch covered by adjacent pixel samples. In calculating the water area of a pond or lake, one needs to consider the actual area viewed by each pixel. In other words, if a pond smaller than 80 x 80 m is contained within one pixel, the pond area is 50 percent of 80 x 80 m (i.e., the IFOV) and not 50 percent of the smaller effective area. Now if this same

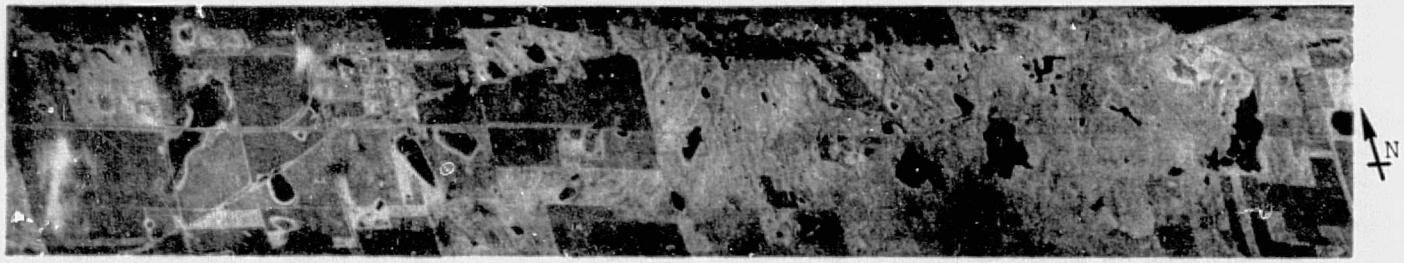

(a) 1.0- to 1.4- μm Electronic Imagery -- 12 May 1973 from 1370 m Altitude.
(The imagery appears skewed due to a pronounced aircraft crab angle.)

(b) 1.0- to 1.4- μm Electronic Imagery -- 12 Aug. 1973 from 1370 m Altitude.

FIGURE 34. AIRCRAFT MULTISPECTRAL SCANNER VIDEO COLLECTED ON A TRANSECT OVER WOODWORTH STATION, NORTH DAKOTA. Approximate along track scale: 1/26,000.

pond was seen in the overlap area of two adjacent pixels it would be inaccurate to use the 80 x 80 m area for each pixel since some portion of the pond would be counted twice. To account for problems of this sort, allowances for adjacent water pixels were made when calculating estimated pond and lake areas. (Any pixel containing water may have been overlapped by up to a maximum of six other pixels containing water - as many as two in the direction of the satellite's velocity vector and as many as four orthogonal to this vector.)

In addition to the pond and lake areal measurements obtained with SKYLAB scanner data, more precise measurements of area were also obtained with the single channel thresholding algorithm applied to low altitude aircraft scanner data. These latter data were used to compare the SKYLAB proportion estimation results against. In Table 7 the results are presented for comparison. Note that neither of the two aircraft observations coincided with the satellite observation but preceded and followed it by 31 and 60 days respectively. From the comparisons, six of the SKYLAB observed water features were reasonably close in area to the aircraft observations (Big and Fish Lakes, Pond 8-14, Glen's Pond, Sargent Pond, and Koening Pond). One water body was underestimated in area (Clark Lake). The remaining six water features were overestimated in area. Thus it would appear that the proportion estimation results tended to either approximate or somewhat overestimate the actual areas of ponds and lakes. This would seem to bear out our earlier suspicions that areas of emergent marsh plants, may in certain cases, be tabulated as open water areas. In particular, Goldwin Lake, Carl's Pond, and Woodworth Marsh are known to have had extensive peripheral deep marsh areas, and the areas of all of these features were notably overestimated. We feel that efforts to effectively estimate open surface water and more especially areas of marsh communities were compromised by inadequate data quality in the visible bandwidths. As noted previously, this lack of quality appears to have been occasioned by the early hour of the SKYLAB observation.

Finally, we present the results of areal water tabulations for the 286 km^2 scene of Figures 30 and 31. These tabulations were

TABLE 7. TABULATION OF AREAL MEASURMENTS OF OBSERVED POND AND LAKE FEATURES

	Computed Areas (Hectares)		
	Aircraft Observation of 12 May 1973 (1)	SKYLAB Observation of 12 June 1973(2)	Aircraft Observation of 12 Aug. 1973 (1)
Limesand Pond	Not Available	6.15	4.49
Goldwin Lake	16.13	23.59	13.78
Pond 9-1	2.41	3.20	2.67
Big Lake	17.56	18.90	16.81
Fish Lake	24.42	24.76	23.53
Clark Lake	11.43	8.36	9.04
Pond 8-14	2.08	1.15	Dry
Glen's Pond	2.43	2.14	Dry
Sargent Pond	0.34	0.28	0.06
Sadie Pond	2.36	2.90	2.53
Koenig Pond	1.25	0.80	Dry
Carl's Pond	1.10	3.43	Dry
Woodworth Marsh	5.75	6.88	3.06

Notes: (1) Pond areas were computed by thresholding a 1.5- to 1.8- μm waveband of scanner data. Observation was made from an altitude of 1370 m.

(2) Pond areas were computed by proportion estimation processing of SKYLAB multispectral scanner data.

accomplished using the computer program described in Appendix A. This program is not able to take account of differences in area represented by the scanner's IFOV and the digital sample (pixel) nor of pixel overlap. Therefore, the results can be compared only in a qualitative sense. Table 8 presents a comparison of numerical and area tabulations of water features for the 286 km^2 test area using both the threshold and proportion estimation algorithms. This comparison indicates that the total number of ponds and lakes delineated by proportion estimation processing was 189 percent of the total number obtained with the single channel threshold algorithm. The results of proportion estimation processing of LANDSAT data for the identical scene are also tabulated in Table 8. It is significant to note that proportion estimation processing of both SKYLAB and LANDSAT data delineated nearly an equal number of water features. The distribution of pond numbers within size classes particularly the smaller classes differs because the basic pixel sizes were different*; this difference allowed the ponds to be clustered somewhat differently into the size classes shown in the table.

*Pixel size for the LANDSAT data was 57 x 79 m. The SKYLAB pixel after we had line straightened and scaled the data was 58 x 71 m.

TABLE 8. COMPARISON OF TABULATIONS OF PONDS AND LAKES

SKYLAB Observation of 12 June 1973				LANDSAT Observation of 7 June 1973	
Computed Using the Thresholding Algorithm		Computed Using the Proportion Estimation Algorithm		Computed Using the Proportion Estimation Algorithm	
Area (Acres)*	Frequency	Area (Acres)*	Frequency	Area (Acres)*	Frequency
0.25 to 0.50		0.25 to 0.50	109	0.25 to 0.50	72
0.51 to 1.00	56	0.51 to 1.00	35	0.51 to 1.00	71
1.01 to 2.00	26	1.01 to 2.00	52	1.01 to 2.00	62
2.01 to 3.00	11	2.01 to 3.00	33	2.01 to 3.00	31
3.01 to 4.00	11	3.01 to 4.00	18	3.01 to 4.00	19
4.01 to 6.00	16	4.01 to 6.00	24	4.01 to 6.00	21
6.01 to 8.00	10	6.01 to 8.00	21	6.01 to 8.00	20
8.01 to 10.00	9	8.01 to 10.00	6	8.01 to 10.00	11
10.01 to 15.00	10	10.01 to 15.00	15	10.01 to 15.00	15
15.01 to 20.00	13	15.01 to 20.00	10	15.01 to 20.00	7
20.01 to 25.00	5	20.01 to 25.00	7	20.01 to 25.00	5
25.01 to 30.00	0	25.01 to 30.00	5	25.01 to 30.00	3
30.01 to 40.00	3	30.01 to 40.00	2	30.01 to 40.00	4
40.01 to 50.00	6	40.01 to 50.00	8	40.01 to 50.00	6
OVER 50.00	17	OVER 50.00	19	OVER 50.00	14
TOTAL	193	TOTAL	364	TOTAL	361

*Although Metric units of measure are generally used throughout this text, the computer software in current use clustered water features according to English units of areal measure (acres).

REFERENCES CITED

Braithwaite, J. and P. Lambeck. 1975. ERIM contributions to the S-192 sensor performance evaluation. Final Rep. 102800-51-F, Environmental Research Institute of Michigan, Ann Arbor. 185 pp.

Burge, W. G. and W. L. Brown. 1970. A study of waterfowl habitat in North Dakota using remote sensing techniques. Tech. Rep. No. 2771-7-F, Willow Run Labs., Inst. of Sci. and Technol., The University of Michigan, Ann Arbor. 61 pp.

Clayton, L. 1967. Stagnant-glacier features of the Missouri Coteau in North Dakota. pp. 25-46 in Midwest Friends of the Pleistocene in south-central North Dakota, 18th Annual Field Conference, 19-21 May 1967, Guidebook and miscellaneous short papers, Glacial geology of the Missouri Coteau and adjacent areas: North Dakota Geol. Survey Misc. Ser. 30.

Cooch, F. G. 1969. Waterfowl-production habitat requirements. pp. 5-10 in Saskatoon Wetlands Seminar, Canadian Wildlife Service Report Series No. 6, Ottawa, Ontario.

Crissey, W. F. 1957. Forecasting waterfowl harvest by flyways. Trans. N. Am. Wildl. Conf. 22:256-268.

Crissey, W. F. 1969. Prairie potholes from a continental viewpoint. pp. 161-171 in Saskatoon Wetlands Seminar, Canadian Wildlife Service Report Series No. 6, Ottawa, Ontario.

Gates, D. M., H. J. Keegan, J. C. Schleter, and V. R. Weidner. 1965. Spectral properties of plants. Applied Optics 4(1):11-20.

Gausman, H. W. 1974. Leaf reflectance of near-infrared. Photogrammetric Engineering 40(2):121-218.

Geis, A. D., R. K. Martinson, and D. R. Anderson. 1969. Establishing hunting regulations and allowable harvest of mallards in the United States. J. Wildl. Mgmt. 33(4):848-859.

Henry, C. D., D. R. Anderson, and R. S. Pospahala. 1972. Aerial surveys of waterfowl production in North America, 1955-71. Special Scientific Rep.--Wildlife No. 160, U.S. Fish and Wildlife Service, Washington, D. C. 48 pp.

Horwitz, H. M., R. F. Nalepka, R. D. Hyde, and J. P. Morgenstern. 1971. Estimating the proportions of objects within a single resolution element of a multispectral scanner. pp. 1307-1320 in Proc. of 7th Internat'l Symp. on Remote Sensing of Environ., Willow Run Labs., Inst. of Sci. and Technol., The University of Michigan, Ann Arbor.

McDowell, D. Q. 1974. Spectral distribution of skylight energy for two haze conditions. Photogrammetric Engineering 40(5):569-571.

Morgenstern, J. P., R. F. Nalepka, R. Cicone, J. Sarno, P. Lambeck, and W. A. Malila. 1975. S-192 analysis: conventional and special data processing techniques. Final Rep. 101900-63-F, Environmental Research Institute of Michigan, Ann Arbor. 172 pp.

Myers, V. I., M. D. Heilman, R. J. P. Lyon, L. N. Namken, D. Simmonett, J. R. Thomas, C. L. Wiegand, and J. F. Woolley. 1970. Soil, water and plant relations. pp. 253-297 in Remote Sensing with Special Reference to Agriculture and Foresty, National Academy of Sciences, Washington, D. C.

Nalepka, R. F., H. M. Horwitz, and P. D. Hyde. 1972. Estimating proportions of objects from multispectral data. Tech. Rep. No. 31650-73-T, Willow Run Labs., Inst. of Sci. and Technol., The University of Michigan, Ann Arbor. 47 pp.

National Aeronautics and Space Administration. 1973. SKYLAB program: EREP investigator's information book. Document NSC-07874, Lyndon B. Johnson Space Center, Houston, Texas

National Aeronautics and Space Administration. 1974. Earth Resources Experiment Package (EREP) experiment calibration data. Document MSC-07744, revision B, change 2, Lyndon B. Johnson Space Center, Houston, Texas.

Nelson, H. K., A. T. Klett, and W. G. Burge. 1970. Monitoring migratory bird habitat by remote sensing methods. Trans. N. Am. Wildl. and Nat. Resour. Conf. 35:73-84.

Olson, C. E., Jr. 1969. Early remote detection of physiologic stress in forest stands. pp. 37-52 in E. B. Knipling, ed. Proceedings of the Workshop in Aerial Color Photography in the Plant Sciences held 5-7 March 1969 at the University of Florida, Gainesville.

Rohde, W. G. and C. E. Olson, Jr. 1970. Detecting tree moisture stress. Photogrammetric Engineering 36(6):561-566.

Smith, A. G., J. H. Stoudt, and J. B. Gollop. 1964. Prairie potholes and marshes. pp. 39-50 in Linduska, J. P., ed., Waterfowl Tomorrow: U.S. Fish and Wildlife Service, Washington, D. C.

Stewart, R. E., A. D. Geis, and C. E. Evans. 1958. Distribution of populations and hunting kill of the canvasback. J. Wildl. Mgmt. 22(4):333-370.

Stewart, R. E. and H. A. Kantrud. 1973. Ecological distribution of breeding waterfowl populations in North Dakota. J. Wildl. Mgmt. 37(1):39-50.

Sverdrup, H. U., M. W. Johnson, and R. H. Fleming. 1942. The oceans. Prentice-Hall, Inc., Englewood Cliffs, N. J. 1087 pp.

Work, E. A., Jr. 1974. Application of the Earth Resources Technology Satellite for monitoring the breeding habitat of migratory waterfowl in the glaciated prairies. Master's Thesis, The University of Michigan. 107 pp. (available from University Microfilms, Ann Arbor, Michigan.--Thesis Abstr. M-6698.).

Work, E. A., Jr. and F. J. Thomson. 1974. A study of waterfowl habitat in North Dakota using remote sensing techniques: Phase II. Tech. Rep. No. 101000-12-T, Environmental Research Institute of Michigan, Ann Arbor. 96 pp.

Work, E. A., Jr., D. S. Gilmer, and A. T. Klett. (in press). Utilization of ERTS-1 for appraising changes in continental migratory bird habitat. Type III Final Report prepared for NASA/Goddard Flight Center.

APPENDIX A

DESCRIPTION OF COMPUTER PROGRAM FOR GENERATING WATER BODY AREA AND PERIMETER STATISTICS

The software program, APSTAT (Area, Perimeter Statistics), is designed to delineate bodies of open surface water and to generate statistics (area, perimeter, and shape factor) on these water bodies. APSTAT has evolved from an older program, MAPLKS, also developed by the Environmental Research Institute of Michigan. Both programs utilize the same decision criteria for classifying a grouping of pixels as a pond or lake. Both programs compute the area of any specific closed feature (i.e., a pond or lake) one line at a time, summing the areas in each scan line to determine the area of the specific feature. MAPLKS takes account of increases in the spatial field of view (and thus an increase in pixel area) as scan angles increase from the nadir position. APSTAT does not take account of variations in pixel area but instead assumes that all scene pixels are of a constant area. Thus APSTAT is suitable for use with satellite data where scan angles subtend no more than 12 or 15 angular degrees. Specifically, APSTAT has been designed to operate on data collected using LANDSAT and SKYLAB/EREP scanners both of which have approximate lateral fields of view of 11°.

Although APSTAT was developed primarily for the tabulation and analysis of pond and lake occurrence, application of the program need not be limited to water bodies. Its statistical enumerating capability can be applied to any scene feature having a closed perimeter such as forests or agricultural crops provided there exists digitized data in which the scene feature of interest can be delineated on the basis of a discrete voltage range in a single data channel (as, for example, a classification tape or water features which exhibit uniquely low radiance values in a near infrared waveband).

Specifically, APSTAT can identify any class of data which may be defined by one of two modes of operation defined by the following level slicing algorithms:

1. If: $0 \leq$ (pixel voltage count on channel ICODE) $<$ VHI,
   the pixel is assigned to the scene class of interest.
   Otherwise: the pixel is assumed not to belong to that class.
2. If: VOLTS(ϕ) $\leq$ (pixel voltage on channel ICOD) $\leq$ VOLTS(1),
   the pixel contains PC(ϕ)% of the class of interest.
   If: VOLTS(1) $\leq$ (pixel voltage on channel ICODE) $\leq$ VOLTS(2),
   the pixel contains PC(1)% of the class of interest.
   If: VOLTS(2) $\leq$ (pixel voltage on channel ICODE) $\leq$ VOLTS(3),
   the pixel contains PC(2)% of the class of interest.
   If: VOLTS(3) $\leq$ (pixel voltage on channel ICODE) $\leq$ VOLTS(4),
   the pixel contains PC(3)% of the class of interest.
   Otherwise: the pixel does not belong to that class.
   Where ICODE, VOLTS(0). . .VOLTS(4) and PC(1). . .PC(3) are
   user specified.

The first algorithm is the normal (default) mode of classification. The second is the "proportion estimation" mode and must be called by the user. The proportion estimation mode assumes the availability of multiple channel tape with each material present in the scene represented by one channel -- the integer scale on the channel being representative of the proportion of that material present within each pixel. Only one channel (i.e., one material class) of a proportion estimation tape can be processed at a time.

APSTAT also incorporates the following features:

(a) The program will accommodate up to 1040 points per linear scan line.

(b) The program can accommodate multiple channel input (to a maximum of 13) but must operate on only one of these channels.

(c) A maximum of 3250 lines of data may be processed each time the program is run.

(d) The program lists the position of each identified feature by the last (highest) scan line on which it appears and the last (highest) point of the feature on that scan line. Optionally, the feature may also be identified by the latitude and longitude of that point.

Algorithm Descriptions

1) AREA

In the normal (default) mode of area calculation, the area of a feature (such as a lake) is equal to the number of feature pixels times the area of a pixel (always constant). In mathematical terms:

Feature Area = Number of Feature Pixels x Pixel Length x Pixel Width

where pixel length and width are user specified.

In the proportion estimation mode

$$\text{Feature Area} = \text{Pixel Length} \times \text{Pixel Width} \times \sum_{i=0}^{3} (\text{number of feature pixels which are PC(i)\%})$$

2) PERIMETER

The following examples illustrate the definition of perimeter:

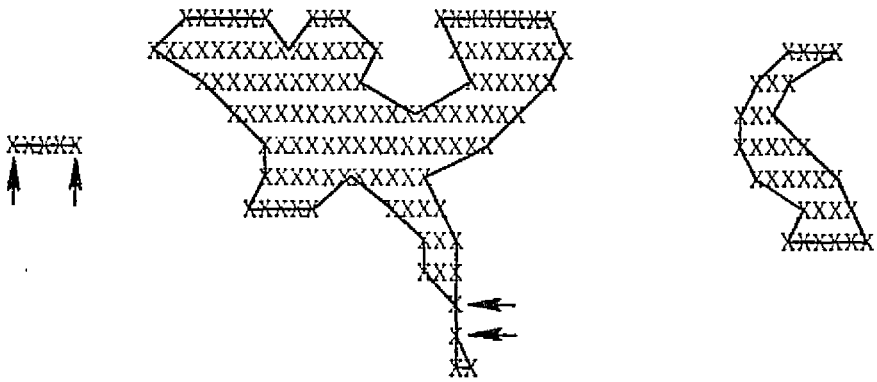

Each pixel identified as the specified feature is shown as an X. The calculated perimeters are shown by the solid dark lines, and the arrow points to line segment whose lengths are counted twice. The following characteristics are noted:

(a) Perimeter measurements are made from pixel centers, not from pixel margins.

(b) Perimeter calculations cannot be performed in the proportion estimation mode.

(c) The perimeter of features which overlap a scene (or universe of interest) boundary will include a false boundary. For example:

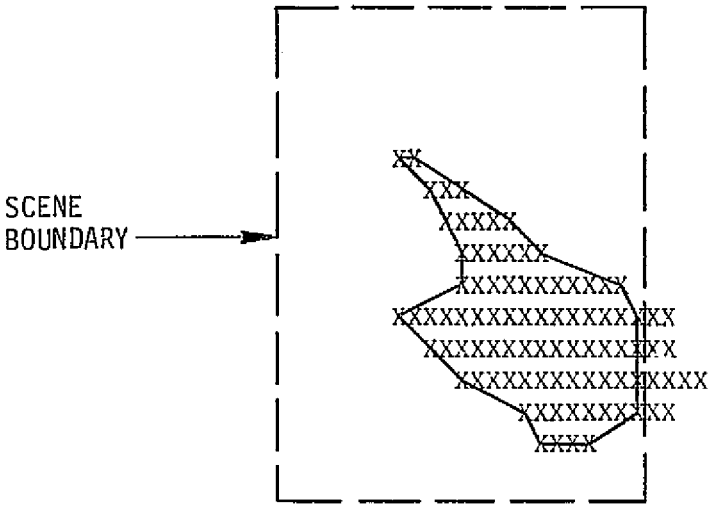

Although the above lake continues beyond the scene boundary, the perimeter is calculated as the sum of the line segments shown.

3) SHAPE

The shape factor is defined as the ratio of the perimeter to the square root of the area normalized to one (1.0) for a round lake. The larger the shape factor, the more irregular is the lake's shoreline. Mathematically the shape factor may be represented as follows:

$$\text{Shape Factor} = \frac{\text{Perimeter}}{\sqrt{\text{Area}}} \times \frac{1}{2\sqrt{\pi}}$$

where $\frac{1}{2\sqrt{\pi}}$ is the normalization factor.

Because perimeter measurements are made from pixel centers, not from pixel margins, shape factors for lakes of size less than 10 or 12 pixels may not be valid.

4) LATITUDE/LONGITUDE

The latitude and longitude of a feature are defined as the latitude and longitude of the last (highest numbered) point of that feature on the last (highest numbered) scan line on which the feature occurs. Transformation coefficients to convert from line and point coordinates to geographic coordinates are input by the user and are obtained by a linear regression analysis external to this program. (Because the coefficients currently in use are first order terms and because lines of latitude converge toward the poles, the areal extent over which one set of coefficients can be applied should be no greater than 25 x 25 nautical miles. In order to preclude this problem in future usage, the use of the Universal Transverse Mercator coordinate system is contemplated.

5) CLASSIFICATION

Recognized features (lakes) are delineated by certain rules of classification algorithms. The following examples illustrate the rules by which pixels are grouped into an areally limited feature (lake):

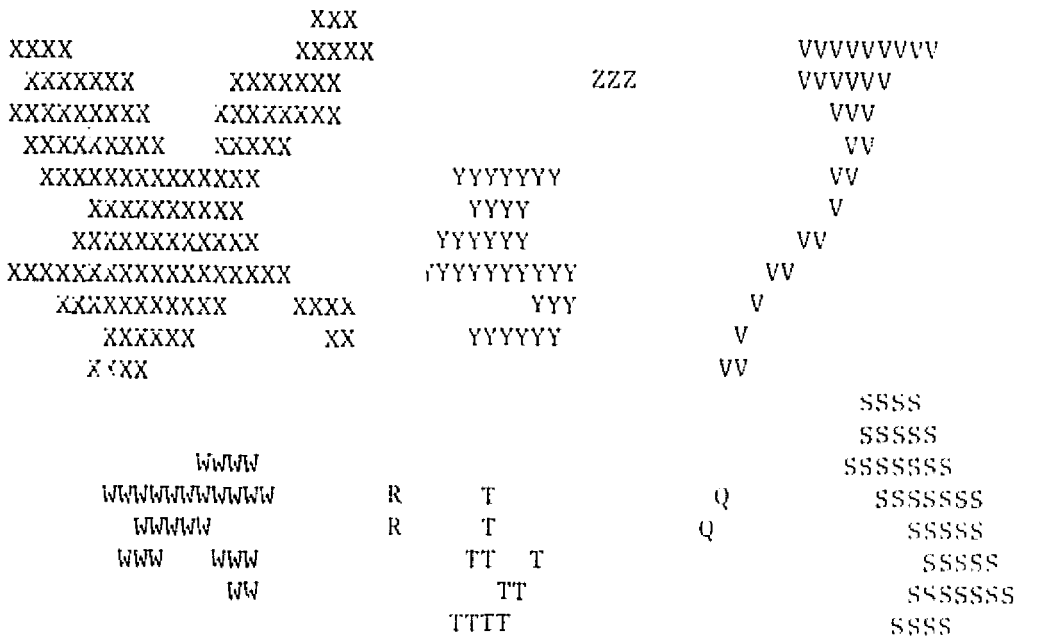

Each letter (Q, R, S, T, V, W, X, Y, Z) represents a pixel. Groups of the same letter represent regions which would be classified together as forming one lake (if this is the feature being recognized). Briefly the rules used to group the pixels are as follows:

(a) A continuous series of pixels on a scan line will be considered as constituting a lake as in lake Z, or a part of a lake as in Y, V. W, and S. A discontinuity in water pixels may be bridged and counted as water only if the bridging option is utilized (see 6 below).

(b) Pixels in a subsequent scan line are again grouped if (a) above applies, and the water segment will be linked to pixels in the previous scan line if any, some, or all of the pixels are vertically or diagonally adjacent to any, some or all of the water pixels in the previous scan line. Lake R illustrates the simple case of a lake consisting of one pixel in each of two adjacent lines, the pixels being vertically adjacent. Lake Q is a two pixel lake consisting of one pixel in each of two adjacent lines, the pixels being diagonally adjacent. By means of this algorithm it is possible for several arms of one lake to be connected as in Lake X.

6) BRIDGING

Pixels not originally identified as water by level slicing may be redefined as water by the bridging algorithm, where the user specifies:

(a) the maximum number of adjacent non-water pixels on a single scan line which may be bridged and

(b) the minimum number of adjacent water pixels on a single scan line which must be in the water intervals on each side of any non-water segment for the non-water segment to be bridged.

NOTES: (i) Bridging is not possible when the proportion estimation mode of classification is specified.

(ii) Bridging only occurs on one scan line, never between scan lines.

7) AREAL STRATIFICATION

The user may wish to stratify the statistical results. The program is capable of sequentially processing any number of strata (scenes). However, a scene must consist of no more than ten rectangles each of which are specified in terms of beginning and ending scan lines and beginning and ending points. For example:

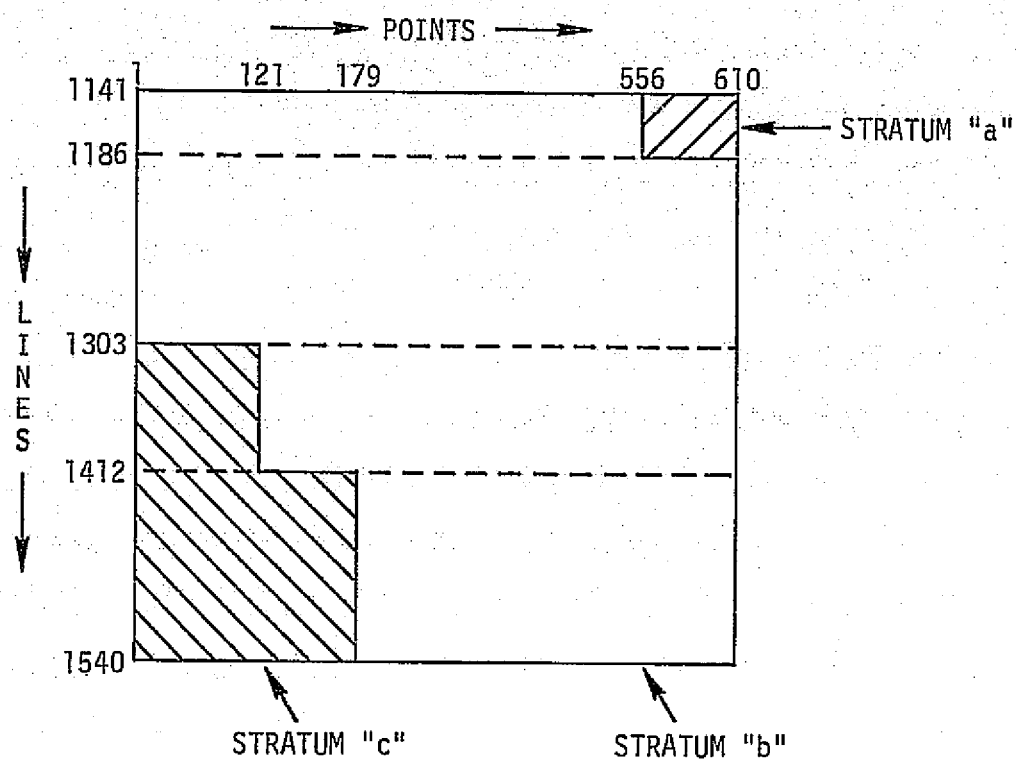

In the above example stratum "a" consists of one rectangle, stratum "b" of an aggregation of four rectangles, and stratum "c" of two rectangles. The size of each stratum is limited only in the number of rectangles which may be grouped to comprise a stratum (ten), and by the maximum number of scan lines (3250) and maximum number of points within a line (1040) which the program can handle. Appendix B exemplifies a typical APSTAT statistical listing for two strata of data.

APPENDIX B

TABULATION OF POND AND LAKE STATISTICS

This appendix includes a tabulation of recognized ponds and lakes identified throughout the study area using SKYLAB/EREP multispectral scanner data collected on 12 June 1973. Based on physiographic differences, the study area was divided into two strata -- the coteau stratum and the drift plain stratum respectively. The drift plain stratum was further subdivided into units labeled "drift plain west" and "drift plain east". This subdivision was necessary because the raw data were divided between two separate computer compatible tapes which could not be abutted for processing. The following diagram and table indicates the vertices in geographic coordinates of the several strata and substrata.

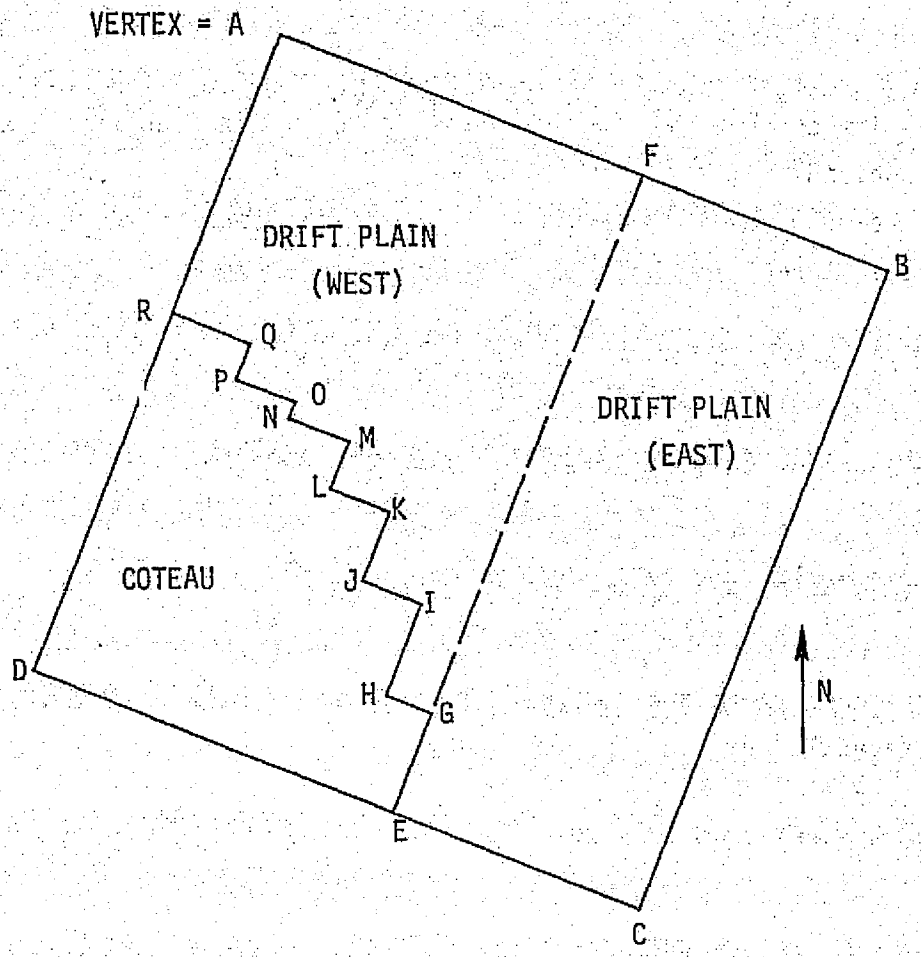

STUDY AREA AND STRATA GEOGRAPHIC COORDINATES

Vertex Code	Vertex Coordinates (degrees)	
	Latitude	Longitude
A	47.595	99.401
B	47.356	98.431
C	46.972	98.648
D	47.210	99.618
E	47.069	99.043
F	47.453	98.826
G	47.129	99.009
H	47.147	99.080
I	47.201	99.050
J	47.224	99.144
K	47.265	99.121
L	47.288	99.215
M	47.317	99.199
N	47.341	99.293
O	47.350	99.287
P	47.374	99.382
Q	47.396	99.369
R	47.427	99.495

The computer tabulations which follow list each water feature recognized in the stratum by enumerating the location and size of the feature. The location is defined using each of two coordinate systems based (1) on a scan line and point number scheme and (2) on a more conventional geographic or latitude and longitude scheme. The convention used to reference each water body has been to locate the body at the position of the last (highest numbered) scan line with at least one pixel in the water body and the last (highest numbered) water body pixel of that scan line. The water feature area is given in terms of both English (acre) and metric (hectare) units. Following this enumeration, the assigned name of the scene is listed along with a description of the scan lines and points which comprise the scene. Next the computed size of the scene is printed followed by several user supplied parameters which the program has utilized in carrying out its computations. The final listing is a summary of the water body size distribution for the scenes (stratum).

LAKE AND POND STATISTICS

SKYLAB/EREP S-192 DATA OF 12 JUNE 1973

STRATUM: NORTH DAKOTA COTEAU

S192 NORTH DAKOTA DATA M*. 2 S* 0* 9 GMT* 12*56* 3.0354 12-06-73

000000000000000000000000000000000000000000000000000000000000000000000000000

TABULATION OF RECOGNIZED WATER BODIES

LAT	LONG	SCAN LINE	POINT	AREA (ACRES)	AREA (HECTARES)
47.3035	99.5651	285	164	1.227	.497
47.2260	99.6068	287	29	6.136	2.483
47.3272	99.5455	291	208	47.861	19.369
47.2118	99.6097	292	9	1.227	.497
47.2403	99.5936	292	56	36.816	14.899
47.2113	99.6079	294	6	1.227	.497
47.3886	99.5047	297	318	1.227	.497
47.2909	99.5589	298	147	44.179	17.879
47.2153	99.5975	302	16	19.635	7.946
47.2367	99.5844	303	54	1.227	.497
47.2349	99.5823	306	52	9.818	3.973
47.3134	99.5370	307	190	1.227	.497
47.3377	99.5222	308	233	1.227	.497
47.3325	99.5088	324	230	7.363	2.980
47.2012	99.5799	327	1	1.227	.497
47.2007	99.5781	329	1	1.227	.497
47.2937	99.5256	329	164	29.453	11.919
47.2318	99.5565	333	57	1.227	.497
47.2718	99.5318	335	128	142.355	57.611
47.2765	99.5189	345	140	1.227	.497
47.2760	99.5171	347	140	1.227	.497
47.3762	99.4463	361	321	2.454	.993
47.2097	99.5382	363	30	7.363	2.980
47.3552	99.4561	363	285	1.227	.497
47.2423	99.5096	373	91	3.682	1.490
47.1957	99.5339	375	10	7.363	2.980
47.2436	99.5068	375	54	4.909	1.987
47.2065	99.5196	383	32	3.682	1.490
47.2872	99.4730	384	174	4.909	1.987
47.2219	99.5058	388	61	3.682	1.490
47.2091	99.5120	389	39	2.454	.993
47.3614	99.4259	389	306	1.227	.497
47.3730	99.4174	391	327	30.680	12.416
47.1855	99.5110	403	3	1.227	.497
47.2602	99.4688	403	134	103.084	41.718
47.1915	99.5065	404	14	1.227	.497
47.1879	99.5076	405	8	6.136	2.483
47.1886	99.5051	407	10	4.909	1.987
47.2328	99.4206	410	264	6.136	2.483
47.3665	99.4016	410	323	8.590	3.477
47.2991	99.4366	413	206	1.227	.497
47.2999	99.4320	417	209	1.227	.497
47.2857	99.4349	422	186	3.682	1.490
47.2761	99.4383	424	170	6.136	2.483
47.3057	99.4185	427	223	2.454	.993
47.2086	99.4652	435	56	12.272	4.966

47.2512	99.4401	436	131	4.909	1.987
47.2189	99.4542	440	76	2.454	.993
47.2977	99.4058	440	214	1.227	.497
47.2812	99.4170	442	186	4.909	1.987
47.2517	99.4316	444	135	1.227	.497
47.3478	99.3732	448	305	1.227	.497
47.2415	99.4323	449	119	6.136	2.483
47.2100	99.4470	452	65	33.134	13.409
47.2916	99.3958	457	210	309.253	125.155
47.1764	99.4557	462	10	28.225	11.423
47.2612	99.4068	463	159	4.909	1.987
47.2379	99.4179	465	119	1.227	.497
47.2847	99.3863	470	203	1.227	.497
47.2794	[illegible]3884	471	194	8.590	3.477
47.2299	99.4143	473	108	25.771	10.430
47.2597	99.3954	475	161	1.227	.497
47.2535	99.3968	477	151	3.682	1.490
47.2821	99.3807	477	201	1.227	.497
47.2042	99.4206	481	66	1.227	.497
47.2234	99.4036	487	102	2.454	.993
47.2551	99.3847	488	158	7.363	2.980
47.1724	99.4211	498	17	1.227	.497
47.2450	99.3730	505	147	17.181	6.953
47.1773	99.4092	507	29	200.039	80.953
47.1933	99.4002	507	57	17.181	6.953
47.2007	99.3960	507	70	31.907	12.913
47.3232	99.3237	510	286	28.225	11.423
47.3289	99.3204	510	296	2.454	.993
47.2534	99.3621	511	164	7.363	2.980
47.1957	99.3865	519	66	6.136	2.483
47.3071	99.3215	521	262	56.451	22.846
47.1747	99.3933	524	31	14.726	5.960
47.1943	99.3781	528	67	7.363	2.980
47.1899	99.3785	530	60	44.179	17.879
47.1990	99.3734	530	76	18.408	7.450
47.1894	99.3767	532	60	11.045	4.470
47.2539	99.3403	532	173	1.227	.497
47.3018	99.3132	532	257	1.227	.497
47.1753	99.3775	535	38	1.227	.497
47.1683	99.3805	540	28	3.682	1.490
47.2006	99.3612	541	83	79.768	32.282
47.2092	99.3513	546	100	39.270	15.893
47.1945	99.3675	548	75	52.769	21.356
47.3046	99.2902	553	270	1.227	.497
47.2142	99.3402	554	112	31.907	12.913
47.3100	99.2831	557	281	3.682	1.490
47.2097	99.3376	559	106	87.131	35.262
47.3284	99.2706	559	314	3.682	1.490
47.2146	99.3338	560	115	2.454	.993
47.3234	99.2714	561	306	4.909	1.987
47.2142	99.3321	562	115	2.454	.993
47.3041	99.2802	563	273	1.227	.497
47.3452	99.2570	563	345	3.682	1.490
47.2297	99.3212	564	143	99.403	40.228
47.2850	99.2900	564	240	25.771	10.430
47.2367	99.3152	566	156	126.401	51.155
47.3422	99.2556	566	341	2.454	.993
47.2498	99.3069	567	179	11.045	4.470
47.3333	99.2566	570	327	1.227	.497
47.1762	99.3443	571	52	15.954	6.456

47.1684	99.3467	573	35	1.227	.497
47.2828	99.2810	574	24C	6.136	2.483
47.1685	99.3445	575	4C	1.227	.497
47.294C	99.2737	575	26C	69.950	28.309
47.3058	99.266C	576	2E1	3.682	1.49C
47.3124	99.2612	577	293	11.045	4.47C
47.2420	99.3CCC	578	17C	1.227	.497
47.3148	99.2978	579	29E	1.227	.497
47.3187	99.2525	582	3C6	1.227	.497
47.3204	99.2516	582	3C9	2.454	.993
47.3347	99.2435	582	334	2.454	.993
47.2722	99.2747	586	226	12.272	4.966
47.2996	99.2593	586	274	3.682	1.49C
47.1567	99.3385	587	24	1.227	.497
47.3299	99.24C1	588	328	4.909	1.987
47.2858	99.264C	589	251	13.499	5.463
47.3183	99.2456	589	3C8	1.227	.497
47.1937	99.315C	59C	9C	1.227	.497
47.2933	99.2577	591	265	1.227	.497
47.1870	99.3167	592	79	107.993	43.705
47.330C	99.2349	593	33C	1.227	.497
47.2978	99.2521	594	274	4.909	1.987
47.2884	99.2563	595	258	3.682	1.49C
47.2016	99.3C23	598	1C7	2.454	.993
47.3C70	99.2418	599	292	2.454	.993
47.2928	99.2477	6C1	268	34.361	13.906
47.3042	99.2413	6C1	288	6.136	2.483
47.2730	99.2569	6C3	234	1.227	.497
47.2815	99.252C	6C3	249	33.134	13.409
47.1826	99.3C69	6C4	7E	19.635	7.946
47.2782	99.2519	6C5	244	11.045	4.470
47.2902	99.2451	6C5	265	2.454	.993
47.1417	99.328C	6C6	5	1.227	.497
47.2061	99.2885	6C9	119	93.267	37.745
47.2298	99.2741	61C	1E1	4.909	1.987
47.3136	99.2267	61C	3C8	6.136	2.483
47.2601	99.2549	612	215	88.358	35.758
47.1635	99.3C85	613	46	4.909	1.987
47.2854	99.2386	614	26C	8.590	3.477
47.2481	99.2587	615	195	42.952	17.383
47.2995	99.2275	617	2F6	2.454	.993
47.3207	99.2156	617	323	2.454	.993
47.3102	99.2205	618	3C5	1.227	.497
47.2170	99.2721	619	142	9.818	3.973
47.2392	99.2596	619	1E1	487.196	197.168
47.2757	99.2396	619	245	3.682	1.49C
47.1760	99.2932	621	71	2.454	.993
47.2747	99.2375	621	244	1.227	.497
47.2136	99.2689	624	138	1.227	.497
47.2456	99.2488	626	195	42.952	17.383
47.2673	99.2365	626	233	1.227	.497
47.2315	99.2547	628	171	23.317	9.436
47.2828	99.2257	628	261	7.363	2.980
47.1919	99.2761	629	1C2	2.454	.993
47.2415	99.245C	632	19C	3.682	1.49C
47.2660	99.2311	632	233	1.227	.497
47.1374	99.3C27	633	8	1.227	.497
47.2108	99.26C2	634	137	58.905	23.839
47.1347	99.3C22	635	4	6.136	2.483
47.2237	99.252C	635	16C	6.136	2.483

47.2608	99.2310	635	225	3.682	1.490
47.2813	99.2194	635	261	7.363	2.980
47.2816	99.2182	636	262	1.227	.497
47.2227	99.2505	637	155	6.136	2.483
47.2609	99.2289	637	226	4.909	1.987
47.2196	99.2512	638	154	2.454	.993
47.1376	99.2955	640	11	1.227	.497
47.2826	99.2115	642	266	3.682	1.490
47.3113	99.1933	644	317	1.227	.497
47.2871	99.2059	645	275	1.227	.497
47.1457	99.2837	647	28	2.454	.993
47.2610	99.2186	647	230	12.272	4.966
47.2545	99.2213	648	219	1.227	.497
47.2778	99.2091	648	260	2.454	.993
47.2634	99.2152	649	235	1.227	.497
47.2736	99.2094	649	253	33.134	13.409
47.2609	99.2156	650	231	1.227	.497
47.2660	99.2127	650	240	47.861	19.369
47.1557	99.2740	651	47	4.909	1.987
47.2549	99.2179	651	221	2.454	.993
47.1974	99.2454	656	122	1.227	.497
47.1983	99.2438	657	124	1.227	.497
47.2637	99.2055	658	235	1.227	.497
47.2694	99.2026	658	245	1.227	.497
47.2950	99.1881	658	294	1.227	.497
47.2995	99.1825	661	303	2.454	.993
47.1515	99.2651	662	44	2.454	.993
47.1681	99.2557	662	73	2.454	.993
47.2605	99.2035	662	235	6.136	2.483
47.2719	99.1971	662	256	2.454	.993
47.2534	99.2065	663	223	29.453	11.919
47.1534	99.2620	664	48	8.590	3.477
47.2809	99.1689	665	272	1.227	.497
47.2571	99.2003	667	231	9.818	3.973
47.2090	99.2265	668	147	76.086	30.792
47.2475	99.2037	669	215	9.818	3.973
47.1505	99.2555	672	46	4.909	1.987
47.1814	99.2359	674	101	20.862	8.443
47.1946	99.2264	676	125	1.227	.497
47.2677	99.1852	676	253	11.045	4.470
47.1260	99.2642	677	5	4.909	1.987
47.2806	99.1769	677	276	1.227	.497
47.1719	99.2372	678	86	67.496	27.316
47.2402	99.1976	679	206	8.590	3.477
47.2034	99.2143	683	143	11.045	4.470
47.2576	99.1837	683	238	7.363	2.980
47.2368	99.1944	684	202	4.909	1.987
47.1305	99.2535	685	16	3.682	1.490
47.2035	99.2122	685	144	1.227	.497
47.2143	99.2061	685	163	95.721	38.738
47.1947	99.2161	686	125	3.682	1.490
47.2415	99.1897	686	211	18.408	7.450
47.2494	99.1822	689	226	1.227	.497
47.2549	99.1781	690	236	2.454	.993
47.2076	99.2027	692	154	65.041	26.322
47.1685	99.2207	696	87	1.227	.497
47.1948	99.2059	696	133	1.227	.497
47.2288	99.1856	697	193	2.454	.993
47.2482	99.1747	697	227	1.227	.497
47.1359	99.2360	699	31	14.726	5.960

47.2049	99.1971	699	152	7.363	2.980
47.2496	99.1647	7CE	233	1.227	.497
47.2346	99.1721	7C7	2C7	1.227	.497
47.1379	99.2257	7C8	38	28.225	11.423
47.1303	99.2290	7C9	25	44.179	17.879
47.2307	99.1723	7C9	2C1	4.909	1.987
47.1466	99.2187	710	54	1.227	.497
47.1786	99.2007	71C	11C	9.818	3.973
47.2182	99.1691	719	183	3.682	1.490
47.1651	99.1960	722	91	1.227	.497
47.2120	99.1675	724	174	8.590	3.477
47.2412	99.1490	726	226	2.454	.993
47.3228	99.1029	726	369	2.454	.993
47.3250	99.1016	726	373	6.136	2.483
47.1172	99.2180	727	9	2.454	.993
47.1395	99.1951	737	52	34.361	13.906
47.1771	99.1739	737	118	11.045	4.470
47.1159	99.2074	738	11	4.909	1.987
47.2526	99.1292	739	251	11.045	4.470
47.1788	99.1695	740	122	1.227	.497
47.1791	99.1687	741	123	1.227	.497
47.1881	99.1632	741	140	1.227	.497
47.1655	99.1743	743	1CC	2.454	.993
47.1787	99.1669	743	123	2.454	.993
47.1913	99.1577	745	146	1.227	.497
47.1408	99.1821	749	99	6.136	2.483
47.2053	99.1457	749	172	2.454	.993
47.1451	99.1756	753	68	6.136	2.483
47.1112	99.1937	754	9	31.907	12.913
47.1460	99.1741	754	70	2.454	.993
47.2098	99.1350	757	183	2.454	.993
47.1256	99.1784	761	37	2.454	.993
47.1212	99.1789	763	3C	69.950	28.309
47.2145	99.1251	764	194	4.909	1.987
47.1427	99.1606	769	7C	1.227	.497
47.1365	99.1539	779	63	23.317	9.436
47.1567	99.1383	783	1CC	12.272	4.966
47.1500	99.1401	785	89	6.136	2.483
47.1234	99.1510	789	44	119.038	48.175
47.2689	99.0637	794	3C1	8.590	3.477
47.1472	99.1314	795	88	1.227	.497
47.1460	99.1291	798	87	1.227	.497
47.1078	99.1455	8C3	22	30.680	12.416
47.1602	99.1159	8C3	114	15.954	6.456
47.1368	99.1261	8C6	74	44.179	17.879
47.1737	99.1021	8C9	14C	1.227	.497
47.1747	99.1006	81C	142	4.909	1.987
47.1257	99.1261	812	57	34.361	13.906
47.1037	99.1315	819	21	1.227	.497
47.1468	99.1061	82C	97	1.227	.497
47.0929	99.1355	821	3	18.408	7.450
47.1290	99.1079	828	69	2.454	.993
47.1655	99.0873	828	133	1.227	.497
47.1237	99.1099	829	6C	2.454	.993
47.1247	99.1062	832	63	1.227	.497
47.1017	99.1182	833	23	85.904	34.765
47.1045	99.1166	833	28	2.454	.993
47.1226	99.1054	834	6C	2.454	.993
47.1643	99.0768	839	135	1.227	.497
47.1669	99.0742	84C	14C	1.227	.497

47.1670	99.0721	842	141	1.227	.497
47.1312	99.0903	844	79	1.227	.497
47.1036	99.1049	845	31	2.454	.993
47.1179	99.0968	845	56	15.954	6.456
47.1032	99.1031	847	31	4.909	1.987
47.1168	99.0953	847	55	8.590	3.477
47.1366	99.0832	848	90	8.590	3.477
47.1118	99.0961	849	47	3.682	1.490
47.1439	99.0760	851	104	2.454	.993
47.1627	99.0653	851	137	3.682	1.490
47.1021	99.0986	852	31	2.454	.993
47.1395	99.0764	853	97	11.045	4.470
47.1501	99.0694	854	116	7.363	2.980
47.0910	99.0987	858	14	8.590	3.477
47.1047	99.0909	858	38	8.590	3.477
47.1173	99.0839	858	60	2.454	.993
47.1412	99.0703	858	102	3.682	1.490
47.1231	99.0785	860	71	4.909	1.987
47.1446	99.0654	861	109	1.227	.497
47.1180	99.0763	865	64	1.227	.497
47.1385	99.0647	865	100	1.227	.497
47.1437	99.0618	865	109	7.363	2.980
47.1002	99.0832	868	34	3.682	1.490
47.0852	99.0907	869	8	3.682	1.490
47.1240	99.0688	869	76	9.818	3.973
47.0978	99.0819	871	31	2.454	.993
47.0885	99.0858	872	15	14.726	5.960
47.1368	99.0575	873	100	17.181	6.953
47.0959	99.0769	877	30	8.590	3.477
47.1153	99.0655	877	64	1.227	.497
47.1188	99.0636	877	70	4.909	1.987
47.1197	99.0620	878	72	2.454	.993
47.0869	99.0795	879	15	23.317	9.436
47.1061	99.0676	880	49	1.227	.497
47.1118	99.0644	880	59	2.454	.993
47.0945	99.0752	881	29	8.590	3.477
47.0979	99.0712	881	35	45.406	18.376
47.2331	98.9949	881	272	14.726	5.960
47.1005	99.0687	882	40	1.227	.497
47.1380	99.0466	883	106	2.454	.993
47.1282	99.0469	888	91	7.363	2.980
47.1347	99.0413	890	103	6.136	2.483
47.0968	99.0616	891	37	3.682	1.490
47.0989	99.0594	892	41	3.682	1.490
47.1248	99.0407	896	88	1.227	.497
47.0760	99.0642	900	4	29.453	11.919
47.1188	99.0400	900	79	11.045	4.470
47.0944	99.0517	902	37	2.454	.993
47.0740	99.0612	904	2	3.682	1.490
47.0838	99.0536	906	20	2.454	.993
47.0831	99.0376	922	25	40.497	16.389
47.0715	99.0432	923	5	19.635	7.946

SCENE N.D. COTEAU

LINES	285	THRU	425	POINTS	1	THRU	380
LINES	426	THRU	530	POINTS	1	THRU	341
LINES	531	THRU	635	POINTS	1	THRU	324

```
LINES   636 THRU   740    POINTS     1 THRU   273
LINES   741 THRU   845    POINTS     1 THRU   201
LINES   846 THRU   924    POINTS     1 THRU   106

SCENE AREA=   348 SQ. MI.
          =   902 SQ. KM.

PIXEL LENGTH=  71.944 METERS   PIXEL WIDTH=  69.031 METERS

MODE= NORMAL
POINTS COUNTED IF VOLTAGE IS GREATER THAN OR EQUAL TO   0 AND
LESS THAN OR EQUAL TO  10
```

S192 NORTH DAKOTA DATA M* 2 S* C* 9 GMT* 12*56* 3.0354 12-06-73

0000000000000000000000000000000000000000000000000000000000000000000000

SCENE	N.D. COTEAU	LINES	285 THRU	425	POINTS	1 THRU	380
		LINES	426 THRU	530	POINTS	1 THRU	341
		LINES	531 THRU	635	POINTS	1 THRU	324
		LINES	636 THRU	740	POINTS	1 THRU	273
		LINES	741 THRU	845	POINTS	1 THRU	201
		LINES	846 THRU	924	POINTS	1 THRU	106

DISTRIBUTION OF RECOGNIZED WATER BODIES IN THE SCENE

BY AREA

AREA (ACRES)	AREA (HECTARES)	FREQUENCY
.25 TO .50	.10 TO .20	0
.50 TO 1.00	.20 TO .40	0
1.00 TO 2.00	.40 TO .81	98
2.00 TO 3.00	.81 TO 1.21	51
3.00 TO 4.00	1.21 TO 1.62	27
4.00 TO 6.00	1.62 TO 2.43	23
6.00 TO 8.00	2.43 TO 3.24	31
8.00 TO 10.00	3.24 TO 4.05	19
10.00 TO 15.00	4.05 TO 6.07	19
15.00 TO 20.00	6.07 TO 8.09	12
20.00 TO 25.00	8.09 TO 10.12	4
25.00 TO 30.00	10.12 TO 12.14	8
30.00 TO 40.00	12.14 TO 16.19	13
40.00 TO 50.00	16.19 TO 20.23	10
50.00 TO 75.00	20.23 TO 30.35	7
75.00 TO 100.00	30.35 TO 40.47	8
100.00 TO 150.00	40.47 TO 60.70	5
150.00 TO 200.00	60.70 TO 80.94	0
OVER 200.00	OVER 80.94	3

LAKE AND POND STATISTICS

SKYLAB/EREP S-192 DATA OF 12 JUNE 1973

STRATUM: NORTH DAKOTA DRIFT PLAIN (WEST)

S192 NCRTH CAKCTA CATA M* 2 S* D* 9 GMT* 12*56* 3.0354 12-06-73

CCCCGOCOCGGCCCCCCCCCCCCCCCCCCCCCCCCCCCCCCCCCCCCCCOCCCCGGGCCCCCGGCCCCCCCCCCCCCCCC

TABULATICN CF RECOGNIZED WATER BCCIES

LAT	LCNG	SCAN LINE	PCINT	AREA (ACRES)	AREA (HECTARES)
47.4835	99.399C	348	5C4	4.909	1.987
47.4657	99.4C59	351	474	2.454	.993
47.4761	99.398C	353	493	29.453	11.919
47.4702	99.4C03	354	483	1.227	.497
47.4688	99.4CC1	355	481	1.227	.497
47.5319	99.2897	428	62C	2.454	.993
47.5347	99.2800	436	628	6.136	2.483
47.4592	99.2582	499	52C	1.227	.497
47.4483	99.251C	512	5C6	3C.680	12.416
47.5032	99.1627	568	624	1.227	.497
47.5028	99.16C9	57C	624	1.227	.497
47.3817	99.1627	635	437	22.C90	8.94C
47.4623	99.11CC	642	581	19.635	7.946
47.3782	99.1565	643	434	51.542	2C.859
47.3594	99.1354	674	413	13.499	5.463
47.3814	99.1168	68C	454	117.811	47.678
47.3335	99.C886	734	391	15.954	6.456
47.4396	99.C102	792	584	1.227	.497
47.4114	98.9668	81C	557	1.227	.497
47.3119	98.9954	837	392	1.227	.497
47.3913	98.9434	844	535	36C.795	146.C14
47.4484	98.8507	9C3	658	6.136	2.483

SCENE									
DRIFT PLAIN WEST	LINES	285	THRU	425	PCINTS	381	THRU	675
	LINES	426	THRU	530	PCINTS	342	THRU	675
	LINES	531	THRU	635	PCINTS	325	THRU	675
	LINES	636	THRU	74C	PCINTS	274	THRU	675
	LINES	741	THRU	845	PCINTS	2C2	THRU	675
	LINES	846	THRU	924	PCINTS	107	THRU	675

SCENE AREA= 480 SC. MI.
= 1244 SC. KM.

PIXEL LENGTH= 71.944 METERS PIXEL WICTH= 69.C31 METERS

MCDE= NCRMAL
PCINTS CCUNTEC IF VCLTAGE IS GREATER THAN CR EQUAL TC C ANC
LESS THAN CR ECUAL TC 1C

S192 NCRTH CAKCTA CATA M* 2 S* C* 9 GMT* 12*56* 3.0354 12-06-72

CCOCCOCCOCCCCCCCCCCCCCCCCCCCCCCCCCCCCCCCCCCCCCCCCCCCCCCOCOCCCOCCCCOCCOOOCCCCCCC

SCENE	CRIFT PLAIN WEST	LINES	265 THRU	425	PCINTS	381 THRU	675
		LINES	426 THRU	530	PCINTS	342 THRU	675
		LINES	531 THRU	635	PCINTS	325 THRU	675
		LINES	636 THRU	740	PCINTS	274 THRU	675
		LINES	741 THRU	845	PCINTS	2C2 THRU	675
		LINES	846 THRU	924	PCINTS	107 THRU	675

CISTRIBUTION CF RECCGNIZED WATER BCDIES IN THE SCENE

BY AREA

AREA (ACRES)	AREA (HECTARES)	FREQUENCY
.25 TC .50	.1C TC .2C	0
.50 TC 1.C0	.20 TC .4C	0
1.00 TO 2.CC	.4C TO .81	8
2.00 TO 3.CC	.81 TC 1.21	2
3.C0 TC 4.CC	1.21 TC 1.62	C
4.C0 TC 6.CC	1.62 TC 2.43	1
6.C0 TC 8.CC	2.43 TC 3.24	2
8.00 TC 1C.CC	3.24 TC 4.C5	0
10.C0 TC 15.CC	4.C5 TC 6.C7	1
15.00 TC 2C.CC	6.C7 TC 8.C9	2
2C.00 TO 25.CC	8.C9 TC 1C.12	1
25.00 TC 3C.CC	1C.12 TC 12.14	1
30.C0 TC 4C.CC	12.14 TC 16.19	1
40.00 TC 5C.CC	16.19 TC 2C.23	0
5C.C0 TC 75.CC	2C.23 TC 3C.35	1
75.00 TC 1CC.CC	3C.35 TC 4C.47	C
100.C0 TC 15C.CC	4C.47 TC 6C.7C	1
150.00 TC 2CC.CC	6C.7C TC 8C.94	0
CVER 2C0.CC	CVER 8C.94	1

LAKE AND POND STATISTICS

SKYLAB/EREP S-192 DATA OF 12 JUNE 1973

STRATUM: NORTH DAKOTA DRIFT PLAIN (EAST)

S192 NORTH DAKOTA DATA M*, 2 S* C* 9 GMT* 12*56* 3.0354 12-06-73

CCC000CCC00CCCCCCCCCCCCCCCCCCCCCCCCCCCCCCCCCCCCCCCCCCCCCCCCCC0CCCCC00CCCCC00CCCCCCCCC

TABULATION OF RECOGNIZED WATER BODIES

LAT	LONG	SCAN LINE	POINT	AREA (ACRES)	AREA (HECTARES)
47.0785	99.0321	930	20	1.227	.497
47.0691	99.0333	934	5	1.227	.497
47.4128	98.8248	948	613	49.088	19.866
47.3995	98.8313	949	590	3.682	1.490
47.4195	98.8149	954	627	3.682	1.490
47.2795	98.8930	955	382	11.045	4.470
47.1659	98.9541	958	164	1.227	.497
47.1671	98.9513	960	187	1.227	.497
47.4427	98.7957	960	670	3.682	1.490
47.3253	98.8548	967	467	4.909	1.987
47.0743	98.9833	980	32	1.227	.497
47.3297	98.8329	986	462	6.136	2.483
47.2600	98.8692	989	361	1.227	.497
47.2587	98.8668	992	360	1.227	.497
47.2616	98.8652	992	365	1.227	.497
47.2577	98.8653	994	359	3.682	1.490
47.2634	98.8621	994	369	1.227	.497
47.4178	98.7688	1000	642	3.682	1.490
47.3335	98.8143	1002	495	2.454	.993
47.3347	98.8137	1002	497	1.227	.497
47.1706	98.9022	1006	211	12.272	4.966
47.3121	98.8172	1011	461	15.954	6.456
47.2736	98.8349	1015	395	1567.128	634.217
47.3428	98.7938	1017	517	4.909	1.987
47.2683	98.8317	1021	388	3.682	1.490
47.2994	98.8131	1022	443	1.227	.497
47.1107	98.9176	1024	113	1.227	.497
47.2762	98.8242	1024	403	1.227	.497
47.2773	98.8236	1024	405	1.227	.497
47.1446	98.8914	1031	175	3.682	1.490
47.2278	98.8443	1031	321	2.454	.993
47.2259	98.8444	1032	318	181.625	73.504
47.2628	98.8226	1033	383	6.136	2.483
47.2009	98.8565	1034	275	1.227	.497
47.2409	98.8339	1034	345	28.225	11.423
47.2802	98.8117	1034	414	1.227	.497
47.1928	98.8556	1036	272	6.136	2.483
47.2342	98.8357	1036	334	31.907	12.913
47.2427	98.8308	1036	349	3.682	1.490
47.1704	98.8696	1038	223	4.909	1.987
47.2195	98.8316	1048	313	1.227	.497
47.2421	98.8179	1049	353	23.317	9.436
47.1637	98.8611	1050	216	1.227	.497
47.2251	98.8254	1051	324	4.909	1.987
47.2310	98.8016	1071	342	1.227	.497
47.2218	98.7802	1097	336	1.227	.497

47.2203	98.7769	1101	335	6.136	2.483
47.1684	98.7878	1119	291	765.769	309.907
47.0846	98.8168	1137	111	1.227	.497
47.1363	98.7313	1152	223	31.907	12.913
47.2292	98.6757	1155	387	1.227	.497
47.2291	98.6727	1158	368	3.682	1.490
47.2323	98.6699	1159	364	3.682	1.490
47.0742	98.7561	1202	118	1.227	.497
47.0728	98.7559	1203	116	1.227	.497
47.0705	98.7541	1206	113	1.227	.497
47.0679	98.7545	1207	109	1.227	.497
47.0642	98.7526	1211	104	1.227	.497
47.1958	98.6772	1212	335	3.682	1.490
47.0615	98.7520	1213	100	2.454	.993
47.0590	98.7524	1214	98	1.227	.497
47.2330	98.6542	1214	401	1.227	.497
47.1292	98.7077	1219	221	1.227	.497
47.2265	98.6517	1220	392	7.363	2.980
47.1848	98.6722	1223	320	1.227	.497
47.1518	98.6887	1225	263	17.181	6.953
47.2329	98.6378	1230	407	1.227	.497
47.2600	98.6215	1231	459	26.998	10.926
47.1318	98.6919	1233	231	49.088	19.866
47.2534	98.6211	1235	445	3.682	1.490
47.2600	98.6163	1236	467	1.227	.497
47.2522	98.6187	1238	444	6.136	2.483
47.2309	98.6298	1239	407	1.227	.497
47.2592	98.6128	1240	467	4.909	1.987
47.1923	98.6474	1243	341	11.045	4.470
47.2459	98.6171	1243	435	2.454	.993
47.1843	98.6387	1256	332	25.771	10.430
47.1800	98.6370	1260	326	13.499	5.463
47.2277	98.6039	1266	412	85.904	34.765
47.2273	98.6021	1268	412	1.227	.497
47.0739	98.6836	1273	145	3.682	1.490
47.1595	98.6250	1283	299	1.227	.497
47.1612	98.6241	1283	302	4.909	1.987
47.1000	98.6576	1284	195	215.986	87.410
47.2090	98.5940	1286	387	18.408	7.450
47.3445	98.5134	1290	626	2.454	.993
46.9886	98.7093	1295	4	997.709	403.773
47.1587	98.6112	1297	302	1.227	.497
47.2263	98.5689	1301	423	1.227	.497
46.9864	98.7033	1302	3	2.454	.993
47.1897	98.5869	1304	360	7.363	2.980
47.1531	98.6041	1307	297	11.045	4.470
47.0954	98.6285	1315	199	1.227	.497
47.1775	98.5740	1323	346	1.227	.497
47.1707	98.5757	1325	335	3.682	1.490
47.0838	98.6156	1334	186	122.719	49.665
47.1046	98.5895	1348	228	9.818	3.973
47.0312	98.6187	1360	104	3.682	1.490
47.0794	98.5874	1364	190	203.714	82.443
47.1125	98.5687	1364	248	61.360	24.832

SCENE DRIFT PLAIN EAST LINES 925 THRU 1364 POINTS 1 THRU 675

SCENE AREA= 569 SQ. MI.
= 1475 SQ. KM.

PIXEL LENGTH= 71.944 METERS PIXEL WIDTH= 69.031 METERS

MODE= NORMAL
POINTS COUNTED IF VOLTAGE IS GREATER THAN OR EQUAL TO 0 AND
LESS THAN OR EQUAL TO 10

S192 NORTH DAKOTA DATA P* 2 S* 0* 9 GMT* 12*56* 3.0354 12-06-73

0000000000000000000000000000000000000000000000000000000000000000000000000000000000000000000000000000

SCENE DRIFT PLAIN EAST LINES 925 THRU 1364 POINTS 1 THRU 675

DISTRIBUTION OF RECOGNIZED WATER BODIES IN THE SCENE

BY AREA

AREA (ACRES)	AREA (HECTARES)	FREQUENCY
.25 TO .50	.10 TO .20	0
.50 TO 1.00	.20 TO .40	0
1.00 TO 2.00	.40 TO .81	40
2.00 TO 3.00	.81 TO 1.21	6
3.00 TO 4.00	1.21 TO 1.62	15
4.00 TO 6.00	1.62 TO 2.43	6
6.00 TO 8.00	2.43 TO 3.24	7
8.00 TO 10.00	3.24 TO 4.05	1
10.00 TO 15.00	4.05 TO 6.07	5
15.00 TO 20.00	6.07 TO 8.09	3
20.00 TO 25.00	8.09 TO 10.12	1
25.00 TO 30.00	10.12 TO 12.14	3
30.00 TO 40.00	12.14 TO 16.19	2
40.00 TO 50.00	16.19 TO 20.23	2
50.00 TO 75.00	20.23 TO 30.35	1
75.00 TO 100.00	30.35 TO 40.47	1
100.00 TO 150.00	40.47 TO 60.70	1
150.00 TO 200.00	60.70 TO 80.94	1
OVER 200.00	OVER 80.94	5